1968

Intrinsic and Extrinsic Control of Cardiac Performance

John Blaise Pace
Loyola University Chicago

INTRINSIC AND EXTRINSIC CONTROL OF CARDIAC PERFORMANCE

by

John Blaise Pace

A Dissertation Submitted to the Faculty of the Graduate School
of Loyola University in Partial Fulfillment
of the Requirements for the Degree of
Doctor of Philosophy

June

1968

BIOGRAPHY

John B. Pace was born on January 12, 1942, in Chicago, Illinois. He attended Lane Technical High School, and then continued his studies at Loyola University Undergraduate School at the Lake Shore Campus, receiving a Bachelor of Science in Biology in 1964.

In the summer of 1964, he began graduate training in the Department of Physiology, of Loyola University Graduate School, under the supervision of Dr. Walter C. Randall, Chairman of the Department. He served as a Graduate Assistant from 1964 to 1968, being supported by a Research Training Grant of the National Institutes of General Medical Sciences, of the National Institutes of Health.

ACKNOWLEDGMENTS

I am pleased to have this opportunity for expressing my sincere graditude to Dr. Walter C. Randall, Chairman of the Department of Physiology, for his continued support and guidance throughout the course of this investigation.

I would also like to take this opportunity to thank my parents without whose unending encouragement this work could not have been completed.

TABLE OF CONTENTS

TABLE OF CONTENTS

LIST OF TABLES

LIST OF FIGURES

LIST OF FIGURES

CHAPTER I

STATEMENT OF PROBLEM

While studying the affects of efferent vagal nerve stimulation on pulmonary and aortic pulsatile flow, large peak flow velocities and flow accelerations were observed during vagal bradycardia. These flow pulses were associated with low aortic pressure and reduced left intraventricular pressures along with depressed rates of intraventricular pressure development. It became apparent that in order to understand the mechanisms responsible for pulsatile flow changes in the ascending aorta, the instantaneous pressure gradient across the aortic valve must be known. This conclusion provided the stimulus to study the hemodynamic determinants of the pressure gradient across the aortic valve. To implement this study, the techniques of right heart bypass were employed in order to independently control the aortic pressure and stroke volume.

The cardiovascular drug isoproterenol has been shown to elicit large pressure gradients across the aortic valve (216). Isoproterenol was employed in this study in order to generate functional systolic pressure gradients across the aortic valve.

The relationships of the changes in magnitude and form of the isoproterenol induced pressure gradients were compared with the contour of the corresponding flow pulse in the ascending aorta. In addition, pressure flow relations across the aortic valve were recorded during sympathetic nerve stimulation.

Large intraventricular pressure gradients have been recorded in the right ventricle as the result of isoproterenol administration (216). Right ventricular pressure gradients are generated within the confines of the right ventricle and develop across the infundibular region.

Other inotropic interventions such as calcium chloride and digoxin have been shown to elicit pressure gradients across the infundibular zone of the right ventricle (17). The effects of sympathetic nerve stimulation on the development of infundibular pressure gradients was investigated in an attempt to demonstrate the possibility of neural control of infundibular pressure gradients.

Ventricular outflow tract pressure gradients have been reported clinically. Inspection of the hearts of individuals who have demonstrated ventricular ejection gradients has revealed no anatomic obstruction. The presence of ventricular ejection pressure gradients without anatomical obstruction has been termed functional stenosis. If the sympathetic nervous system can be shown to influence pressure gradients in the right and left ventricles, this could provide a possible explanation for functional

obstruction of ventricular outflow.

Recently it has been found that the vagus nerve can exert a negative inotropic influence on the left ventricle and has been shown to be involved in reflex cardiovascular adjustments (45,46,47,48,111). However, vagal negative inotropic effects have not been shown in the right ventricle.

In experiments involving the affects of vagal stimulation on the paced heart, large increases in right ventricular end diastolic pressure with little or no change in peak systolic pressure have been observed. On this basis the existence of a vagal negative inotropic influence on right ventricular function may be proposed.

In short, the purpose of this dissertation is to evaluate the hemodynamic determinants of the pressure gradient across the aortic valve, as well as the effects of autonomic nerve stimulation on intrinsic mechanisms of ventricular function.

CHAPTER II

LITERATURE REVIEW

A. Cardiac and Vascular Hemodynamics.

The function of the heart has been characterized primarily by its ability to move blood into and through the arterial system. The early experiments of Frank and Starling provide the basis for most current concepts of cardiac function (55,209). The length active tension relationships first established by Otto Frank for cardiac muscle, formed the foundation for Starling's work in the intact heart (55). In his Linarce lecture of 1915, Starling stated that "the energy of contraction is a function of the length of the muscle fiber". Hence, the contractile force of the myocardium increases with increases in muscle length and in the intact preparation, increases in cardiac muscle length have their expression in the volume or pressure in the ventricles prior to the onset of systole (209). Hamilton and Burton have discussed the importance of the Starling relationship in the intact circulation, and have concluded that the primary function of this relationship is to maintain the outputs of the right and left ventricles equal (29,72).

Increases in fiber length in the intact ventricle resulting from increased filling yield elevated stroke volumes. In the Newtonian sense the heart does work on the blood in moving it into the large arteries. Stroke work is expressed as the product of the stroke volume times the mean arterial pressure during ejection. The relationship between stroke work and left ventricular end diastolic pressures (LVEDP) has been termed a ventricular function curve (186,187). This relation has been employed to evaluate the contractile state of the heart. Sarnoff and Mitchell demonstrated that from any given end diastolic pressure or fiber length, the ventricle produces more external stroke work and more external stroke power, and concluded an increase in ventricular contractility occurred (193). Function curves have been derived which show how inotropic interventions alter the basic length tension relation developed by Starling. Interventions such as norepinephrine infusion cause the relation between end diastolic ventricular volume and the work function to be shifted so that more work can be done without encroachment on fiber length (186).

Changes in cardiac function which are accompanied by alteration in fiber length have been termed heterometric autoregulation, and are exemplified by the Starling concept (193). Sarnoff et al have coined the term homeometric autoregulation to characterize intrinsic changes in cardiac function resulting in increased external work without concomitant increases in fiber

length (189, 195). Anrep was the first to recognize that the heart adapted to increases in aortic pressure and stated that "if the blood pressure be maintained steady at its new height, the heart always reacts in such a manner that it tends to return more or less to its normal volume, whether the change in pressure has been one of diminution or increase" (7). Peserico has shown in the tortoise heart that when arterial resistance was raised with constant cardiac output the ratio of work to end diastolic ventricular volume (w/v) increased, indicating that increases in external work were not accompanied by equal increases in fiber length (144). Stainsby et al were the first to show that elevations in mean aortic pressure caused the heart to perform more stroke work from a given end diastolic pressure (208). Independent work by Sarnoff and Rosenblueth have shown that the cardiac responses to elevations in aortic pressure is not dependent upon an increased coronary perfusion pressure (170,195). Homeometric autoregulation in response to elevations in mean aortic pressure have also been shown by Sonnenblick in the cat heart (205). These results tend to indicate that the level of mean aortic pressure may be an important determinant of the contractile state of the heart (205).

Other workers have shown that elevations in outflow resistance presented to the left ventricle can alter the performance of the heart (49,89,143). Otto Frank was probably the first to demonstrate that the velocity flow during ejection decreased

continuously with increasing afterload (55). Imperial et al have shown that increases in outflow resistance caused a reduction in peak aortic flow and stroke power (89). Wilken et al demonstrated a decrease in peak flow and the maximum acceleration of blood during ejection in the first few beats following increased outflow resistance (238).

It should be mentioned that the oxygen consumption or energy utilization of the heart is not directly related to work per se (29). Cardiac oxygen consumption is less when identical work is performed in moving large volumes at low pressures than when the heart moves smaller volumes at high pressures (29). Muscle demands an increased rate of energy consumption proportional to the tension developed rather than to the work load (88). The experiments of A.V. Hill have demonstrated that extent and duration of tension depends upon the active state of the muscle during contraction, and energy must be supplied to maintain the active state (79).

The work of A.V. Hill on skeletal muscle mechanics has lead the way for more precise characterization of the contractile state of the myocardium. Abbott and Mommaerts have shown that the muscle mechanics elucidated by A.V. Hill in skeletal muscle are applicable to cardiac muscle (1). In contrast to skeletal muscle, maximum isometric force generated by cardiac muscle can occur at resting tensions which are greater than the active tension developed (1). Sonnenblick has shown that increases in

initial muscle length do not alter the maximum velocity of shortening in unloaded muscles, but do increase the maximum force developed (203). These relationships prevail during each instant of muscle shortening (204). Inotropic interventions cause increases in the initial velocity of shortening with or without an increase in the maximum isometric force generated by the muscle (203). Changes in the maximum velocity of shortening with or without a change in developed force is indicative of a change in the contractile state of the heart muscle. These principles have been extended to better define muscle mechanics in the intact heart.

Fry et al have demonstrated a method in which force, velocity, and tension can be analyzed during the course of a single beat in the intact heart (61). This method involves the theoretical consideration of the left ventricle as a sphere and the volume of blood ejected per unit time taken to represent the circumferential shortening of the ventricular muscle. In this way the instantaneous radius of the ventricle could be calculated from the volume equation of a sphere (61). Utilizing this method, Levine and Britman have shown a reciprocal relationship between force and velocity in the intact heart (107).

The relation between force and velocity has been shown to be altered by the level of aortic pressure. Levine et al and Ross et al have shown that sudden increases in afterload between beats caused increases in developed tension together with

reductions in muscle fiber shortening velocity (108,171). These results indicate that both LVEDP and the level of afterload can influence the velocity of ejection (171). As is the case in isolated cardiac muscle, increases in fiber length (LVEDP) produced concomitant increases in maximum wall tension without change in the maximum velocity of muscle fiber shortening. In addition, inotropic interventions such as norepinephrine infusion produced increases in both velocity of muscle fiber shortening and maximum ventricular wall tension (171).

The force velocity method of assessing cardiac function in the intact heart may represent a more sensitive index of the contractile state of the myocardium than the ventricular function curve. Covell et al have shown that infusions of 0.03 μg/Kg/min norepinephrine did not produce significant changes in the ventricular function curves (stroke work as a function of LVEDP), but did shift the relationship between the velocity of shortening of the contractile elements in the myocardium and the wall tension, so that greater contractile element velocity was obtained for a given wall tension (39). Similar shifts in the force velocity relationship were observed with elevated heart rates and hypothermia (39).

Studies concerned with understanding the mechanisms of myocardial force development and muscle mechanics provide important indices by which we can assess the contractile state of the heart and its performance. In terms of the movement of blood

from the heart into the major arteries, the forces generated by the contractile elements in the myocardium must ultimately be transferred into a pressure gradient responsible for the movement of blood. The heart pulses the circulatory system with a given volume of blood and the frequency of pulsations is determined by the heart rate. Hence, there is a repetitive oscillation of pressure and flow pulses across the aortic valve, and it becomes evident that the understanding of such a system is dependent upon the relationships between pulsatile pressure and flow in the circulatory system.

The relationships of pulsatile pressure to flow in elastic tubes and their application to the mammalian circulatory system have stemmed largely from the efforts of J.K. Womersley (239,240). Most of this work involves mathematical formulations with which I am unfamiliar and fail to fully understand. However, certain conceptual formulations can be mentioned concerning this work.

Utilizing the Navier-Stokes boundary equations for flow of a Newtonian fluid, Womersley showed that a nondimensional parameter (alpha) controlled the behavior of such flow (239). The formula for the parameter is given by (77):

$$\alpha^2 = \frac{r_o^2 w}{v} \qquad (1)$$

where r_o is the tube radius, w the angular frequency, and v is the kinematic viscosity of the fluid. Assuming a sinusoidal

pressure gradient to be acting along the axis of the tube, it follows that the resultant fluid velocity in the axial direction will also be sinusoidal, having a certain amplitude and phase lag with respect to pressure. The amplitude and phase of the velocity are functions of the tube radius, the kinematic viscosity, as well as the frequency. The solution of this equation enabled Womersley to resolve the sinusoidal pressure gradient in a rigid tube into two components, one in phase with flow, the functional gradient from which fluid resistance could be calculated and one in phase with the acceleration of flow from which fluid inductance could be calculated (60). As α increases the phase lag of the flow with respect to the pressure gradient tends to approach 90°. Reductions in α result in flow which is characterized primarily by the Poiseuille relationship (60). Fry et al have attempted to evaluate the effects of changing values of α on the ratio of hydraulic inductance to fluid resistance. The value of α was increased by increasing the frequency of a sinusoidal pump which forced fluid oscillations in a small tube. The ratio of hydraulic inductance to fluid resistance remained relatively constant over values of α^2 ranging from 100 to 10,000 (60). The constancy of inertance and resistance with changes in α has caused Fry to postulate the use of constant coefficients representing inertance and resistance for the computation of pulsatile flow from the pressure gradient (62,63).

The application of the pressure gradient technique for

the computation of pulsatile blood flow has been developed primarily by the efforts of Womersley, Fry and Porjé (62,149,239). Fry et al have resolved Womersley's pressure gradient equation into the following form:

$$v = \frac{980\ P}{\sqrt{a^2 + (2p\Delta\ x\ \pi f)^2}} \qquad (2)$$

where P is the lateral pressure difference between two points in the axial flow stream, a^2 is a proportionality constant between blood velocity and the frictional pressure drop between the two points X_1 and X_2 where lateral pressures are being measured and ρ is the fluid density (62). This equation is applicable only to the case of sinusoidal waves. Utilizing this equation, a very close relationship was shown between the fluid velocity calculated from the pressure gradient and that taken empirically from the characteristics of the pump (62).

Further application of this method to pulsatile blood flow resulted in the development of the following formulation (63):

$$P = \rho\ \Delta x \frac{du}{dt} + au \qquad (3)$$

This linear differential equation combines the inductance and resistance components of the change in pressure across a segment of vessel. The solution of this equation can be derived with a simple computer. In the above equation P is the instantaneous pressure difference, ρ is the blood density, Δx is the separation of the pickup points on the change in pressure catheter, $\frac{du}{dt}$ is

blood acceleration, a represents the coefficient of friction and u the blood velocity. Although the pressure gradient technique neglects vessel compliance this does not introduce a significant error (63).

Utilizing the pressure gradient technique in the ascending aorta of man, Barnett et al have shown that norepinephrine infusions resulting in elevations in systemic arterial pressure above 150 mm Hg caused the peak flow velocity along with the peak pressure gradient to be decreased, while administration of isoproterenol caused an increase in the aortic blood velocity and peak pressure gradient (11). Employing the pressure gradient method, Rudewald and Porjé demonstrated that at the onset of the Valsalva maneuver the Δp was slightly increased in the ascending aorta then decreased rapidly below control levels (173).

Utilizing high speed cinematography, McDonald has demonstrated that in a segment of femoral artery the peak pressure gradient was associated with the maximum rate of flow change, and zero pressure gradients with peak forward flow (125). Such relationships between pressure and flow are based on inertial properties, in that the pressure gradient acts mainly to accelerate and decelerate the blood column in a segment of vessel. The pressure oscillations had both negative and positive components, and the positive components were accentuated by a reduction in the mean pressure level in the vessel (125).

Measurements in the rabbit abdominal aorta indicated that peak forward flow velocity can reach 60 cm/sec, and a high vascular resistance distally reduced the velocity of systolic flow (126). Spencer and Denison have demonstrated that inertial flow dominates in the thoracic aorta, and is accentuated when the flow rate is minimal, the resistance component on the other hand, became accentuated when flow rate or cardiac output was elevated (198).

The results of McDonald and Spencer have shown that flow in the arterial system of mammals is primarily inertia, indicating that the resistance offered to blood flow in arteries is minimal (125,198). Utilizing a differential pressure technique across the aortic valve, Spencer and Greiss have shown that left ventricular ejection is also dominated by the inertial characteristics of the blood (201). Consequently, left ventricular pressure exceeded aortic pressure for approximately 27 to 63% of the ejection period, the remainder of forward flow during ejection took place against the pressure gradient (201). Spencer recorded mean flow accelerations in thoracotomized dogs ranging from 1.8 to 8.8 x 10^3 cm/sec/sec and the peak pressure gradient across the aortic valve ranged between 4.9 and 16.1 mm Hg. Rushmers group has presented acceleration in conscious dogs ranging from 5.1 to 7.0 g (g = 980 cm/sec/sec) (56,177,184,185). Recently, Noble et al reported maximum accelerations during ejection which ranged between 5 and 11 g (138). In the experiments of Spencer on thoracotomized dogs the peak pressure gradient across the aortic

valve was associated with the point of maximum acceleration on the flow pulse and zero pressure gradient with peak flow velocity (201).

Okino and Spencer have shown that inertial flow also characterizes right ventricular ejection dynamics. However, right ventricular pressure exceeded pulmonary arterial pressure for approximately 30 to 40% of open valve time. The maximum acceleration during ejection was 600 cm/sec/sec and peak pressure gradients average 1 mm Hg/cm of artery (140). The ejection dynamics across the pulmonic semilunar valves are probably influenced by the geometry of the pulmonary artery (64).

The early experiments of Hamilton and Bracket illustrating aortic and ventricular pressures during ejection showed that left ventricular pressure exceeded aortic pressure throughout the total period of ejection (72). Such results indicate that blood flow during ejection is based on the viscous properties of blood and changes in flow can be explained utilizing the classical formulation of Poiseuille which has been simplified to the following form by Green (70):

$$Q = \frac{\Delta p}{r} \qquad (4)$$

where Q is the volume flow, Δp is the pressure drop across the resistance r.

Driscoll and Eckstein have recently confirmed the results of Hamilton and Bracket by demonstrating that the pressure

reversal across the aortic valve during the latter phase of systole was a function of the placement of the tip of the aortic cannula in respect to the aortic valve (51). When the aortic cannula was placed immediately above the valve no systolic reversal of pressure could be observed. However, when the aortic cannula was placed from 1-3 cm distal to the valve a negative pressure was recorded across the valve during the latter phase of systole, thus confirming Spencer's results.

Rushmer has interpreted the results of Spencer et al to mean that the ventricles act as impulse generators, which apply a large force for a given period of time on the blood resulting in flow acceleration into the ascending aorta (177). Since the flow properties which prevail during ventricular ejection are primarily inertial, the system may be represented by Newton's second law of motion:

$$F(t) = M \, \Delta V/\Delta t \qquad (5)$$

where F(t) is the ventricular impulse, M is the mass, and ΔV is the change in instantaneous velocity with time. This equation indicates that the flow acceleration during ejection will be a direct function of the peak pressure gradient across the aortic valve, as well as the time over which it acts.

The rate of change of intraventricular pressure has been used as an index of the contractile state of the myocardium (68,162). Increasing attention is now being given the maximum acceleration of blood in the ascending aorta as another

means of assessing the contractile state of the myocardium. Noble et al have shown that when the myocardium of unanesthetized dogs was stimulated with intracoronary injections of calcium gluconate and isoproterenol the maximum acceleration of blood in the ascending aorta during ejection showed greater increases than did dP/dt (138). Noble and colleagues have shown that the maximum acceleration and deceleration of blood during ejection is not altered by changes in posture; however, the maximum flow velocity was increased and this effect was responsible for the increased stroke volume observed (137). In the reclining position the diastolic size of the heart is increased and the stroke volume augmented (175). The results of Noble et al tend to indicate that maximum acceleration is not exclusively a function of LVEDP. However, Weissler et al have shown in humans that the mean rate of left ventricular ejection was increased as a function of the stroke volume (227).

Wiggers has shown that both pressure pulses and phasic flow can be modified by vascular factors such as compliance of the vessels (232). Peterson has shown that pressures in the arterial system generating flow are composed of inertial, resistance, and compliant forces, and changes in any one of these factors can change the characteristics of the pressure wave form (147). Pressures generated by a constant flow device introduced into the ascending aorta developed first a rapid step up, the acceleration transient, a slower rising component, the

resistive force and a gradually developing pressure, the force required to overcome vessel compliance (147). The acceleration transient was believed to result from the inability of the vascular wall to follow the rapid fluid ejection because of its inherent resistance to stretch. Spencer et al have implicated vessel compliance as contributing to the 180° phase difference between the resonant pressure waves in the upper and lower aorta (202). Alexander has stated that reflected pressure waves originate from the diaphram and the femoral vascular bed, and are responsible for the generation of the aortic standing wave (3). The distensibility of the ascending aorta has been shown to decrease with increases in mean pressure from 50 to 200 mm Hg (13, 104). Bergel and Cope have shown that the compliance of the aorta is slightly increased under dynamic conditions with pulsation frequencies in the physiologic range (14,37).

In summary, the contractile forces generated by the heart are directed primarily in developing sufficient force to accelerate the blood into the aorta (199). The pressures generated in the aorta during the rapid entry of blood are dependent upon the flow acceleration, the volume ejected, and the compliance of the aorta. Consequently, the pressure gradient across the aortic valves represents a complex sum of forces, which have both cardiac and vascular components.

Extrinsic neural control of the pressure gradient across the aortic valve is mediated by the autonomic nervous system and

must be intimately related with changes in cardiac function resulting from activation of the sympathetic pathways to the heart.

B. Sympathetic Control of Ventricular Function.

Early studies concerned with the effects of cardiac nerve stimulation on ventricular function elucidated the accelerator function of these nerves. Utilizing a tambour device, Hendersen and Barringer demonstrated that accelerator nerve stimulation could increase ventricular stroke and amplitude. However, these authors considered this an exception, and concluded that accelerator nerve stimulation could not alter amplitude or stroke independent of the beat frequency (78). Cullis and Tribe demonstrated that the action of epinephrine on ventricular contraction remained after transection of the A.V. node, and concluded that the ventricles received an abundant supply of sympathetic nerves which did not pass by way of the A.V. bundle (41). In 1920 Wiggers and Katz showed that stellate ganglion stimulation reduced the systolic period to cycle length ratio below that expected from a theoretical relation based on beat frequency (234). Further studies by Katz showed that the duration of systole was altered before cycle length at the onset of stellate ganglion stimulation, thus demonstrating that the accelerator nerves have a specific influence on the duration of ventricular systole (95).

In independent studies Tulgan and Samaan were able to demonstrate that the accelerator nerves have a tonic influence on

heart rate, and implied the involvement of the cardiac nerves in the reflex control of blood pressure (185,218).

Shipley and Gregg observed that stellate stimulation resulted in large elevations in arterial blood pressure as well as right intraventricular pressure (197). These workers also showed that the work output of the heart could be increased by stimulation of the stellate ganglion. However, Eckstein and Stroud have demonstrated that sympathetic nerve stimulation increases the oxygen consumption of the heart disproportionately to the external work (53). Recent studies by Sarnoff et al have shown that catecholamines can increase ventricular performance without elevating myocardial oxygen consumption (192).

Cardiac sympathetic nerve stimulation has been shown to result in a reduction in heart size (6). Similar changes in ventricular dimensions were observed by Gauer during exercise (65). These changes are intrinsically related to the increase in myocardial contractility which results from sympathetic nerve stimulation.

Independent studies by Randall and Anzola have demonstrated that cardiac nerve stimulation could result in an increased strength of myocardial contraction (6,159). Randall and Rohse concluded that stellate ganglion stimulation could induce the heart to perform more external work without changes in fiber length (159). This concept was employed by Sarnoff and associates in the elaboration of the ventricular function curve (186,

187,189). These workers demonstrated that sympathetic nerve stimulation altered the performance of the ventricles such that more external work could be produced without change in initial fiber length. The intensity of the stimulation determined the level of external work generated from a given fiber length or end diastolic pressure (189,194).

Sympathetic nerve stimulation has been shown to increase contractility of all the cardiac chambers (219). Wallace et al have demonstrated that the difference between mean left atrial pressure (MLAP) and left ventricular end diastolic pressure (LVEDP) is independent of aortic pressure, stroke volume, and heart rate over certain ranges (221). Mitchell et al have reported that during sympathetic nerve stimulation MLAP is lower for any given LVEDP (130). However, Ulmer and Randall have shown instances during stellate ganglion stimulation in which MLAP becomes elevated (219).

Sympathetic nerve stimulation has been shown to facilitate the pattern of mitral valve closure by increasing the contractility of the left atrium (191).

Linden et al showed a curvilinear relation between myocardial segment length and left ventricular diastolic pressure. Atrial systole caused a substantial increase in myocardial segment length when the ventricle was on the more sensitive part of its pressure length curve (113). Distensibility and pressure-volume relations in the intact left ventricle appear to be

unaffected by cardiac sympathetic nerve stimulation (131,207).

Studies by Randall et al have demonstrated differences in cardiac function resulting from stimulation of the right and left stellate ganglion (158). Outflows from the right stellate ganglion were shown to innervate predominately the S.A. node and conductile tissue, while the left sympathetic trunk and stellate ganglion provided the principle sympathetic supply to the ventricles (154). Sympathetic fibers to the heart were shown to originate from T-1 through T-5. These results have been confirmed by Mizeres (133).

In 1926, Cannon concluded that the increment in heart rate he observed in excited cats after bilateral superior cervical and stellate ganglion removal was due to accelerator fibers reaching the heart from the sympathetic chain below the stellate ganglion (31). However, recent investigations by Levy et al have shown that the communicating rami entering the paravertebral chain below the stellate ganglia funnel up through the stellate ganglia and the ansa subclavia (112). Apparently, no sympathetic outflows to the heart in the dog leave the paravertebral chain below the stellate ganglia (112,133).

Rushmer and West have shown that changes in left ventricular performance during exercise appear to be directly influenced by neural reflexes (183). Intravenous infusions of catecholamines in physiological doses produced changes in ventricular performance which differed significantly from those

observed during exercise, particularly with reference to heart rate. Further studies by Rushmer et al demonstrated that during exercise, heart rate increased, left ventricular diameter decreased, left ventricular end diastolic pressure decreased, but stroke power and dP/dt both increased (181). Infusion of isoproterenol induced changes similar to those recorded during exercise.

In addition, Rushmer has shown that stroke volume remains constant during exertion (176). This has been confirmed by Wang et al who showed that stroke volume had little or no change even when cardiac output increased 2.4 times (225). On the other hand, experiments by Warner and Toronto utilizing dogs with electrically paced hearts have shown that cardiac output during exercise can be regulated by stroke volume at rates between 140 and 250 beats per minute (226). Increases in stroke volume during stellate stimulation have been reported by Kelso and Randall (98).

The left ventricle ejects approximately 46% of its end diastolic volume with each stroke and retains approximately 54% of its end diastolic volume at the end of systole (86). Similarly the right ventricle empties in a fractional manner and on the average ejects 39% of its end diastolic volume (87).

Braunwald et al have shown that increases in stroke volume resulted in small but definite increases in the ejection period (19). The mean rate of ejection (stroke volume divided by the ejection period), increased greatly per beat. In addition,

these workers have shown that the mean ejection rate was elevated at higher heart rates with stroke volume constant. No lengthening of the duration of systole was observed at various levels of aortic pressure (75-125 mm Hg), and sympathomimetic amines caused the ejection period to decrease and the mean rate of ejection to become elevated (19). Mitchell et al demonstrated that with increases in aortic pressure the mean rate of ventricular ejection (MRE) increased, along with stroke work and stroke power (132). With further elevations in aortic pressure MRE decreased but stroke work and stroke power increased. Infusions of norepinephrine resulted in elevated MRE with no change in stroke volume.

Sonnenblick et al have shown that at a constant level of external ventricular work, myocardial oxygen consumption correlated most closely with the velocity of ventricular contraction (206). In these experiments the mean rate of ventricular ejection was taken as an index of myocardial fiber shortening velocity. When the contractile state of the myocardium was augmented by norepinephrine or paired electrical stimulation, the time tension index became an unreliable measure of myocardial oxygen consumption (206).

Although the rate of ventricular muscle fiber shortening can be altered by the left ventricular end diastolic volume, it appears that the mean contracted length of the ventricular muscle at the end of systole is dependent upon the inotropic state of the muscle (214).

Probably the first definitive study on the action of sympathomimetic amines on the cardiovascular system was performed by Barger and Dale (10). These workers demonstrated that certain compounds such as phenylephrine had a profound affect on systemic arterial pressure. Studies by Wiggers demonstrated that epinephrine increased the isometric pressure gradient in the left ventricle, as well as the rate of ventricular relaxation (231). The experiments of Cannon and Rosenblueth showed the existence of two epinephrine-like substances released at sympathetic nerve endings which they called sympathins E and I (33,34,35). Dale termed adrenergic those postganglionic sympathetic fibers which have an adrenaline-like effect on the organ they innervated (43). Von Euler has presented considerable evidence to support the contention that the adrenergic transmitters are epinephrine and norepinephrine (220).

Studies concerned with the effects of exogenous administration of epinephrine and norepinephrine on cardiac performance have dealt primarily with their effects on the mechanics of the cardiac cycle. Remington and Hamilton have shown that neosynephrine (phenylephrine) infusion did not alter the length of systole, even though the arterial pressure was increased and stroke volume decreased (165). Stellate ganglion stimulation resulted in an augmented stroke volume and ventricular work, but decreased the duration of systole. Further studies by Hamilton and Remington showed that administration of isoproterenol

resulted in elevated stroke volume and stroke work (73). The reduction in the length of systole which accompanies the administration of either epinephrine or isoproterenol is independent of the heart rate (164). In addition to reducing the period of systole, epinephrine and isoproterenol have been shown to abbreviate the systolic ejection period (166). On the other hand, norepinephrine caused the ejection period to lengthen.

Under the influence of isoproterenol, myocardial force has been shown to increase over 250% from control (38).

The actions of exogenous epinephrine and norepinephrine on cardiovascular function appear to be linked with their secondary action on blood pressure. Infusions of norepinephrine and epinephrine in some instances leads to an increase in the diastolic size of the left ventricle (228), which is probably the result of the elevations in aortic pressure induced by these drugs (228).

Epinephrine and norepinephrine not only affect the processes by which the ventricles are emptied, but also affect those which contribute to ventricular filling. Studies by Brecher indicate that epinephrine and norepinephrine contribute to ventricular filling by augmenting negative diastolic pressures (20,21).

The changes in the contractile state of the myocardium resulting from catecholamine infusion appears to be linked to the activity of the phosphorylase enzyme. The degree of isometric

tension development resulting from drug administration has been shown by Kurovetz and Mayer to be closely correlated with the level of phosphorylase activity (101,122). Isoproterenol is one of the most potent activators of the phosphorylase enzyme in cardiac tissue.

During isoproterenol infusion, the end systolic volume of the ventricle is reduced (100). Krasnow et al have implied that the augmented stroke volume resulting from isoproterenol administration is the result of the reduction in arterial pressure which prevails during isoproterenol infusions (100).

Piemme et al have recently shown that isoproterenol infusions result in elevated flow accelerations in the ascending aorta and methoxamine had the opposite affect on flow acceleration (148).

Remington has shown a definite phase difference between the point at which left ventricular pressure reaches aortic diastolic pressure and the upstroke of the aortic pressure wave (163). This lag was not attributed to slow pulse wave transmission through the aortic valve. The extent of the phase lag was magnified by epinephrine and isoproterenol and was reduced by phenylephrine and heart failure (163).

Isoproterenol appears to have little or no affect on conduction velocity in the Purkinje system (94). However, isoproterenol will induce spontaneous firing in isolated Purkinje fibers (94).

On the basis of a reduction in activation time between the left and right ventricles during stellate stimulation, Priola and Randall concluded that the cardiac nerves can increase conduction velocity through the bundle branches (151). However, Wallace et al have shown that isoproterenol administration reduced the A.V. nodal delay, but produced little or no change of conduction velocity in the Purkinje system (222,223).

In addition to its strong inotropic action, isoproterenol has been shown to induce large pressure gradients across the aortic valve in patients with muscular subaortic stenosis (18, 235). This action of isoproterenol appears to be linked to its inotropic properties. In addition, other inotropic drugs, such as the digitalis glycosides, can also induce large pressure gradients across the aortic valve (17).

Reductions in the end systolic volume of the ventricle induced by isoproterenol has been thought to be instrumental in the generation of large pressure gradients across the aortic valve (22,69). However, Gorlin et al have demonstrated that isoproterenol can generate a systolic ejection gradient whether end systolic volume increased or decreased (69).

Wigle has implied that isoproterenol has its greatest contractile effect on the deep constrictor muscles of the left ventricle inducing them to contract to such an extent that they reduce the caliber of the outflow orifice beneath the aortic valve (235). This assumption is based on the observation that

after surgical transection of the deep constrictor muscles of the left ventricle, neither digitalis nor isoproterenol caused the reappearance of any evidence of muscular stenosis (236,237).

Morrow and Braunwald characterized functional aortic stenosis as a malformation characterized by resistance to left ventricular outflow without anatomic obstruction (134). Large pressures recorded during ejection were abolished when the left ventricular catheter was placed immediately below the aortic valve.

Functional aortic stenosis is characterized by a notch or slurr on the rising slope of the left ventricular pressure pulse (16,30). Notching of the left ventricular pulse is believed to signal the onset of narrowing of the subvalvular musculature (30). Individuals possessing functional obstruction of left ventricular outflow are sensitive to inotropic interventions, such as ouabain and isoproterenol (235). Krasnow has shown that dogs subjected to the inotropic effects of isoproterenol develop cardiodynamic alterations which are very similar to functional subaortic stenosis in man (99). Isoproterenol infusions resulted in elevations in the rate of intraventricular pressure development. However, the systolic flow rate increased proportionately less than the developed pressure gradient. This was interpreted as a decrease in outflow tract area.

Large pressure gradients have been recorded from the left ventricle to the ascending aorta approximately 30-45 minutes

after the onset of hemorrhagic shock (121). Cinefilms taken of the heart during shock indicate that the apical region of the left ventricle is devoid of contrast material during ejection (121). Criley has postulated that a high pressure pocket develops in the left ventricular apex which may be responsible for the elevated pressure gradients recorded during inotropic interventions (40). When the orifice of the pressure catheter was withdrawn from the apical region of the left ventricle, the characteristic pressure gradients were not recorded during isoproterenol infusion (40).

These data tend to indicate that a high pressure area is developed near the base of the left ventricular outflow tract and the resulting pressure gradients recorded during isoproterenol administration may not be related to a narrowing of ventricular musculature beneath the valve ring (40).

Functional stenosis has also been reported in the right ventricular outflow tract. The infundibular region of the right ventricle hypertrophies in response to elevated outflow resistance resulting from valvular pulmonic stenosis (54). After the valvular stenosis has been corrected, large pressure gradients continue to prevail across the infundibular region until the hypertrophied infundibular musculature returns to normal size. Engle et al have interpreted the pressure gradients after valvotomy to be due to forceful contractions of the hypertrophied infundibular region during right ventricular systole (54).

Campeti et al, utilizing high speed cinematography, have demonstrated in the normal heart that the maximum infundibular systolic diameter equalled the diameter of the pulmonic valve ring (31). In pulmonary valvular stenosis, infundibular diameters were enlarged due to the hypertrophy of the right ventricular musculature in this region.

Johnson has demonstrated that contractile or functional infundibular stenosis is characterized by infundibular and right ventricular sinus pressures which have coincident ascents during systole, but during ventricular relaxation the sinus pressure descent falls across the infundibular pressure pulse. The pressure wave recorded from within the infundibulum did not fall until approximately 0.1 second later (90). In the fixed or valvular form of the stenosis the rise and the fall of pressure waves recorded from the infundibular and sinus regions coincide throughout the cardiac cycle. In addition, Johnson has presented evidence which indicates that infundibular contraction commences about 0.1 second after the start of systolic contraction in the sinus or inflow region of the right ventricle, and becomes maximal at the time of right ventricular protodiastole (90,168).

Brock has reported that the pulmonic valves become incompetent at systolic pressures above 26 mm Hg (23). Epinephrine delayed the onset of pulmonic regurgitation. These results prompted Brock to conclude that the tone of infundibular muscle is important in maintaining the competancy of the pulmonary bed.

On the basis of anatomical evidence, Robb and Robb concluded that the deep sinospiral muscles which encircle the infundibular region of the right ventricle function to maintain the pulmonary circulation (167). Mall, in his early anatomical studies on the heart, showed the existence of a circular band of muscle fibers surrounding the conus of the right ventricle (116). Hypertrophy of these muscle structures may be involved in the production of infundibular stenosis in man (117).

The functional basis of right ventricular outflow appears to be intrinsically related to the anatomical and embryological development of this region. The early studies of Keith have shown that the infundibular region of the right ventricle is derived embryologically from the bulbus cordis (96,97). The bulbus cordis is the muscular structure which surrounds the common aortic stem from which the pulmonary artery and aorta eventually develop. The bulbus cordis becomes obliterated on the left side of the heart while in the course of right ventricular development the bulbus cordis becomes incorporated into the musculature of the infundibular region of the right ventricle. The bulbus cordis remains as loops which encircle the terminal portion of the infundibulum (97). Keith concluded from his studies that "from a structure and historical point of view, we have every reason to suspect that the infundibulum of the right ventricle must play a particular and distinct role in the physiology of the pulmonary circulation" (96).

The turtle heart has been used to study the functional characteristics of the bulbus cordis since this structure is both anatomically and functionally discrete in this species. Woodbury and Robertson have demonstrated in hemorrhaged turtles that the muscular tissue at the orifice of the pulmonary artery became contracted during the last part of systole (241). These workers concluded that this mechanism was useful in diverting blood from the right ventricle through the interventricular foramen into the systemic circuit where it would be of advantage during hemorrhage. March recorded cinefilms of the turtle heart which showed that during early systole the bulbus cordis became distended with blood. Later in systole the bulbus cordis underwent a vigorous contraction which resulted in movement of blood into the pulmonary artery (118). These studies tend to indicate that the bulbus cordis or infundibular region is the last area to become activated at the onset of systole.

Further studies by March, utilizing cinematographic methods on dogs, have revealed mechanisms operating in the right ventricular outflow tract similar to those recorded in turtle hearts (119,120). Right ventricular ejection was observed to occur as the inflow or sinus region contracted and the outflow tract bulged. In late systole the outflow tract contracts and generates a constriction which remained constricted until the onset of inflow filling. Additional studies utilizing strain gauges showed a 20 msec delay in the onset of contraction

between the sinus and infundibular region of the right ventricle (119). Other studies utilizing cinematographic methods have shown that during early systole the cavity of the lower and posterior portions of the right ventricle is reduced in volume primarily because of the spherical shape assumed by the left ventricle in early systole. These initial changes in ventricular geometry apparently cause right ventricular blood to be stored in the infundibular region during isometric contraction (27). On the other hand, Anzola utilizing mercury strain gauges sutured to various areas of the right ventricle, did not show alterations in the contractile sequence between the sinus and infundibular or conus regions of the right ventricle (5).

Puff employed high-speed cinematography to study changes in ventricular configuration during systole (152,153). He reported that the inflow and outflow tracts contract consecutively generating peristaltic waves along the main blood pathway through each ventricle. Priola et al have shown that pressure in the inflow area of the left ventricle exceeds that in the outflow tract in the initial phases of systole, but during ejection outflow exceeds inflow pressure (150). Constriction of the aorta which resulted in an elevation of end diastolic pressure reduced the pressure differentials between the inflow and outflow tracts.

Sympathetic nerve stimulation has been shown to alter the sequence of contraction between the right and left ventricles

Measurements from the beginning of the P-wave to the initial rise in chamber pressure revealed that pressure in the left ventricle began to rise approximately 20 msec prior to that in the right ventricle. This interval was significantly shortened during electrical stimulation of the stellate ganglion (151). Similarly, stellate stimulation has been shown to reduce the time interval between the onset of contraction of muscle segments on the base and apical regions of the left ventricle (141). Thus, stellate stimulation caused the contraction of myocardial segments to become more synchronous (141). As a consequence of this, one would expect to abolish the inflow-outflow pressure gradients in the left ventricle, since it is the sequential contraction of the myocardium which is responsible for this effect.

Tobin et al have shown that the administration of inotropic drugs caused a marked increase in the pressure gradient recorded across the infundibular zone of the right ventricle in dogs (216). In this study isoproterenol induced pressure gradients across the infundibulum in excess of 40 mm Hg. Isoproterenol did not alter the temporal relationships of peak electromyographic potentials recorded directly from sinus and infundibulum of the right ventricle. It was concluded that the pressure gradients recorded across the infundibular zone of the right ventricle were due to forceful contractions of the infundibular region.

There is sufficient evidence to believe that infundibular

contraction during systole results in a reduction of the effective outflow area in this region (27,31,54,90). Consequently, high flow velocities through this region may result in attenuated lateral pressure measured from this area. Meisner and Rushmer have shown that streaming and vortex formation can originate at the aortic valve leaflets and can contribute to the development of turbulence (128). Disturbed flow has been shown to exist in the aorta under normal conditions (57). It is conceivable that streaming effects and disturbed flow through the infundibular region could contribute to the large pressure gradients recorded during inotropic interventions (216).

Left ventricular contraction appears to have an important effect on right ventricular function. Starr and Jeffers observed that after complete cauterization of the right ventricular mass, the central venous pressure was unaffected in acute experiments (210). Bakos has shown that complete cauterization of the right ventricle does not significantly affect right intraventricular pressure nor systolic and diastolic pulmonary pressures (9). Bakos concluded that force generated by the contracting fibers of the left ventricle is transmitted to the "dead" right ventricular musculature through the deep and superficial sino-spiral and bulbo-spiral muscles which are continuous with both ventricles (9). However, it has been shown that after complete cauterization of the right ventricle the response to elevated pulmonary arterial resistance is unchanged, indicating

that the deep layers of right ventricular musculature are unharmed by the cauterization process (93).

Rushmer has shown that right ventricular contraction is accomplished primarily by a shortening of the chamber along its longitudinal axis, the distance between the free wall of the right ventricle and the septum varying only slightly during contraction (179,180). On the other hand, left ventricular contraction during systole takes place through a reduction in circumferential length (75,178).

Rushmer has shown that the initial filling of the ventricles occurs more rapidly than ejection during systole (182). On the basis of pressure volume curves recorded during filling of the isolated right ventricle, Buckley et al have attempted to evaluate the factors contributing to changes in filling impedance (26). These authors have shown that increased venous return was accompanied by a reduction in filling impedance, while increased heart rates were associated with an elevated impedance to filling. Inotropic drugs such as epinephrine and strophanthin-K resulted in decreased impedance to ventricular filling (25).

Sympathetic nerve stimulation has been shown to result in elevated right intraventricular pressure. However, the dynamic changes in the inflow and outflow tracts of the right ventricle during stellate ganglion stimulation have not been described. In addition, the parasympathetic control of right ventricular function has not been investigated.

C. Parasympathetic Control of Ventricular Function.

The effects of efferent vagal stimulation on the heart have been studied by various investigators for over 75 years. Wiggers demonstrated that vagal stimulation had a direct depressant effect on atrial musculature (233). Experiments involving the effects of vagal stimulation on the ventricular myocardium has provided conflicting reports as to whether the vagus has a functional cholinergic innervation to the ventricles.

Bayliss and Starling concluded that efferent vagal stimulation could influence conduction from atria to ventricles, but has an insignificant depressant effect on ventricular myocardium (12). In experiments in which ventricular rate was held constant, Drury could not show depression of right or left ventricular contractile force during efferent vagal stimulation (52). In addition, Drury reported that the length of the ventricular refractory period was unaffected by vagal stimulation. Rothberger and Scherf concluded that the vagus did not have a negative inotropic influence on the ventricles, but had a profound accelerator function (172). Hoffman et al found that vagal stimulation had no effect on ventricular excitability (84). In experiments in which cardiac output and aortic pressure were controlled, Schreiner et al could not show any changes in ventricular function and coronary flow resulting from efferent vagal stimulation (196). However, infusions of acetylcholine resulted in auricular-ventricular block, decreased atrial and ventricular contractility

and reduced coronary flow. Carlsten et al could not show a reduction in aortic pulse pressure during vagal bradycardia in man and on this basis concluded that the vagi had no effect on the ventricles (36). Rushmer concluded that the vagi do not effect ventricular performance; however, his records show that efferent vagal stimulation resulted in decreased left ventricular pressure along with elevated end diastolic pressures (174). Denison and Green reported that efferent vagal stimulation had no effect on left ventricular contraction, and had neither a constrictor nor dilator effect on the coronary vessels (50). Utilizing strain gauges to record myocardial contractile force, Reeves and Hefner could not show left ventricular depression during vagal stimulation (161). According to Sarnoff et al, when left ventricular stroke work is plotted as a function of left ventricular end diastolic pressure, efferent vagal stimulation does not alter this relationship. However, when stroke work is plotted as a function of mean left atrial pressure, vagal stimulation results in depressed stroke work for a given MLAP (189).

In 1888, MacWilliam showed that when a stimulating current was applied to the ventricle during vagal arrest, the resulting contraction was reduced in amplitude (114). On this basis he concluded that the vagi could weaken the ventricular beat. Howell and Duke concluded that vagal stimulation could depress ventricular myocardium (88). Patterson showed that vagal stimulation slowed the rate of rise of intraventricular pressure

and concluded that the vagus has a direct effect on the ventricles (142). Gesell reported vagal depression of the ventricles during ventricular pacing with heart block (66). Straub concluded that the vagi could reduce the force of ventricular contraction (211). Further experiments by MacWilliam demonstrated vagal inhibition in ventricles which were devoid of blood, thus eliminating changes in ventricular filling resulting from vagal bradycardia (115). However, the vagus had little or no effect on the ventricles in the paced heart. Peterson has presented evidence that the vagus may alter ventricular contractility in man (146). He showed that the bradycardia resulting from carotid sinus stimulation did not produce the characteristic large pulse pressure. Wang et al found a decrease in external cardiac work and elevated coronary sinus outflow associated with efferent vagal stimulation (224). Recently DeGeest et al have shown in the isovolumetric paced left ventricle that efferent vagal stimulation resulted in depression of ventricular systolic pressure which was related to the stimulus frequency (46,48). In addition, these workers have shown a parabolic relationship between stimulus frequency and the percent decrease in rate and force during vagal stimulation (48). These results are in complete accord with the parabolic relationships described by Rosenbleuth for the autonomic nervous system (169). Daggett et al have recently shown that efferent vagal stimulation resulted in depressed left ventricular function which was associated with reduced

dP/dt and elevated left ventricular end diastolic pressures (42). Coronary sinus oxygen content increased during vagal stimulation. These investigators have also provided preliminary evidence for reduced contractility in the right ventricle (42).

Levy et al have shown that the vagi can exert a reflex depressant effect on the left ventricle during baroreceptor stimulation (109). DeGeest et al have demonstrated that hypoxia at the carotid chemoreceptor reflexly depressed ventricular contractility through the vagus nerve (45). After vagotomy, chemoreceptor hypoxia resulted in a slight increase in peak left ventricular pressure (45). Gilmore and Sarnoff have shown that during baroreceptor hypotension ventricular function is increased and catecholamine levels in the ventricular musculature became elevated (190). These changes in ventricular contractility appear to be mediated through the sympathetic nervous system by way of the ansa subclavia (47).

Anatomical evidence for vagal innervation of the ventricles is scarce. Woollard found ganglion cells on the posterior atrial wall and concluded that the main innervation of the ventricular musculature is by the sympathetic nervous system (242). On the other hand, Tcheng has shown ganglion cells within the musculature of the right ventricle (215). Truex et al showed that the majority of atrial ganglion cells were structurally immature at birth, and vagal stimulation resulted in negligible cardiac slowing in puppies (217). According to Hirsch,

parasympathetic ganglion cells are present within the ventricular musculature (82). Further studies by Hirsch have disclosed an appreciable decrease in the amount of fibrils in the perimysial plexus in hearts after bilateral cervical vagotomy. Hirsch has interpreted these results to mean that the perimysial plexus receives parasympathetic nerve fibrils (80,81). Napolitano has described postganglionic nerves in the atria and ventricles after total extrinsic denervation (135). If extrinsic cardiac nerves represent parasympathetic elements this gives evidence for vagal innervation of the ventricles. Bielecki and Lewartowski have shown large reductions in the acetylcholine content of the ventricles after hemicholinium administration (15). Since hemicholinium acts to reduce acetylcholine in nerve endings these experiments may provide evidence for cholinergic innervation of the ventricles.

Both Woollard and Saaman have postulated the existence of sympathetic cardiac accelerator fibers in the vagosympathetic trunk (185,241). Nonidez has shown a mixing of sympathetic and parasympathetic fibers in nerve trunks from the caudal cervical ganglion (139).

Jourdan and Nowak have shown in cross-circulation studies in which the head of the recepient animal had all neural connections cut except the vagus, that cephalic ischemia resulted in bradycardia which was reversed to tachycardia after atropine (91). In addition, these investigators were able to induce

cardiac acceleration by stimulating the vagal rootlets from the medulla. Randall and Peiss have recently considered the importance of the medullary outflows to the vagus in reflex cardiovascular adjustments (155). Kabat showed that the accelerator functions of the vagus became active in acute animals, thus confirming the results of Jourdan and Nowak (92). However, Kabat could not induce acceleration by stimulating the vagal rootlets without atropine. Haney has shown that the accelerator function of the vagus may be involved in reflex baroreceptor responses to acetylcholine induced hypotension (74). In completely sympathectomized and adrenalectomized dogs, acetylcholine infusion caused an elevation in heart rate. Haney concluded that this effect was mediated by sympathetic fibers present in the vagus. Recent work by Randall et al have shown that vagal stimulation after atropine can induce ventricular augmentation along with cardioacceleration (156,157). These responses could be blocked by propranolol.

Daly and Hebb have shown the existence of pulmonary constrictor fibers in the vagosympathetic trunk of the dog (44). Recently, Szidon has shown that stellate ganglion stimulation resulted in elevated resistance in the pulmonary vascular bed (213).

Vagal innervation of the myocardium appears to be nonuniformly distributed. Vagal stimulation has been shown to affect the refractory period of atrial muscle differently in different regions (2,136). Similarly, stimulation of the right

stellate ganglion appears to alter the electrograms on the anterior surface of the heart while left stellate stimulation influences electrograms recorded from the posterior regions of the ventricles (243). In addition, Szentivanyi et al have shown that the sympathetic innervation of the ventricles is arranged on a segmental level, analogous to the motor unit arrangement in skeletal muscle (212).

The mechanisms by which vagal stimulation after atropine generates changes in ventricular contractility are still largely unknown. Sympathetic fibers in the vagus having a functional innervation to the myocardium is a possible explanation. On the other hand, there is much evidence in the literature to indicate that acetylcholine alone can induce positive inotropic changes in ventricular muscle.

Hoffman et al described positive chrono- and inotropic affects resulting from acetylcholine infusions. These responses were abolished by ergotamine, curare, and nicotine (83). These investigators isolated a perfusate during acetylcholine infusion which stimulated the frog heart and relaxed the small intestine of the rabbit. Hence, it was concluded that acetylcholine produced its positive inotropic and chronotropic affects by releasing catecholamines. Angelakos and Bloomquist reported that acetylcholine released norepinephrine into the perfusate in isolated heart preparations (4). McDowall found that acetylcholine stimulated the heart after atropine administration and the

response to acetylcholine was not blocked by nicotine, but was blocked by ergotoxine (127). McDowall proposed that acetylcholine exerted its stimulating effect through a direct action on the myocardium. Middleton showed that vagal stimulation could induce acceleration after bilateral superior cervical ganglionectomy (129). He concluded that preganglionic fibers in the vagus synapse on adrenergic ganglion cells in the ventricular myocardium. Burn and Rand have postulated that acetylcholine is released at postganglionic nerve endings and causes the release of norepinephrine (28). Lee and Shideman showed that tetramethylammonium, nicotine, and acetylcholine produce a positive inotropic affect on the isolated papillary muscle after atropine. These responses were blocked by hexamethonium. Since no ganglion cells were found in the papillary muscle, these investigators concluded that acetylcholine did not stimulate the myocardium through ganglion cells (106). Leaders demonstrated that in some instances vagal stimulation provoked positive chronotropic responses after the administration of hemicholinium (105). Hollenberg et al have shown that doses of pronethalol, capable of blocking the effects of tyramine had no effect on acetylcholine induced inotropism (85). The results of Hollenberg et al indicate that acetylcholine does not exert its effect by releasing catecholamines from sympathetic nerve endings in the heart. Buccino et al have shown in the cat papillary muscle that the inotropic effects of acetylcholine were not blocked by

atropine or hexamethonium. These investigators have postulated the existence of an acetylcholine receptor in ventricular muscle which is responsible for the positive inotropic responses (24). Friedman et al have shown that acetylcholine augmented tension development in cat papillary muscle contracting at low frequencies (<42); at high frequencies (>70) this positive effect of acetylcholine was abolished. The author concluded that acetylcholine has a dual effect on the myocardium: 1) an action on the muscarinic receptor that reduces contractility and may be blocked by atropine; and 2) a direct effect on cellular membrane permeability to calcium that stimulates contractility (58).

CHAPTER III

MATERIALS AND METHODS

A. Experimental Preparation.

Experiments were performed on mongrel dogs of either sex, ranging in weight from 9 to 25 Kg. The animals were premedicated with an intramuscular injection of phencyclidine (2 mg/Kg). After the preanesthetic had taken effect, alphachloralose (80 mg/Kg) or nembutal (25-30 mg/Kg) was administered intravenously through the cephalic vein. A tracheotomy was performed and the animal placed on positive pressure respiration with an Electro-Med animal respirator which received room air from a compressor. A bilateral thoracotomy was performed through either the fourth or fifth interspace. An electrocautery was used to divide the thoracic musculature. The right or left internal thoracic artery was cannulated with a 15 cm length of PE 100 polyethylene tubing (I.D. 0.034 in), and was used to monitor systemic arterial pressure. The mediastinal septum was ligated 4 cm above the arch of the aorta, and was stripped away from the pericardium along with the pericardial fat pads. The pericardium was incised and the heart suspended in a pericardial cradle. In those experiments

in which the techniques of right heart bypass were employed, the following procedures was followed.

After the administration of heparin (500 units/Kg), the inferior and superior vena cava were cannulated with tygon tubing (I.D. 3/8 in). This tubing was connected to the arms of a glass Y-tube which in turn was fitted to a 150 cm length of tygon tubing (I.D. 3/8 in). Venous blood was drained through this tubing into a large teflon reservoir. Coronary sinus venous outflow was collected through a 150 cm length of tygon tubing (I.D. 1/4 in), fitted with a metal tip which was tied into the right ventricular sinus region. The reservoir was placed approximately 1 m below the heart. In several experiments systemic venous drainage was accomplished through a single cannula tied into the right atrium and inserted through the tricuspid valve into the right ventricle. A purse string suture was placed in the conus region of the right ventricle, and the pulmonary artery was loosely ligated with a strip of umbilical tape. The reservoir was primed with whole blood from a donor animal which was diluted with an equal volume of 0.9% saline or dextrose and saline. An occlusive roller pump (Sarns model No. 3500) was used to return known volume flows of blood to the animal. The pump was calibrated by timing the collection of water in a 2 liter graduate at various r.p.m. The pump occlusion was adjusted to allow a 24 to 36 in column of water to descend in the tubing at a rate of 1 in per min. Determining the occlusion in this way

insured against extensive pump-induced hemolysis.

An incision was made within the confines of purse string suture in the right ventricular outflow tract, and the input cannula from the roller pump was inserted through the right ventricle and passed into the main pulmonary artery. The purse string suture was then drawn tightly around the cannula. Venous drainage was instituted by removing an occlusive clamp from the venous line. The input cannula was tied securely into the pulmonary artery and the roller pump switched on.

Mean aortic pressure was regulated by means of an occlusive clamp placed around the descending thoracic aorta, approximately 4 cm above the diaphragm. In several experiments both femoral arteries were cannulated with stiff, large bore polyethylene and the cannulas connected to a pressure bottle which was used to regulate mean arterial pressure. The experimental setup is illustrated in Figure 1.

Differential pressure across the aortic valve was measured with a Pace single membrane differential transducer. A special cannula (98) was placed in the outflow tract of the left ventricle. This placement usually positioned the cannula tip between the anterior papillary muscle and the septum. A 10 cm length of PE 60 (I.D. 0.030 in) polyethylene tubing was fixed to the cannula and attached to the positive or high end of the differential transducer by means of a Tuohy-Borst adapter and three-way valve. The ascending thoracic aorta was cleared of its fat

FIGURE 1

DIAGRAM OF EXPERIMENTAL TECHNIQUE

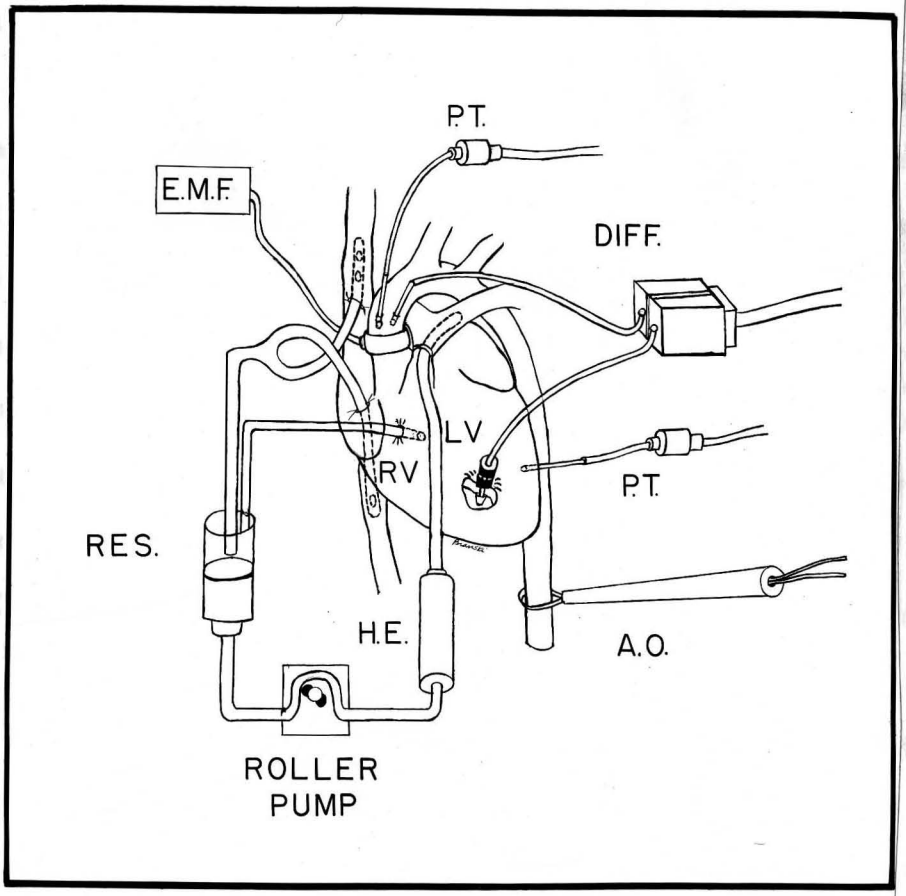

Bypass of the right heart was accomplished by cannulating the inferior and superior vena cava and draining the venous blood into a reservoir (RES). Venous blood was returned to the animal with a roller pump. A heat exchanger (HE) was interposed between the pump and the animal and maintained rectal temperature at 37°C. Pulsatile blood flow in the ascending aorta was measured with an electromagnetic flowmeter (EMF). Differential pressures across the aortic valve were recorded with a Pace single-membrane transducer (DIFF). Pulsatile left ventricular and ascending aortic pressures were recorded with a Statham P23db strain gauge transducer (PT). Mean aortic pressure was regulated with a snare device (AO) placed around the descending thoracic aorta at the level of the diaphragm.

and connective tissue in order to receive an electromagnetic flow probe. The flow probe was positioned around the ascending aorta, approximately 0.5-1.0 cm above the aortic valve ring. A probe size was selected which provided a snug fit around the aorta and limited constriction by only 10 or 15% of the original aortic diameter (198). Another 10 cm length of PE 60 tubing was fitted to a blunt No. 20 needle and inserted through the wall of the ascending aorta, approximately 1 cm rostral to the flow probe. This cannula was adjusted so that its oriface was parallel to the flow stream. The ascending aortic cannula was attached to the low or negative end of the differential pressure system. Pulsatile and left ventricular end diastolic pressure was measured through a No. 19 or No. 18 gauge needle inserted through the lateral ventricular wall and connected to a Statham P23db transducer by a 1 cm length of large bore polyethylene. This transducer was positioned at the level of the tricuspid valve ring through visual approximation. The variation in placement from animal to animal could not have exceeded plus or minus 1 cm. Consequently, variations in LVEDP from animal to animal probably amounted to less than 1 mm Hg. Lateral pulsatile ascending aortic pressure was measured through a No. 20 blunt needle fitted to a 6 cm length of PE 100 polyethylene. This cannula was attached by means of a three-way valve to a Statham P23db transducer.

Pressures and flows were recorded while independently varying cardiac output and aortic pressure. Step changes in

cardiac output were made at 763, 929, 1090, 1222, 1358, 1496, and 1670 ml/min. These increments in cardiac output were carried out at mean aortic pressures of 50, 75, and 100 mm Hg.

The effects of autonomic nerve stimulation on left ventricular ejection dynamics was studied in the intact preparation. After tracheotomy, both the right and left cervical vagi were separated, by blunt dissection, from the common carotid artery and loosely ligated with a strip of umbilical tape. Following bilateral thoracotomy through the fourth interspace and sternal transection, the left stellate ganglion was isolated. A bipolar wire electrode was secured to the common ansa subclavia and caudal pole of the ganglion. The electrode was then sutured to the thoracic wall. An AEL model 104 stimulator was used to electrically excite the stellate ganglion and cervical vagi. Individual pulses were of 5 msec duration 10-30 cps and 2-4 volts intensity. Vagal stimulation was accomplished with bipolar Porter electrodes. The stimulator was connected in parallel with a Tektronix 502 dual beam oscilloscope which was employed to monitor the stimulation parameters.

Differential pressures across the aortic valve in intact preparations were measured with a Statham P23H differential transducer which is essentially a pair of carefully matched P23Db transducers with an electrical bridge between them. An 8 cm length of PE 50 (I.D. 0.023 in) polyethylene cannula was threaded down the left common carotid artery and the tip positioned flush

with the superior curvature of the aortic arch. Catheter placement was verified by direct palpation. The aortic arch cannula was fitted to a plastic tubing adapter and attached by means of a three-way valve to the low end of the differential transducer. A second catheter of identical bore and length was fixed to a special ventricular cannula and was attached to the high end of the transducer (98). This cannula is constructed of teflon having a threaded shaft with a flanged tip. The end of the cannula is secured to the endocardial wall with a knurled nut which turns on the shaft of the cannula and is apposed to the epicardial surface. Hence, the cannula is virtually locked to the myocardial wall. Prior to placement, the ventricular cannula was attached to a 2 cc syringe filled with 2000 units of heparin in saline. After insertion through the ventricular wall the contents of the syringe (heparin-saline) was forced into the ventricular chamber, thus minimizing the possibilities of clot formation at the catheter tip and within the general circulation.

Pressures and flows were recorded during autonomic nerve stimulation and after a single injection of isoproterenol (0.5 μg/Kg). Traces were recorded at the maximum paper speed (250 mm/sec) at the height of the responses resulting from autonomic nerve stimulation or isoproterenol administration. The intensity of vagal stimulation was adjusted so that a steady bradycardia was induced and high-speed recordings were taken during this response.

Right ventricular pressures were recorded with either a

pace differential transducer or a Statham P23H differential transducer. A special cannula was inserted through the free wall of the outflow tract, approximately 0.5 cm below the pulmonic valve ring (98). This placement positioned the cannula in the conus region of the right ventricle. The conus arteriosus forms the terminal portion of the infundibulum of the right ventricle. A second special cannula was placed in the inflow region of the right ventricle approximately 1.5 cm below the tricuspid valve ring. In the majority of experiments right ventricular outflow tract pressure gradients were measured with the Statham differential system. Both right and left stellate ganglia and right and left cervical vagi were isolated. Stimulation pulses were monitored in these experiments with a Hewlett Packard cathode ray oscilloscope. Right ventricular responses to both right and left stellate ganglion stimulation were recorded on a Grass model 5 polygraph. After responses to both right and left stellate ganglion stimulation were recorded, 0.5 mg/Kg of atropine sulfate was administered intravenously. Both vagi were tied and cut and the distal end stimulated through bipolar Porter electrodes. Responses to nerve stimulation were recorded at a paper speed of 100 mm/sec.

The heart was electrically paced in those experiments involving the effects of efferent vagal stimulation on ventricular dynamics. A Grass model S5 stimulator provided pulses to the right atrial appendage and triggered a Grass model 4 stimulator

which delivered stimuli to the inflow tract of the right ventricle. The delay between pulses determined the AS-VS interval and was adjusted between 40 and 50 msec. The cervical vagosympathetic trunk was stimulated using bipolar electrodes and an AEL model 104 square wave generator. Stimulation intensity ranged from 3 to 15 volts. Right and left ventricular pressures were recorded. Catheters were placed either in the inflow or outflow region of the right ventricle. Outflow tract pressure was recorded in the left ventricle. In these experiments intraventricular pulse pressures were highly amplified so that changes in ventricular end diastolic pressure could be observed during excitation of the sectioned cervical vagosympathetic trunk.

B. Pressure and Flow Instrumentation.

With the exception of the series of experiments on right ventricular pressure gradients, all pressure and flow pulses were recorded on an Offner Type R pen recorder. The manufacturer states that this instrument has a frequency response of 250 cps. However, the recorder employed in this study was shown to accurately reproduce a sinusoidal voltage from a sine wave generator up to a frequency of 125 cps. The amplitude of input frequencies above 125 cps showed progressive attenuation at the Dynograph output.

The frequency response characteristics of the catheter manometer systems employed in this study were tested according to the method outlined by Wiggers (230). Response characteristics

of the Statham P23dB strain gauge transducer and the Pace (model No. KP15) variable inductance differential transducer were evaluated. A single membrane differential transducer virtually eliminates any error in the differential output resulting from variations in phase lag, since the output signal is the instantaneous pressure difference across the membrane.

The frequency response of a manometer depends upon the physical characteristics of the pressure sensing membrane. In addition, the volume elasticity coefficient $\frac{\Delta V}{\Delta P}$ -- that is, the increment of fluid (ΔV) which enters the system on applying a pressure increment (ΔP) is an important determinant of frequency response. The lower this ratio, the higher the frequency response. The length and diameter of the catheter tubing and parts which make up the catheter manometer system offer resistance to the volumetric displacement of fluid and thus acts to damp the responses to applied pressures. The Statham P23dB pressure transducer has a volume displacement of 0.04 mm^3/100 mm Hg, and an elastic coefficient $\frac{\Delta P}{\Delta V}$ of 2.5×10^3, a high value. Four resistance wires are attached to the pressure sensing membrane of this transducer, and form a bridge circuit. Deformation of the membrane causes the resistance of two of the wires to change, thus generating a voltage imbalance in the bridge, which is the output signal.

The frequency response characteristics of the Statham P23dB transducer and dynograph system were tested in the following

way. The transducer dome was filled with boiled water and bubble formation was meticulously avoided. A 6 to 8 cm length of PE 50 tubing (I.D. 0.023 in) was fitted to a plastic tubing adapter and attached to the transducer by means of a three-way valve. The tip of the catheter tubing was positioned in another transducer dome fitted with a Touhy-Borst adapter. The transducer and dome were firmly secured to a ring stand. The finger tip of a surgical glove was fastened over the transducer dome and the pressure raised to 75 mm Hg by pumping air into the dome reservoir. The frequency switch on the Dynograph was set for a cutoff of 250 cps. The inflated glove tip over the dome reservoir was ruptured with a red-hot cautery blade. The sudden drop in pressure caused the transducer membrane to vibrate and these oscillations were recorded at a paper speed of 250 mm/sec. Recordings made under these circumstances yielded the natural frequency of this system, and were found consistently to be above 120 cps.

According to Wiggers, the amplitude of frequencies up to 33% of the natural frequency will be recorded faithfully. This means that the Statham transducer, with the length and bore of catheter tested, can accurately record the amplitude of frequency components up to 40 cps. Frequency components in a pressure pulse above 40 cps will not be accurately represented with this system. McDonald has shown that the arterial pressure pulse can be accurately constructed with the sum of the first eight harmonics of the fundamental (123). Hence, in a dog having a

maximum heart rate of 4/sec the arterial pulse wave will be made up of frequencies approaching 32 cps. Frequency components within this range can be accurately recorded with the Statham catheter manometer system employed in this study. During stellate ganglion stimulation the rising phase of the ventricular pulse may be composed of frequencies above 40 cps. Since the system is critically damped the recorded response will be progressively decreased above 40 cps. Consequently, during inotropism the recorded values for intraventricular pressure development may be attenuated.

The frequency response characteristics of the Statham P23H differential transducer and the Pace differential transducer were also tested. The Statham P23H had frequency response characteristics identical to the P23dB units.

Although the manufacturers of the Pace differential transducer state that this unit has a uniform frequency response to 600 cps, the high volume displacement (3×10^{-4} cubic inch/500 mm Hg) makes this figure unreasonable. The displacement of the single membrane of the Pace transducer induces a voltage which impresses amplitude modulation on a 4 Kc carrier wave. The transducer is equipped with a demodulator unit (model CD110) which filters the carrier signal.

Frequency response studies on the Pace transducer were carried out using various lengths and diameters of polyethylene to empirically determine the damping ratio. The damping ratio

was calculated from the logarithmic decrement of the natural vibrations of the catheter manometer system. Recordings were made on a 561 Tektronix oscilloscope or on the Dynograph. The output voltage of the demodulator unit is sufficiently high to provide ample gain when this unit was coupled directly to the power amplifier of the Dynograph.

The damping ratio was calculated utilizing the method described by Fry (59). Figure 2, traces A_1 and A_2 show natural frequency responses with PE 60 and PE 100 catheter tubing. Trace A_2 shows the dimensions of the wave form utilized in the calculation of the damping ratio. The following formula was employed in this calculation:

$$h = \sqrt{\frac{(\ln \frac{X_2}{X_1})^2}{\pi^2 + (\ln \frac{X_2}{X_1})^2}} \qquad (6)$$

where h = the damping ratio.

A damping ratio of 0.80 was calculated for a 10-12 cm length of PE 60. Since optimal damping is believed to occur at a damping ratio of 0.75 the calculated value of 0.80 indicates that the system was slightly over damped.

The frequency of damped natural vibration in cycles/sec was measured from the free vibration of the catheter manometer system. Knowing the damped natural frequency and the damping ratio, the undamped natural frequency was calculated from the

Figure 2

DYNAMIC RESPONSE OF PACE DIFFERENTIAL TRANSDUCER

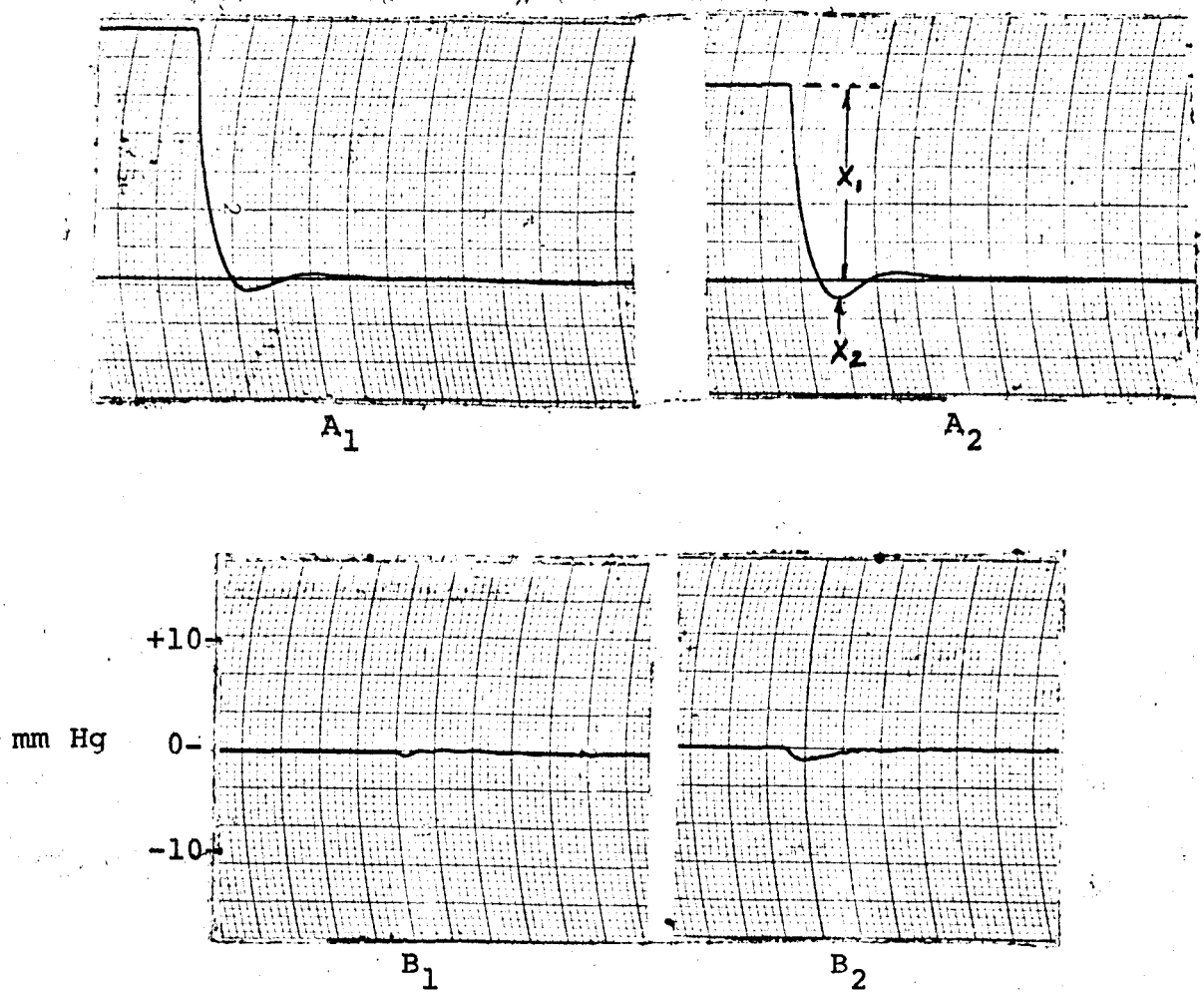

Paper Speed - 250 mm/sec

Traces A_1 and A_2 show free resonance response of Pace differential transducer to step change in pressure. Trace A_1 shows response using 13 cm length of PE 60 (I.D. 0.030) polyethylene tubing. A_2 shows response with 13 cm PE 100 (I.D. 0.034) tubing. X_1 and X_2 in trace A_2 are the dimensions of the free resonance wave used in the calculation of the damping ratio (h). B_1 and B_2 show dynamic imbalance in the differential output induced by instantaneous step change in pressure delivered simultaneously to both chambers of the transducer. Dynamic imbalance was found to be less than 0.9% of full scale pressure calibration. Dynamic imbalance in B_1 is -0.36 mm Hg and -0.72 mm Hg in B_2.

following formula:

$$Wu = \frac{Wd}{\sqrt{1-h^2}} \qquad (7)$$

where, Wu = undamped natural frequency

Wd = damped natural frequency

h = damping ratio

A damping curve was selected on a frequency ratio, amplitude ratio graph which had a damping factor close to 0.80. From this curve it was determined to what frequency the amplitude ratio remained essentially flat. This calculation gave the value in cycles/sec up to which the catheter manometer system will record faithfully. This value was found to be 18.3 cycles/sec, a relatively low value. However, Porjé has shown that only the sum of the first three harmonics are necessary to fully construct the differential pressure pulse in the ascending aorta (149).

Traces B_1 and B_2 in Figure 1 illustrate the results of an experiment designed to test the dynamic imbalance of the Pace differential transducer. Both ports of the differential transducer were connected to a common presssure reservoir and the entire system was flushed with 95% ethanol and filled with water. A sudden drop in the pressure reservoir was instituted by rupturing a rubber diaphragm. Since the instantaneous drop in pressure is transmitted simultaneously to both sides of the transducer, there should be no change in the differential output. However, a small, but real negative imbalance was observed which

averaged 0.6 mm Hg.

The Statham P23H differential transducer was tested with the identical method employed for assessing the dynamic characteristics of the Pace differential transducer. An instantaneous pressure drop at both membranes resulted in the generation of vibrations which were identical in phase and amplitude indicating that the individual transducer membranes were closely matched.

All pressure transducers were statically calibrated at regular intervals with a 136 cm column of water. The calibration was expressed in mm Hg on chart paper. The Pace differential transducer was usually calibrated prior to each experiment.

Left ventricular end diastolic pressures were obtained by taking the pulsatile outputs from the ventricular recordings and directly coupling them to another channel. When recording LVEDP, the pen deflection was electrically limited to prevent interference with recordings on adjacent channels.

Pulsatile flow in the ascending aorta was recorded with a square wave electromagnetic flowmeter (Carolina Medical Electronics Model 420-R). This instrument delivers a 400-cycle square wave to the probe magnet which energies the magnet and generates a magnetic field around the blood vessel. Since blood is a conductor of electricity it will have an induced voltage proportional to the rate at which it cuts through the magnetic field generated by the probe magnet. The manufacturer specifies

that this instrument is capable of faithfully recording pulsatile flow up to 50 cps.

The flowmeter was calibrated utilizing the integration technique described by Spencer (200). The flow probe was placed around an excised blood vessel which was tied between two lengths of tygon (I.D. 3/8 in). One end of the tygon was connected to a 50 cc syringe, and the other to a reservoir containing blood or saline. Blood was withdrawn and returned to the reservoir in 50 cc aliquotes. The resultant flow pulse was recorded on the Dynograph. The calibration was made from the planimetered area under the flow curve according to the formula:

$$\text{total volume injected} \div \text{paper speed (min/mm)} \div \text{area under the flow curve } (mm^2) = \text{cc/min/mm of pen deflection} \quad (8)$$

The effects of changes in pressure gradients across the flow probe was tested in the following way. A strip of dialysis tubing was tied between two lengths of tygon. One end of the tubing was fitted into a constant flow pump which pumped saline from a reservoir through the tubing and back into the reservoir. The flow probe was secured to the dialysis tubing and mean flow recorded on the Dynograph. An adjustable clamp was placed distal to the flow probe and progressive occlusion of the tubing resulted in elevations of pressure at the probe lumen. Changes in pressure from 50 to 150 mm Hg had no effect on the magnitude of the mean flow signal.

C. Data Analysis.

All measurements were taken at a paper speed of 250 or 100 mm/sec, depending upon the recording instrument employed. These measurements were recorded after examination and averaging 3-5 separate cardiac cycles.

The heart rate was obtained by counting the number of cardiac cycles occurring within a period of 20 to 30 sec and converting this value to beats/min.

The excursions of the arterial and ventricular pulse pressures were measured in millimeters of pen deflection and the conversion made to mm Hg on the basis of the prevailing calibration. Ventricular pressures represent the highest value obtained by the ventricular pulse during the cardiac cycle. Arterial diastolic pressure was taken just prior to the upstroke of the anacrotic limb of the arterial pulse wave.

The rate of change of intraventricular pressure (dP/dt) was measured by drawing a line tangent to the fastest changing component on the rising slope of the intraventricular pressure pulse. The distance in millimeters over which the tangent line transected the upper and lower limits of the channel was measured and converted to time in milliseconds. The time factor was then divided into the cross-channel pressure calibration. This calculation gave a value for dP/dt in mm Hg/msec. The dP/dt values were averaged from three separate pulses.

Peak flow (ml/min) in the ascending aorta was obtained

from the flow calibration. Since the blood column in the ascending aorta is essentially stationary during the latter part of diastole, this region of the flow pulse was taken as zero flow reference (63). Velocity flow in the ascending aorta was determined by converting the flow (ml/min) calibration into units of velocity (cm/sec). The following formula was used for this calculation (201):

$$\text{Velocity cm/sec} = \frac{16.6F}{\pi\left[\frac{C/\pi - 2w}{2}\right]^2} \qquad (9)$$

where, F = flow in L/min

C = circumference of the flow probe

w = wall thickness of the ascending aorta

16.6 = conversion factor; converts L/min to cm/sec

Flow acceleration was determined by drawing a line tangent to the point of maximum velocity on the flow pulse. This method was identical to the one employed in the measurements of dP/dt.

Stroke volume was obtained from the area under the flow pulse. A calibration curve was determined by relating the volumetric displacement of known volumes of blood injected through the flow probe to the area under the resulting flow pulse. This relation was linear. The area for three flow pulses were averaged to determine the stroke volume. Flow recordings were made with the pulsatile damping switch set at either the 3 or 10 msec position.

CHAPTER IV

RESULTS

A. Pressure Flow Relations Across the Aortic Valve.

The data presented in the following section were obtained during bypass of the right heart. Table 1 shows changes in left ventricular ejection resulting from sequential alterations in ventricular filling. Measurements were made at four filling levels which represent cardiac output values of 929, 1222, 1496, and 1820 ml/min. The measurements recorded in Table 1 were made while sequentially altering cardiac output at a mean aortic pressure of 50 mm Hg. Tables 2 and 3 show data recorded during sequential elevations in cardiac output at 75 and 100 mm Hg mean aortic pressure respectively. The values under a given cardiac output represent the mean of several experiments. The standard error of the mean (SEM) is given at the right of each figure. The letter N adjacent to the SEM represents the number of experiments from which the mean and SEM values were calculated. Left ventricular filling and cardiac output will be used interchangeably to describe the results in this section, since increments in filling result in concomitant elevations in cardiac output.

Figure 3 illustrates the changes in magnitude of the pressure difference measured from the outflow tract of the left ventricle to the ascending aorta resulting from step increases in ventricular filling. Mean aortic pressure was maintained at 75 mm Hg. Each increment in pump output is associated with an elevation in LVEDP. In addition, there was a concurrent increase in the interval over which LV pressure exceeded aortic pressure. In panel 1, LV pressure exceeded aortic pressure for 41% of the ejection period, and in panel 4, LV pressure remained elevated above aortic pressure for 57% of the total period of ejection. Zero pressure differential occurred 20 msec after the attainment of peak flow in panel 1, and in panel 4, zero pressure differential across the aortic valve occurred 40 msec after peak flow was reached in the ascending aorta. These observations are consonant with the idea that inertial flow dominates during ventricular ejection. The peak flow velocity and the rate of rise (dV/dt) of the velocity pulse increased with ventricular filling. Left ventricular systolic pressure development (dP/dt) increased with increments in filling.

Inspection of Tables 1 through 3 reveals that both systolic and diastolic blood pressures increased slightly with elevations in cardiac output, indicating the presence of small variations in mean aortic pressure resulting from increments in ventricular output. Similarly, peak left ventricular pressure was found to increase with ventricular output. The low SEM values

FIGURE 3

ALTERATIONS IN EJECTION DYNAMICS ACROSS THE AORTIC VALVE INDUCED BY SEQUENTIAL ELEVATIONS IN VENTRICULAR FILLING

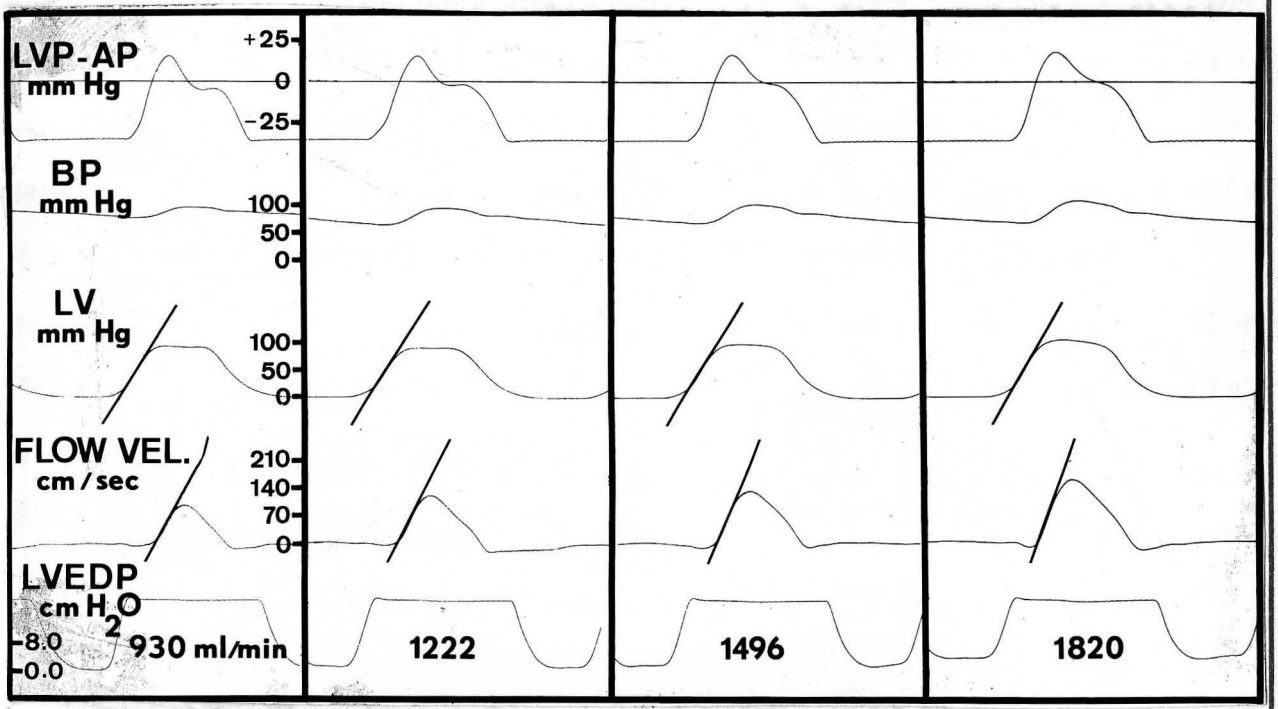

LVEDP increased with ventricular filling and was accompanied by elevations in peak flow velocity. The slope on the velocity pulse which is a measure of flow acceleration increased with ventricular filling. Similarly, the slopes on the left ventricular pressure pulses increased with ventricular filling. In each panel these changes are associated with elevations in the peak pressure gradient along with an increase in the total area under the pulse.

associated with these figures indicate that the increments in peak systolic left ventricular pressure represent important changes resulting from step increases in left ventricular filling.

Heart rate, beats per minute, remained relatively constant, averaging 180 beats/min. In order to standardize cardiac output, the figure for mean flow at the head of each column was divided by the animals' weight in kilograms. Cardiac output varied from 56.6 to 103 ml/min/Kg.

Maximum blood flow in the ascending aorta increased with cardiac output averaging 4491 ml/min at 929 ml/min mean flow and 7578 ml/min at a mean flow of 1820 ml/min. In addition, peak flow velocity (cm/sec) increased with increments in ventricular filling. At the lowest output, peak flow velocity averaged 114 cm/sec and 180 cm/sec at the highest output value. The associated SEM values indicate that these differences are important. Similarly, the maximum acceleration of blood in the ascending aorta increased with ventricular filling, averaging 3451 cm/sec/sec at a mean flow of 929 ml/min and 6299 cm/sec/sec at a mean flow of 1820 ml/min.

Left ventricular end diastolic pressure was increased with each increment in ventricular filling. Although reference is made to cardiac output in conjunction with the above parameters, LVEDP is the basis for observed pressure flow dynamics, since this parameter represents changes in ventricular fiber length. LVEDP ranged from 2.00 to 3.34 mm Hg. Each increment in

LVEDP is associated with a concomitant elevation in stroke volume. Stroke volumes ranged from 5.2 to 11.0 cc. At a cardiac output of 1820 ml/min the stroke volumes at the various aortic pressures were essentially identical. At 100 mm Hg mean pressure, the maximum flow velocity and acceleration in the ascending aorta are reduced below values recorded at 50 mm Hg mean pressure, indicating that the stroke volume is ejected at a slower rate at 100 mm Hg mean aortic pressure.

The rate of change of left ventricular pressure (dP/dt) increased with increments in ventricular filling, ranging from 1.69 to 3.18 mm Hg/sec. Values for dP/dt and LVEDP were generally elevated at 100 mm Hg mean aortic pressure.

Without exception the maximum positive change in pressure across the aortic valve increased concomitantly with elevations in ventricular filling. P values were calculated using the Students *t*-test for unequal group means. In Tables 1 through 3, P values are given adjacent to the mean peak pressure gradient at each level of cardiac output. The level of significance was determined between the value of the peak pressure gradient recorded at 929 ml/min and the pressure gradients recorded at each succeeding level of cardiac output. These calculations indicate that the peak pressure gradient recorded at output levels of 1222, 1496, and 1820 ml/min are all significantly different from the peak pressure gradient at 929 ml/min ($P<0.05$). This degree of significance was obtained at all three levels of aortic pressure

TABLE I

PRESSURE FLOW RELATIONS ACROSS THE AORTIC VALVE
50 mm Hg Mean Aortic Pressure
(range 50-60 mm Hg)

Cardiac Output ml/min	929	SEM	N	1222	SEM	N	1496	SEM	N	1820	SEM	N
Blood Pressure	70	3.7	7	76	4.6	8	85	4.7	8	88	--	3
	46	3.0	7	50	3.6	8	53	5.0	8	49	--	3
Left Ventricular Pressure	79	3.5	8	85	4.9	9	100	5.2	9	121	--	3
Heart Rate	181	9.2	8	179	6.0	9	180	7.0	9	167	11	4
Cardiac Output ml/min/Kg	56.6	2.0	8	73.7	2.5	9	90.3	3.6	9	103	9.2	4
Maximum Flow ml/min	4491	315	8	5628	344	9	6515	402	9	7578	1070	4
Maximum Velocity cm/sec	114	3.8	8	131	5.9	9	150	6.6	9	180	14	4
Maximum Acceleration cm/sec/sec	3451	178	8	4295	365	9	5346	470	9	6299	1090	4
LVEDP	2.0	0.26	8	2.64	0.37	9	3.02	0.36	9	3.34	0.55	4
Stroke Volume cc	5.2	0.26	8	6.8	0.29	9	8.4	0.32	9	11.0	0.69	4
Maximum Positive ΔP mm Hg	18.8	--	8	23.0	P< .005	9	27.4	P< .005	9	29.2	P< .005	4
Duration Pos. ΔP % Ejection	58	2.7	8	65	3.6	9	64	1.8	9	64	3.76	4
Duration Cardiac Cycle (msec)	336	26	8	339	14	9	341	13	9	368	22	4
Forward Flow % Cycle	34	1.1	8	36	1.2	9	37	1.4	9	40	3.9	4
Left Ventricular dP/dt	1.69	0.15	8	1.94	0.15	9	2.27	0.21	9	2.30	0.39	4

TABLE II

PRESSURE FLOW RELATIONS ACROSS THE AORTIC VALVE
75 mm Hg Mean Aortic Pressure
(range 75-85 mm Hg)

Cardiac Output ml/min	929	SEM	N	1222	SEM	N	1496	SEM	N	1820	SEM	N
Blood Pressure	89	1.8	13	94	2.3	13	95	1.7	12	102	5.0	6
	67	2.3	13	68	2.1	13	66	2.7	12	74	4.6	6
Left Ventricular Pressure	98	7.0	15	105	3.7	15	109	4.2	14	114	5.6	7
Heart Rate	174	6.5	15	182	7.2	15	177	6.5	14	173	7.1	7
Cardiac Output ml/min/Kg	52.8	1.7	15	69.6	1.9	15	84.3	2.8	14	99.3	5.1	7
Maximum Flow ml/min	5156	329	12	6241	250	12	7149	410	11	7386	857	4
Maximum Velocity cm/sec	113	5.0	15	136	5.8	15	157	5.9	14	165	5.1	7
Maximum Acceleration cm/sec/sec	4160	427	14	5173	412	14	5797	500	14	5905	676	7
LVEDP	2.46	0.32	15	2.82	0.34	15	3.40	0.27	14	3.98	0.36	7
Stroke Volume cc	5.2	0.2	15	6.8	0.25	15	8.6	0.28	14	10.6	0.53	7
Maximum Positive ΔP mm Hg	20.6	--	15	26.8	$p<.005$	14	29.4	$p<.005$	14	31.6	$p<.005$	7
Duration Pos. ΔP % Ejection	56.1	4	10	63	2.8	10	66	1.6	11	70.0	--	3
Duration Cardiac Cycle (msec)	332	12	10	340	8.4	11	346	11	11	360	--	3
Forward Flow % Cycle	32	1.3	11	34	1.0	10	34	1.2	10	35	--	3
Left Ventricular dP/dt	2.38	0.25	11	2.60	0.30	11	2.58	0.19	11	2.41	0.56	4

TABLE III

PRESSURE FLOW RELATIONS ACROSS THE AORTIC VALVE
100 mm Hg Mean Aortic Pressure

Cardiac Output ml/min	929	SEM	N	1222	SEM	N	1496	SEM	N	1820	SEM	N
Blood Pressure	112	2.6	7	120	3.5	9	122	4.4	8	119	2.7	6
	91	1.9	7	94	3.6	9	90	3.6	8	84	4.0	6
Left Ventricular Pressure	114	4.7	8	122	5.3	9	124	5.0	8	123	6.1	7
Heart Rate	176	6.2	9	174	7.2	9	171	6.0	9	168	8.1	7
Cardiac Output ml/min/Kg	52.6	2.1	9	70.1	2.3	10	84.9	4.4	9	99.3	5.3	7
Maximum Flow ml/min	4709	491	6	5987	682	6	6950	940	6	6386	--	3
Maximum Velocity cm/sec	112	7.4	9	130	8.2	10	153	8.5	8	160	16	5
Maximum Acceleration cm/sec/sec	3327	358	8	4089	436	9	5002	517	9	6108	746	6
LVEDP	3.26	0.52	9	3.53	0.49	10	3.60	0.48	9	3.71	0.75	7
Stroke Volume cc	5.3	0.2	9	7.1	0.27	10	8.8	0.35	9	11.0	0.56	7
Maximum Positive ΔP mm Hg	20.1	--	8	26.0	$P<.05$	9	32.8	$P<.005$	8	38.2	$P<.001$	6
Duration Pos. ΔP % Ejection	61	2.3	5	64	2.16	5	66	1.2	5	71	--	3
Duration Cardiac Cycle (msec)	348	13	5	358	16	5	376	22	5	396	--	3
Forward Flow % Cycle	29	1.6	5	31	1.73	6	31	1.8	5	32	--	3
Left Ventricular dP/dt	2.76	0.37	6	2.99	0.46	7	3.25	0.45	6	3.18	0.51	4

This parameter ranged from 18.8 to 38.2 mm Hg. The duration of positive change in pressure expressed as percent of the ejection period was shown to increase with ventricular filling. This change was observed at each level of mean aortic pressure. Similarly, the period of forward flow, expressed as percent of the cardiac cycle, tended to increase with ventricular filling. However, the associated SEM values suggest that these changes were not important.

Sequential changes in ventricular filling generated identical directional changes at each aortic pressure. However, the magnitude of these changes were influenced by the level of mean aortic pressure. Tables 2 and 3 show data obtained at mean aortic pressures of 75 and 100 mm Hg respectively. The peak pressure gradient recorded at 100 mm Hg is elevated above those recorded at either 50 or 75 mm Hg mean pressure. However, the resultant maximum flow velocity and acceleration are reduced or relatively unchanged from the values obtained at mean pressures of 50 and 75 mm Hg.

The relationships between the peak pressure gradient, cardiac output (expressed per kilogram of body weight), and LVEDP are shown graphically in Figure 4. The peak pressure gradient across the aortic valve increased as a function of LVEDP. This relationship obtained at all three levels of aortic pressure. Points recorded at 100 mm Hg mean pressure appear to be curvilinearly related, and lie below those recorded at 50 and 75 mm Hg,

FIGURE 4

RELATION OF THE PEAK PRESSURE GRADIENT TO LVEDP AND CARDIAC OUTPUT

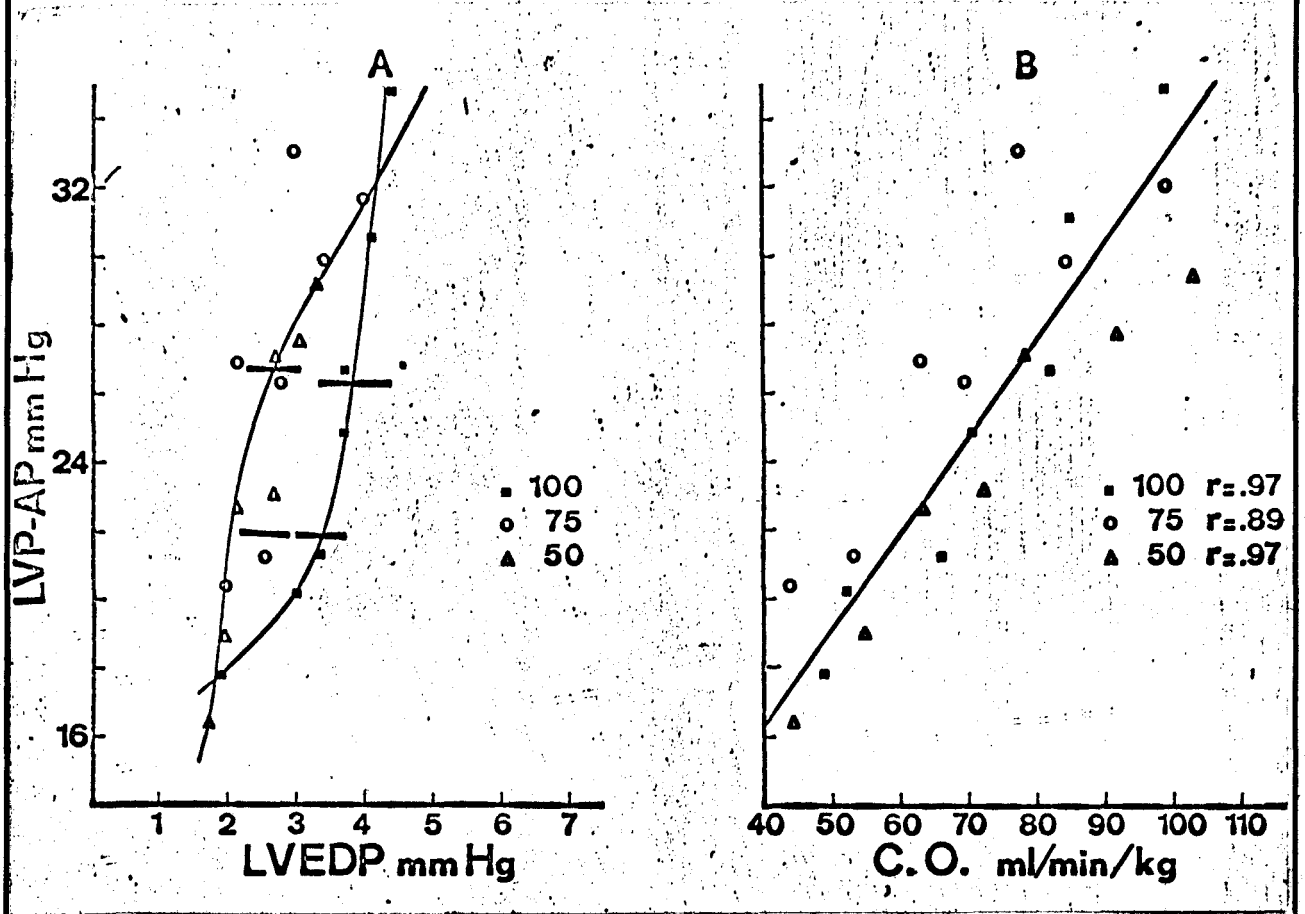

Graphic representation depicting the relationships of the peak pressure gradient across the aortic valve to LVEDP and cardiac output. The pressure gradient increases as a function of LVEDP. The high correlation coefficients (r value) indicate that cardiac output is a linear function of the peak pressure gradient. Horizontal bars on the change in pressure LVEDP graph represent SEM values calculated for LVEDP at those points on the graph.

indicating that for end diastolic pressures between 2 and 4 mm Hg the peak pressure gradient will be less at 100 mm Hg than at either 50 or 75 mm Hg mean pressure. The horizontal bars represent SEM for LVEDP. The points recorded at 50 and 75 mm Hg fall along a similar path; consequently, a single SEM bar was used to represent LVEDP variance for both 50 and 75 mm Hg mean pressure. The SEM bars indicate that the separation between 50 and 75 mm Hg relations is an important change from the peak pressure gradient-LVEDP relation obtained at 100 mm Hg mean pressure. The second graph in Figure 4 depicts the relationship between cardiac output and the peak pressure gradient. The magnitude of the peak pressure gradient appears to be directly related to cardiac output. The calculated correlation coefficients (r value) lend further support to the concept that the peak pressure gradient is a linear function of cardiac output.

Figure 5 shows the graphic relationships which were obtained by plotting maximum flow velocity and maximum acceleration as a function of the peak pressure gradient. The r values at the various aortic pressures indicate that both peak flow velocity and acceleration in the ascending aorta are linear functions of the peak pressure gradient across the aortic valve.

In order to evaluate the influence of mean aortic pressure on pressure-flow relations across the aortic valve, regression equations were formulated from the data illustrated in Figures 4 and 5. These graphs show a regression of Y on X rather

FIGURE 5

RELATION OF THE PEAK PRESSURE GRADIENT TO MAXIMUM FLOW VELOCITY AND ACCELERATION IN THE ASCENDING AORTA

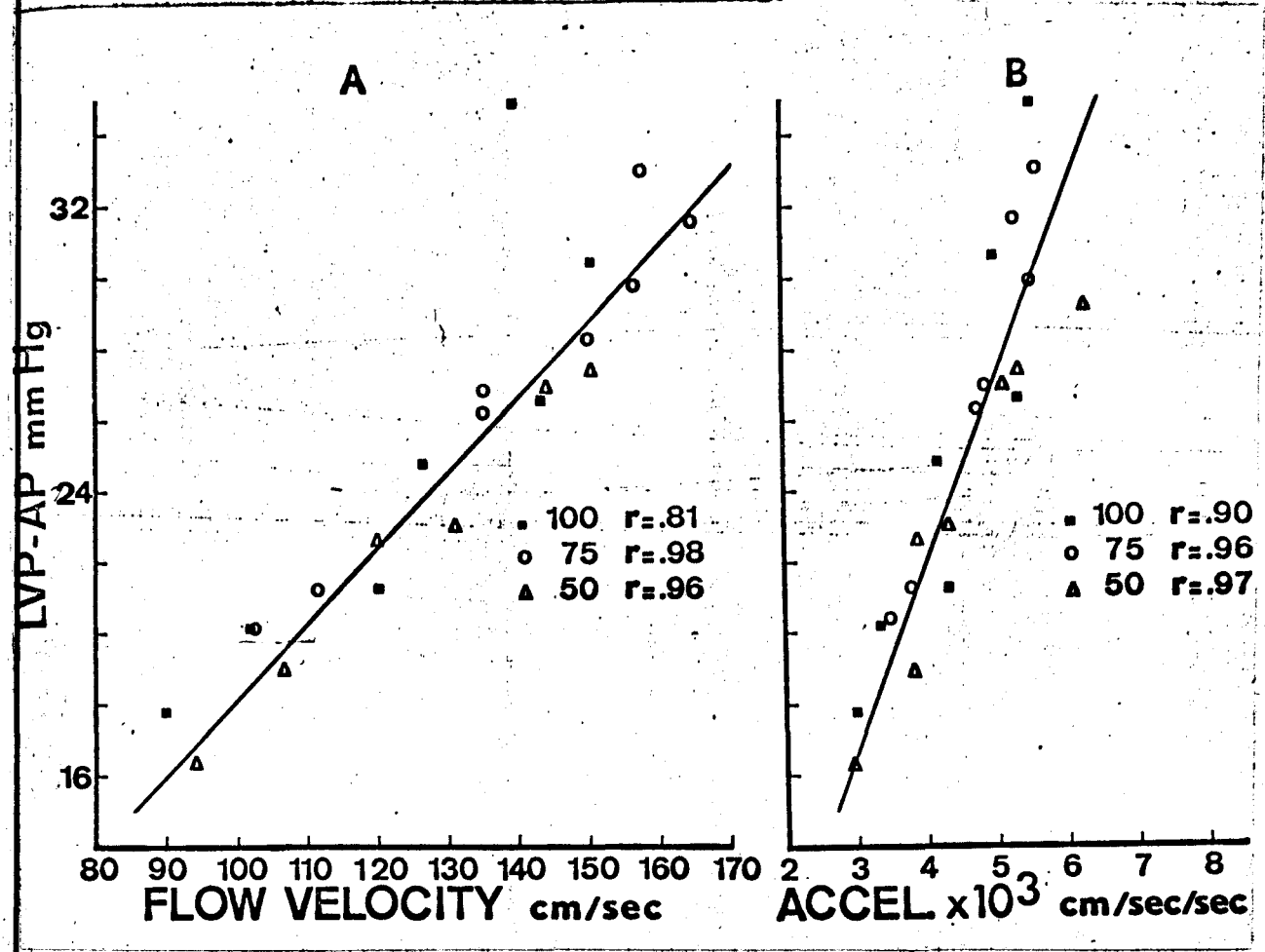

Graphic representation showing the relationships of the peak pressure gradient to flow velocity and acceleration in the ascending aorta. Both flow velocity and acceleration are linear functions of the peak pressure gradient across the aortic valve.

than the conventional X on Y. The results obtained from regression methods are illustrated in Figure 6. The slopes of the lines relating the peak pressure gradient to cardiac output, velocity, and acceleration are reduced with elevations in mean aortic pressure. In each regression equation the value for the slope immediately preceeds the term in parentheses and represents the value increment on the abcissa resulting from a 1 mm Hg increase in the peak pressure gradient. With elevations in mean aortic pressure a unit change in the peak pressure gradient generates less maximum velocity and less maximum acceleration. The SEM values calculated at a cardiac output of 1820 ml/min indicate that the separation of the regression lines for maximum flow and acceleration obtained at 50 and 100 mm Hg mean pressure are important changes. However, the SEM bars on the 75 mm Hg regression lines show considerable overlap with those on the 50 and 100 mm Hg lines.

Similarly, the separation of the regression lines for 50 and 75 mm Hg mean pressure in the cardiac output pressure gradient plot appear to be important on the basis of the SEM bars. A SEM bar is not shown for the 100 mm Hg regression lines, since there is no important separation between it and the 75 mm Hg line.

B. Left Ventricular Responses to Autonomic Nerve Stimulation and Isoproterenol.

Table 4, parts 1 and 2 show the influences of autonomic nerve stimulation and isoproterenol on left ventricular ejection

FIGURE 6

REGRESSION LINES AND EQUATIONS FOR PRESSURE-FLOW RELATIONS

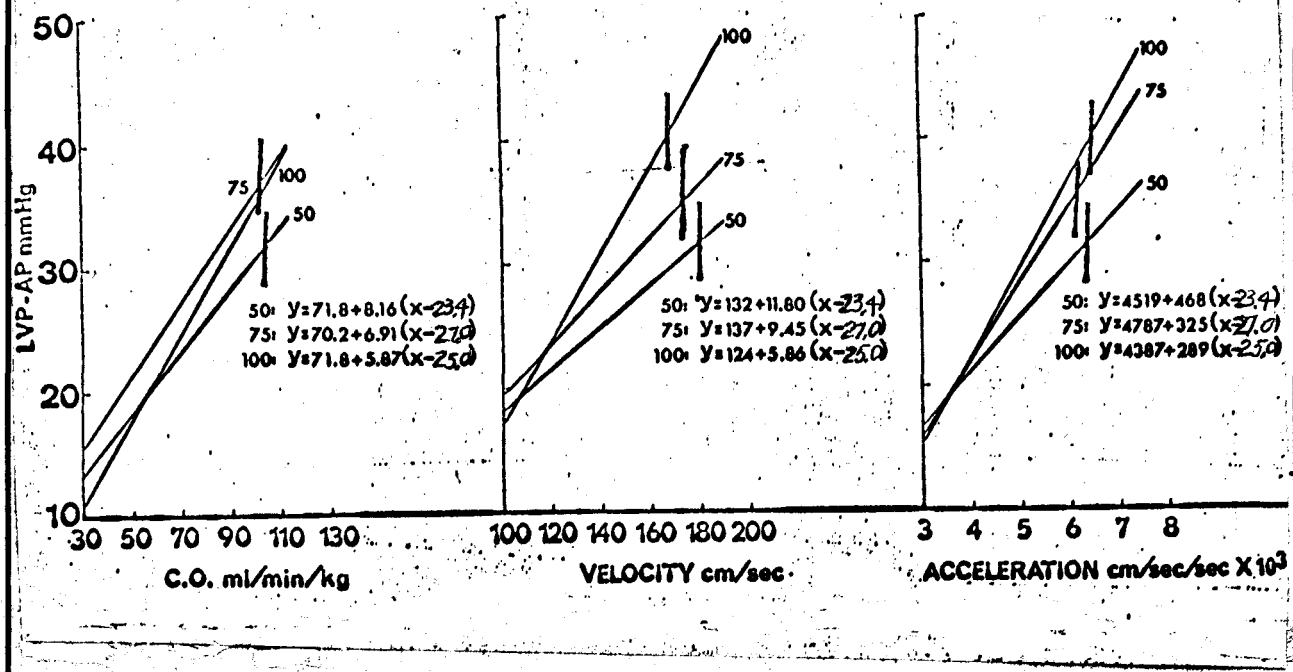

Regression lines calculated from the data illustrated in Figures 4 and 5. The slopes of the regression lines are reduced with elevations in mean aortic pressure. Vertical bars represent SEM values for peak pressure gradient data calculated at a mean cardiac output of 1820 ml/min.

dynamics. The numeral in parentheses associated with each procedure represents the number of animals used to compute mean values. Stimulations were repeated two or three times in each experiment and the mean of the observations calculated. SEM values are given for the mean values recorded in eight different experiments.

During vagal bradycardia the heart rate (H.R.), blood pressure, and left ventricular pressure are reduced. However, all the components of the flow pulse are augmented. Maximum flow showed an average increase of 730 ml/min; the high SEM value associated with this figure questions the importance of this change. Maximum velocity during vagal bradycardia showed an average increase of 15 cm/sec. In addition, ventricular stroke increased 2.7 cc during vagal bradycardia. Maximum acceleration during vagal bradycardia showed a slight increase; however, the large SEM values make this change unimportant.

The rate of change of intraventricular pressure was reduced during vagal bradycardia. This result indicates that the dP/dt during vagal bradycardia does not reflect the magnitude or direction of changes in pulsatile blood flow in the ascending aorta. The average positive ΔP across the aortic valve increased 1.4 mm Hg during vagal bradycardia.

Figure 7 illustrates the dynamic changes in ventricular ejection during a vagal escape beat. Slopes on the left ventricular pressure pulses indicate the rate of change of ventricular

TABLE IV

LEFT VENTRICULAR RESPONSE TO NERVE STIMULATION AND ISOPROTERENOL

Part I

Procedure	Blood Pressure	SEM	LV Pressure	SEM	H.R.	SEM	Cardiac Output ml/min/kg	SEM	Maximum Flow ml/min	SEM	Maximum Velocity cm/sec	SEM
Control (11)	124/94	12.0/9.0	109	10	177	6.6	54.0	8.0	4240	328	95.5	7.8
Vagal Stim. (9)	89/69	10.0/8.5	96	10	86	7.9	42.7	5.9	4970	515	111.0	13.0
L.Stell.Stim. (10)	148/114	15.0/10.0	175	19	192	4.3	72.6	6.2	6960	555	153.0	13.0
Isoproterenol 0.5µg/kg (11)	89/64	8.0/7.4	124	13	206	5.7	73.5	4.6	6190	372	124.0	11.0

Part II

Procedure	Max. Acc. cm/sec^2	SEM	Max. Deacc. cm/sec^2	SEM	Stroke Volume CC	SEM	LV dP/dt mmHg/msec	SEM	Max. Positive ΔP - mmHg	SEM	Max. Positive ΔP-%Ejec.	SEM
Control (11)	3250	327	1540	120	4.8	0.52	2.23	0.17	6.4	0.82	33	4.4
Vagal Stim. (9)	3500	460	1560	460	7.5	0.68	1.74	0.25	7.8	1.1	32	4.8
L.Stell.Stim. (10)	7360	782	3450	556	5.6	0.78	4.90	0.26	30.0	6.4	73	14.0
Isoproterenol 0.5µg/kg (11)	6590	482	3000	401	5.1	0.54	4.03	0.61	45.0	12	96	13.0

pressure. In the control pulses the differential pressure across the aortic valve (DIFF) indicates that LV pressure exceeds aortic pressure for approximately 30% of the ejection period, after which aortic pressure exceeds ventricular pressure. The identical relationships between pressure and flow were recorded during the vagal escape beat. The peak pressure gradient recorded during the control and the escape beat are identical; however, the stroke volume, maximum flow, and maximum acceleration are elevated in the escape pulse. Elevations in the pulsatile flow components during vagal escape are associated with a reduced dP/dt in the LV pressure pulse.

Stellate ganglion stimulation resulted in a general increase of all parameters measured. All components of the flow pulse increased with the greatest changes occurring in maximum acceleration and deceleration. This parameter showed over a two-fold increase during stimulation. As was the case in the control flow pulse, the deceleration was approximately one-half the rate of acceleration. The average stroke was slightly augmented, and the change was not important. Consequently, the elevation in cardiac output resulting from left stellate ganglion stimulation was manifest primarily by the increased heart rate.

The peak pressure gradient across the aortic valve was markedly increased during stellate ganglion stimulation, averaging 30 mm Hg. In addition, the duration of the positive change in pressure expressed as percent of ejection also increased, so

FIGURE 7

ALTERATIONS IN EJECTION DYNAMICS ASSOCIATED WITH VAGAL ESCAPE BEAT

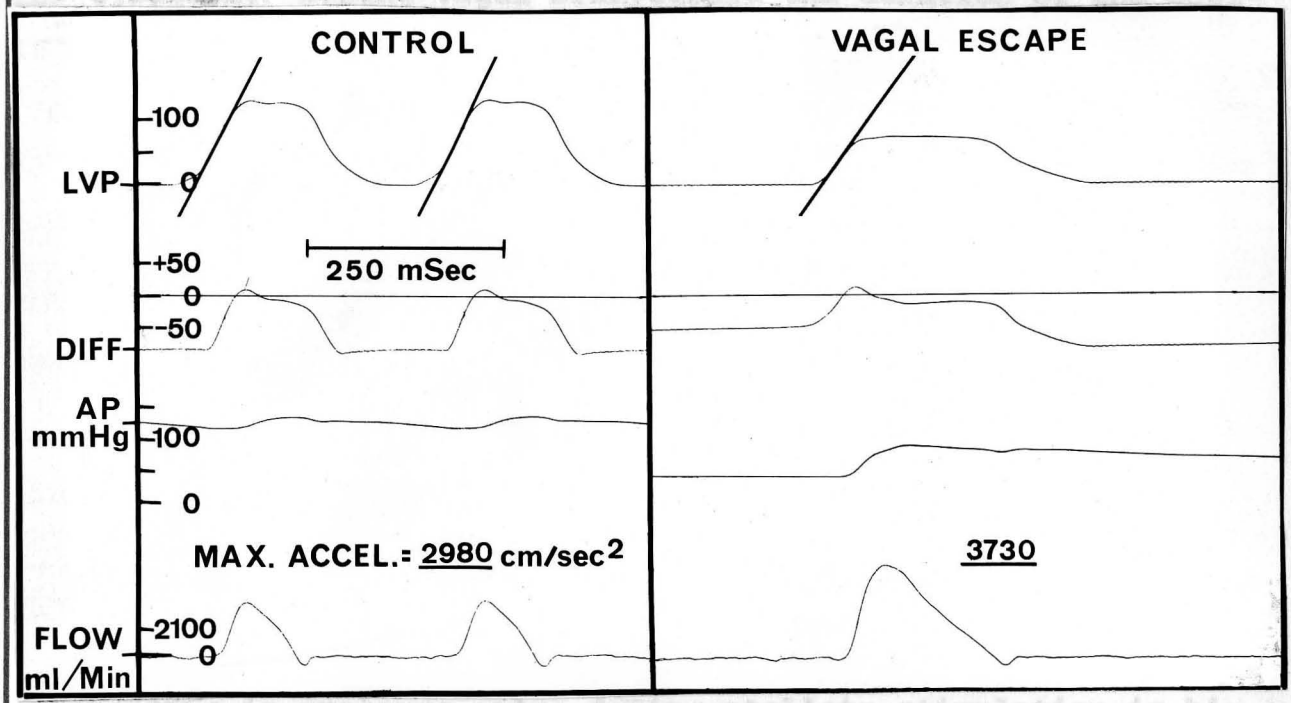

Record showing changes in ventricular ejection dynamics during vagal escape beat. Both aortic pressure and peak LV pressure are reduced. Visual inspection of the slope tangents on the LV pressure pulses reveals a reduction of dP/dt in the vagal escape beat. The peak pressure gradient from heart to aorta is unchanged in the escape beat, and results in an augmented stroke volume and peak flow. Maximum acceleration increased from 2980 cm/sec^2 to 3730 cm/sec^2 in the escape pulse. Records taken from intact animal.

that left ventricular pressure exceeded aortic pressure for 73% of ejection. During vagal bradycardia the duration of the positive ΔP percent ejection was unchanged from control.

Figure 8 illustrates alterations in left ventricular ejection dynamics induced by electrical excitation of the left stellate ganglion. In the control pulse LV pressure exceeded aortic pressure for approximately 30% of the ejection interval. Stimulation resulted in an elevation of the pressure gradient to 30 mm Hg. In addition, during stimulation LV pressure remained elevated above aortic pressure for the entire period of ventricular ejection. Flow acceleration in the ascending aorta was almost doubled with stellate ganglion stimulation. The contour of the change in pressure pulse during stellate stimulation is bimodal. The late systolic rise in the pressure gradient can be correlated with the secondary rise in the LV pressure pulse. This secondary rise in left intraventricular pressure may be due to the development of a high pressure pocket between the anterior papillary muscle and the intraventricular septum (40).

The cardiodynamic responses to a single injection of isoproterenol were directionally similar to those recorded during stimulation of the left stellate ganglion. Stroke volume showed a small increase during the isoproterenol response, and as is the case with stellate ganglion stimulation, the increase in cardiac output is primarily the result of the elevated heart rate.

The average maximum ΔP across the aortic valve during

FIGURE 8

INFLUENCE OF LEFT STELLATE GANGLION STIMULATION ON VENTRICULAR EJECTION

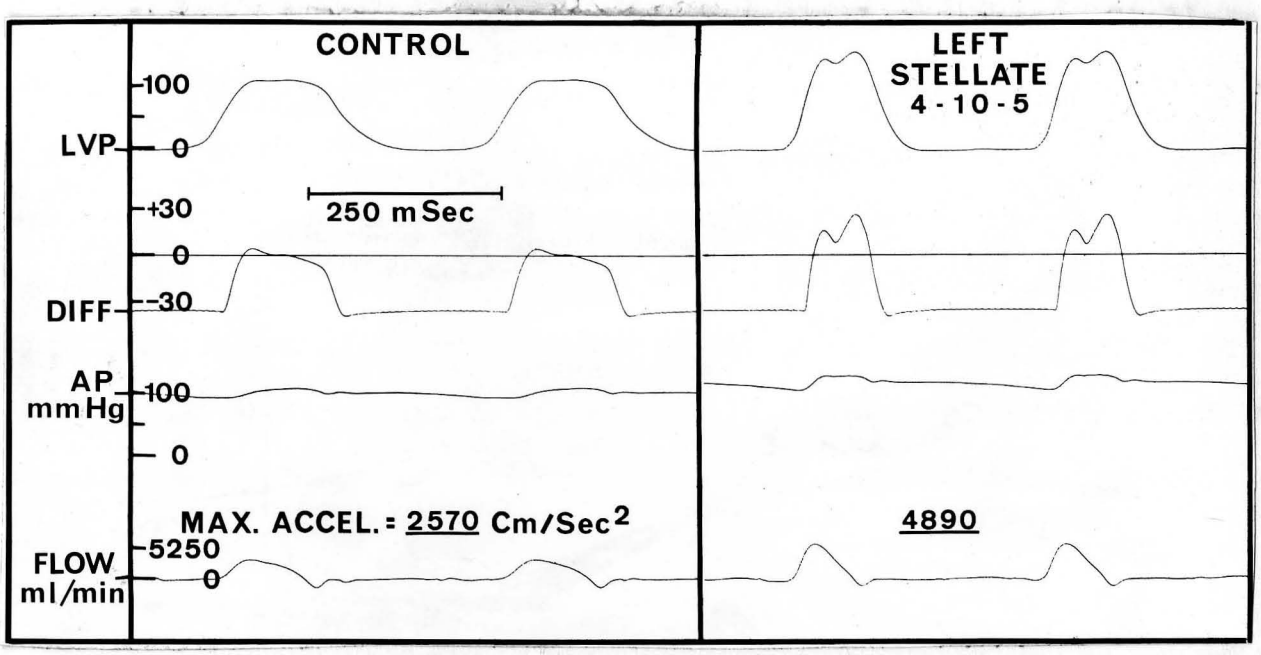

Record showing changes in ventricular ejection dynamics resulting from stimulation of the left stellate ganglion. During stimulation the peak pressure gradient is augmented and left ventricular pressure exceeds aortic pressure for the entire ejection period. Stimulation results in triangulation of the ascending aortic flow pulse with an increase in maximum acceleration from 2570 cm/sec^2 to 4890 cm/sec^2. Notching of the ventricular pressure pulse indicates a secondary rise in intraventricular pressure which begins shortly after the attainment of peak flow in the ascending aorta. Records taken from intact animal.

isoproterenol was 45 mm Hg. In addition, isoproterenol caused the duration of the positive change in pressure to extend for approximately the entire period of ejection.

Both the average systolic and diastolic arterial pressures decreased 30 mm Hg during isoproterenol response. Stellate ganglion stimulation resulted in average increases in peak aortic flow of 2720 ml/min, peak velocity of 57 cm/sec, and maximum acceleration of 4110 cm/sec^2. Isoproterenol, on the other hand, resulted in average increases in peak aortic flow of 1950 ml/min, peak velocity of 28 cm/sec, and maximum acceleration of 3340 cm/sec^2. Left stellate ganglion stimulation and isoproterenol caused identical increases in cardiac output averaging 19.0 ml/Kg/min. The average increase in left ventricular dP/dt was 2.67 mm Hg/msec during stellate ganglion stimulation and 1.80 mm Hg/msec during the isoproterenol response. These data indicate that supramaximal stimulation of the left stellate ganglion induces more profound cardiodynamic changes than 0.5 µg/Kg isoproterenol.

C. Right Ventricular Responses to Autonomic Nerve Stimulation.

Right ventricular responses to autonomic nerve stimulation are presented in Table 5. The results represent the averages of eight separate experiments in eight dogs with associated values for the standard error of the mean (SEM). Stimulation of the right and left cervical vagosympathetic trunk was initiated after the administration of 0.5 mg/Kg atropine. Electrical excitation of the vagosympathetic after atropine resulted in an elevation in

heart rate, with the right vagus having the greater accelerator affect. Both right and left stellate ganglion stimulation resulted in elevated heart rates. Right stellate ganglion stimulation evoked the greatest accelerator response. Right vagosympathetic stimulation increased heart rate to a greater extent than did supramaximal stimulation of the left stellate ganglion.

Pulmonary arterial pressures (PAP) increased with nerve stimulation. The largest increase in systolic pulmonary arterial pressure was elicited during left stellate ganglion stimulation, averaging 12 mm Hg over the control value. Changes in pulmonary pressure associated with right stellate ganglion stimulation are comparable with pulmonary arterial pressures recorded during vagosympathetic stimulation.

The rate of change of right intraventricular sinus pressure was consistently increased with nerve stimulation. Stellate ganglion stimulation elicited the greatest change in sinus dP/dt, showing an average increase of 1.68 mm Hg/msec. Right stellate ganglion stimulation generated a smaller increase in sinus dP/dt which averaged 1.21 mm Hg/msec. Sinus dP/dt values recorded during stellate ganglion stimulation appear to be significantly different from control.

The average rate of right intraventricular pressure rise in the conus region was found to be less than that recorded in the sinus during both control and nerve stimulation. The small SEM values associated with conus dP/dt changes indicate

that dP/dt values in the conus region are markedly altered from control during nerve stimulation. In addition, the difference between conus and sinus dP/dt during nerve stimulation also appear to represent important changes in these experiments.

Peak sinus pressure increased during autonomic nerve stimulation. Left stellate ganglion stimulation showed the largest increase which averaged 29 mm Hg. Right stellate ganglion stimulation generated an average increase in sinus pressure of 22 mm Hg. The large SEM values associated with these figures make their importance questionable. However, in all eight experiments stellate ganglion stimulation resulted in elevations in peak sinus pressure. The magnitude of the elevations were highly variable and this contributed to the large SEM values. Peak sinus pressures were also elevated with vagosympathetic nerve stimulation.

Similarly, autonomic nerve activation induced elevations in peak conus pressure. Inspection of Table 5 reveals that the average increment in peak conus pressure during autonomic nerve stimulation is less than one-half the increment in sinus pressure. The result of this variation in the magnitude of peak systolic pressure is the generation of a pressure gradient across the infundibulum of the right ventricle. In addition, the different rates of pressure development in the sinus and conus regions also contribute to the development of pressure gradients. Stellate ganglion stimulation resulted in 12 mm Hg increase in the peak pressure gradient and vagosympathetic stimulation caused

TABLE V

RIGHT VENTRICULAR RESPONSES TO NERVE STIMULATION

Procedure	Heart Rate beats/ min	SEM	PAP mm Hg	SEM	dP/dt Sinus	SEM	dP/dt Conus	SEM	Peak Sinus Pressure mm Hg	SEM	Peak Conus Pressure mm Hg	SEM	Peak Pressure Differ- ential	SEM
Control	164	6.8	12/ 2.9	1.6 / 0.34	0.51	0.10	0.34	0.07	15.9	2.40	10.2	1.00	9.10	2.30
Right Vagus	190	7.4	14/ 4.3	1.2 / 1.2	1.07	0.27	0.51	0.10	23.7	3.80	10.7	2.10	14.0	4.30
Left Vagus	170	4.6	16/ 5.0	1.5 / 2.6	0.78	0.21	0.44	0.05	27.0	6.90	13.5	1.50	14.0	2.30
Left Stellate	184	6.8	24/ 2.7	7.5 / 0.75	2.19	0.73	1.40	0.39	45.0	8.10	24.0	2.30	21.5	7.70
Right Stellate	204	6.7	17/ 5.0	4.6 / 2.1	1.72	0.52	0.60	0.13	37.6	6.70	17.5	2.20	21.3	4.70

a 6 mm Hg increase.

These results indicate that the sinus and conus regions of the right ventricle are functionally discrete, and can be influenced by adrenergic mechanisms in the autonomic nervous system.

D. Alterations in Ventricular Dynamics Induced by Stimulation of the Vagosympathetic Trunk.

The results in the following section are concerned with experiments designed to evaluate the affect of efferent vagal stimulation on ventricular dynamics. Atropine was not given in this series of experiments. All experiments were performed on electrically paced hearts. Pulsatile pressures were recorded from all four ventricular chambers together with ventricular end diastolic pressures.

Figure 9 illustrates the four cardiac chamber pressure responses elicited by electrical stimulation of the right cervical vagosympathetic. Stimulation resulted in depression of all components of the left atrial pressure complex with complete loss of the a-wave. There was an 8% reduction in systolic left ventricular pressure and no change in right ventricular systolic pressure with concurrent and comparable decline in systemic arterial pressure. Left ventricular dP/dt was reduced from 1.52 mm Hg/msec in the control pulse to 1.49 during vagal stimulation and right ventricular dP/dt was reduced from 0.47 to 0.35 mm Hg/msec. During vagal stimulation, right ventricular end diastolic pressure increased from a control value of 1.30 cm H_2O to 3.00 cm

FIGURE 9

FOUR CHAMBER RESPONSES TO VAGOSYMPATHETIC STIMULATION

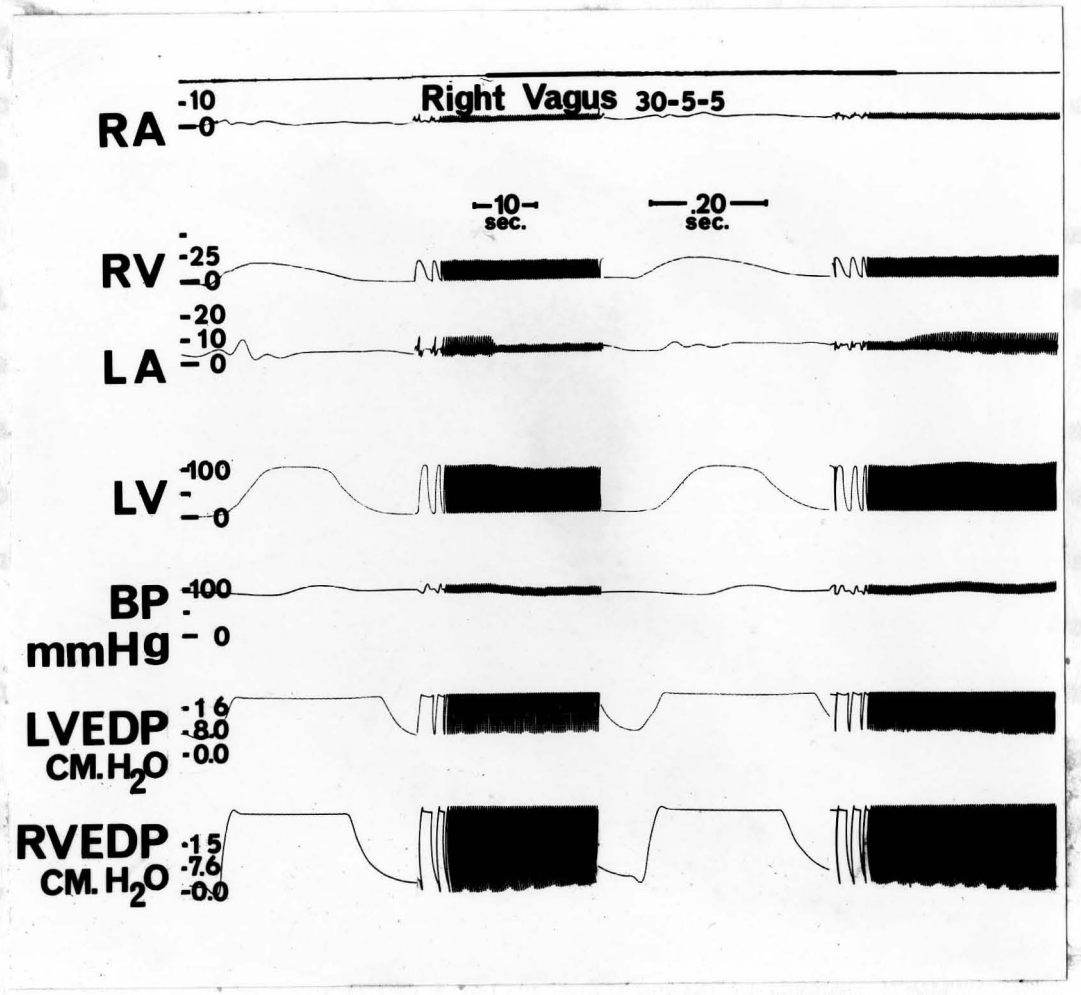

Record showing four cardiac chamber pressure responses during electrical excitation of the right cervical vagosympathetic trunk. The depressed systolic left ventricular pressure (LV) was accompanied by a slight elevation in left ventricular end-diastolic pressure (LVEDP). Peak systolic pressure (RV) was unchanged during stimulation and was accompanied by an elevation in right ventricular end diastolic pressure (RVEDP). RA = right atrium, LA = left atrium, Stimulation parameters were 30 cps, 5 msec, 5 volts.

H_2O and left ventricular end diastolic pressure from a control value of 5.6 cm H_2O to 6.4 cm H_2O. Depressed systolic ventricular pressures or ventricular pressures which show no change in the face of elevated end diastolic pressures are interpreted to indicate depressed ventricular contractility in the context of these experiments.

Figure 10 shows a somewhat different dynamic response resulting from stimulation of the left cervical vagosympathetic. Depression appeared in all components of the left and right atrial pressures. Stimulation resulted in a 12% reduction in systolic left ventricular pressure with no change in right ventricular systolic pressure. Left ventricular dP/dt was elevated from 2.02 mm Hg/msec in the control pulse to 2.50 during vagal stimulation. Systemic arterial pressure decreases from a control value of 120/100 to 105/90. In addition, there was a reduction in LVEDP from 3.68 cm H_2O to 1.60 cm H_2O during stimulation, while RVEDP increased from 0.76 cm H_2O to 3.00 cm H_2O. Both the right and left ventricular pressure pulses showed more rapid decline during diastole. Except for the reduction in left ventricular systolic pressure, the changes in the recorded left ventricular pressure pulse during vagal stimulation are indicative of sympathetic excitation.

On the basis of peak systolic pressure development, inspection of the right ventricular response in Figures 9 and 10 could lead to the conclusion that vagal inhibition of the right

FIGURE 10

FOUR CHAMBER RESPONSES TO VAGOSYMPATHETIC STIMULATION

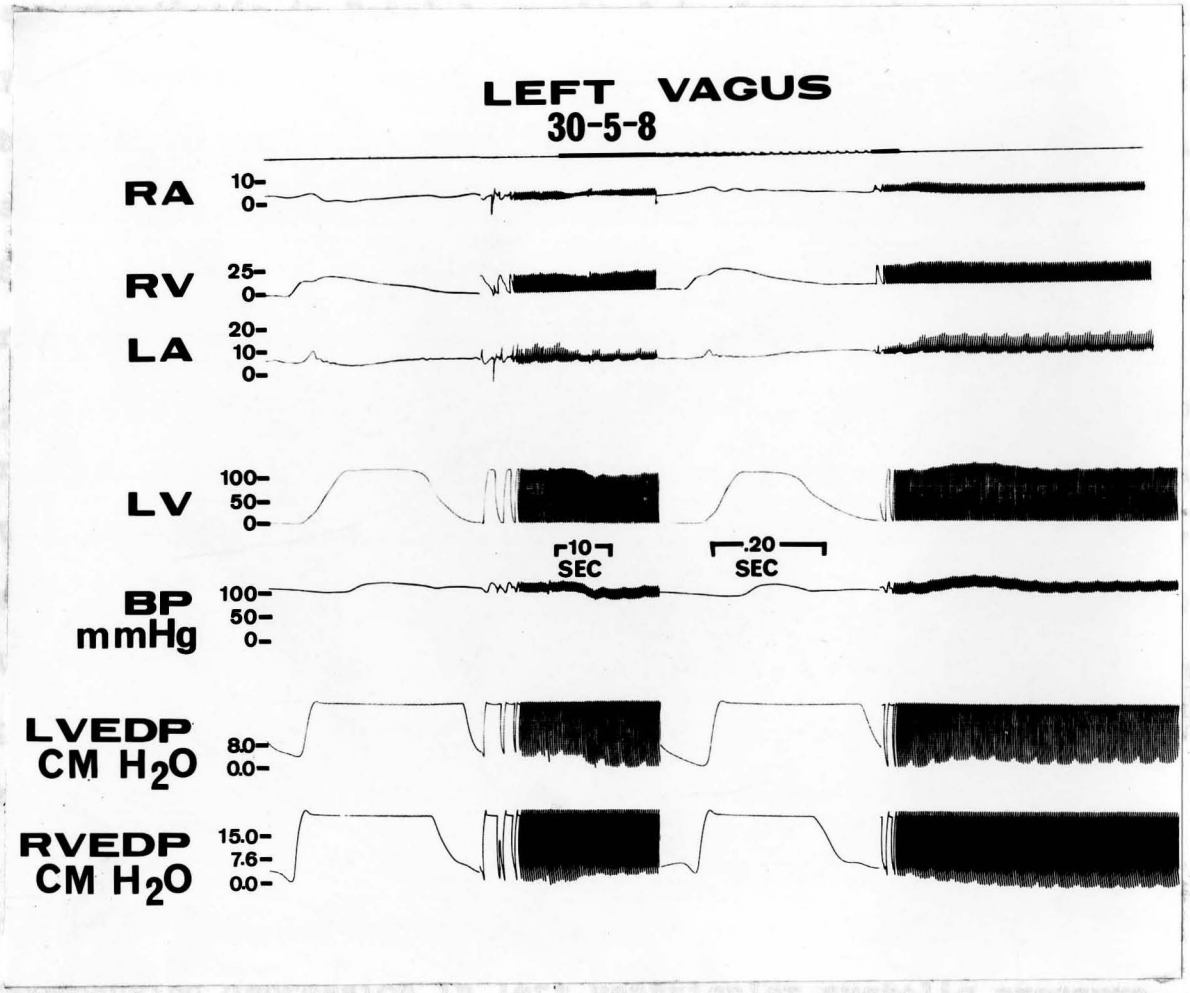

Record showing four chambered cardiac pressure responses resulting from stimulation of left cervical vagus. Unlike responses shown in Figure 9, left ventricular end diastolic pressure decreases along with an elevation in the rate of systolic pressure development. Legends identical to those in Figure 9.

ventricle does not occur. Figure 11 illustrates experiments designed to evaluate the extent of vagal negative inotropic influence on the right ventricle. Stimulation of the right cervical vagosympathetic in Panel A resulted in decreased left ventricular systolic pressure accompanied by a small elevation in LVEDP. At the onset of stimulation, a slight depression in right ventricular pressure was quickly converted to systolic pressure slightly above control. These changes were accompanied by a marked increase in RVEDP from 0.80 cm H_2O during the control to 7.6 cm H_2O during stimulation. Panel B shows the changes in right ventricular systolic pressure which resulted when the elevation in RVEDP recorded during right vagal stimulation was duplicated by partial occlusion of the main pulmonary artery. This increased RV outflow resistance elevated RV systolic pressure from 15.0 mm Hg to 21 mm Hg at a RVEDP identical to that recorded during vagal stimulation.

In 12 experiments an augmented right ventricular systolic pressure was observed during vagal stimulation along with accompanying depression in left ventricular systolic pressure. Figure 12 illustrates these changes. Stimulation of the left cervical vagosympathetics in Panel A resulted in an initial slight depression in right ventricular systolic pressure accompanied by a corresponding increase in RVEDP. Similar changes occurred in the left ventricle. However, the latter did not show an augmentation in systolic pressure. The fast traces in Panel A

FIGURE 11

EFFECTS OF PULMONARY ARTERIAL PRESSURE ON

RIGHT VENTRICULAR SYSTOLIC PRESSURE

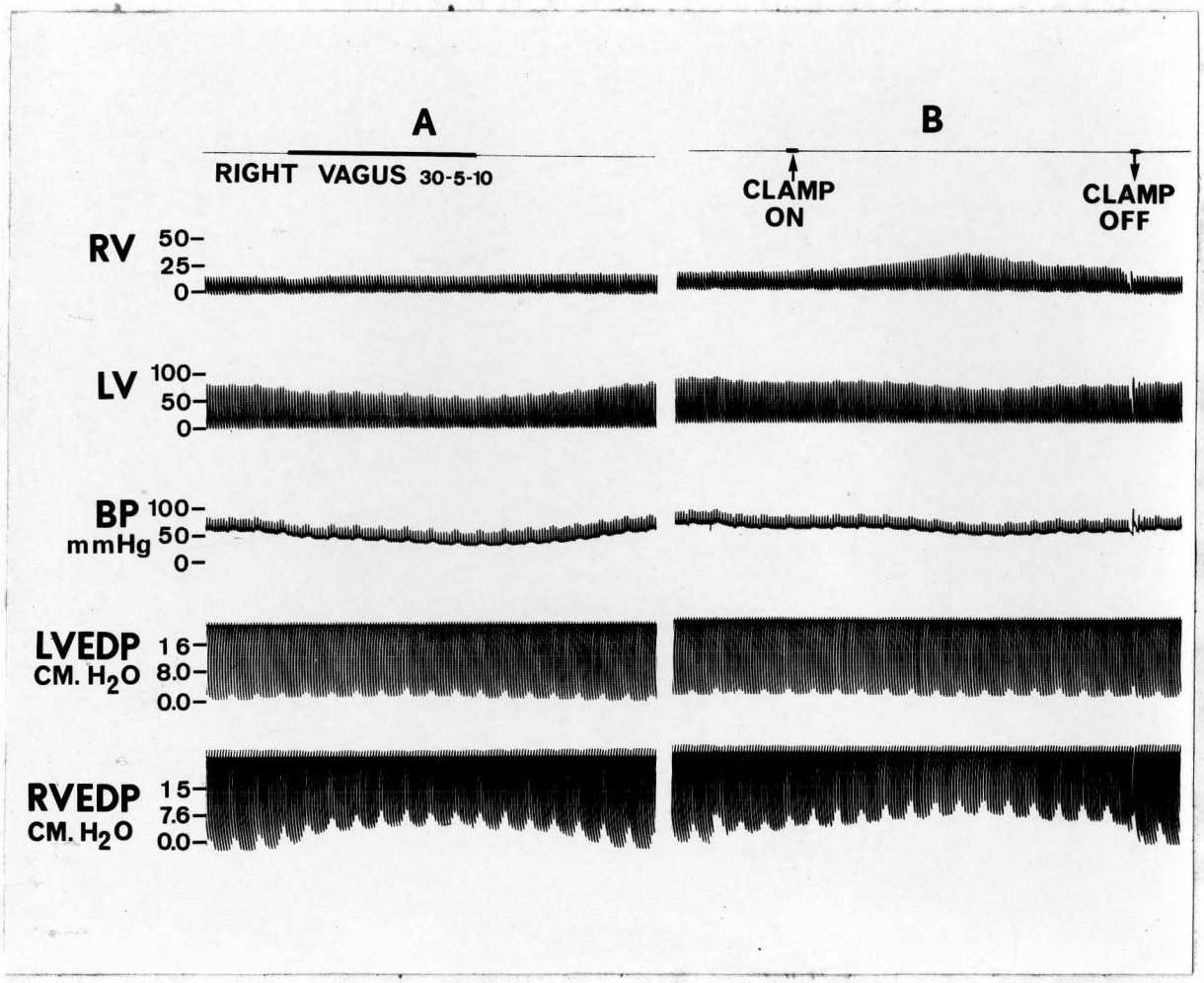

Record showing intraventricular pressure responses resulting from stimulation of the right cervical vagus. Panel A shows pressure responses observed during stimulation. In Panel B, arrow marks point at which a non-traumatic clamp was closed around the origin of the main pulmonary artery, and occlusion adjusted such that the elevation in RVEDP matched the peak value recorded during stimulation. Peak right ventricular systolic pressures recorded during occlusion are elevated above those obtained during stimulation.

FIGURE 12

EFFECTS OF PROPRANOLOL ON VAGOSYMPATHETIC STIMULATION

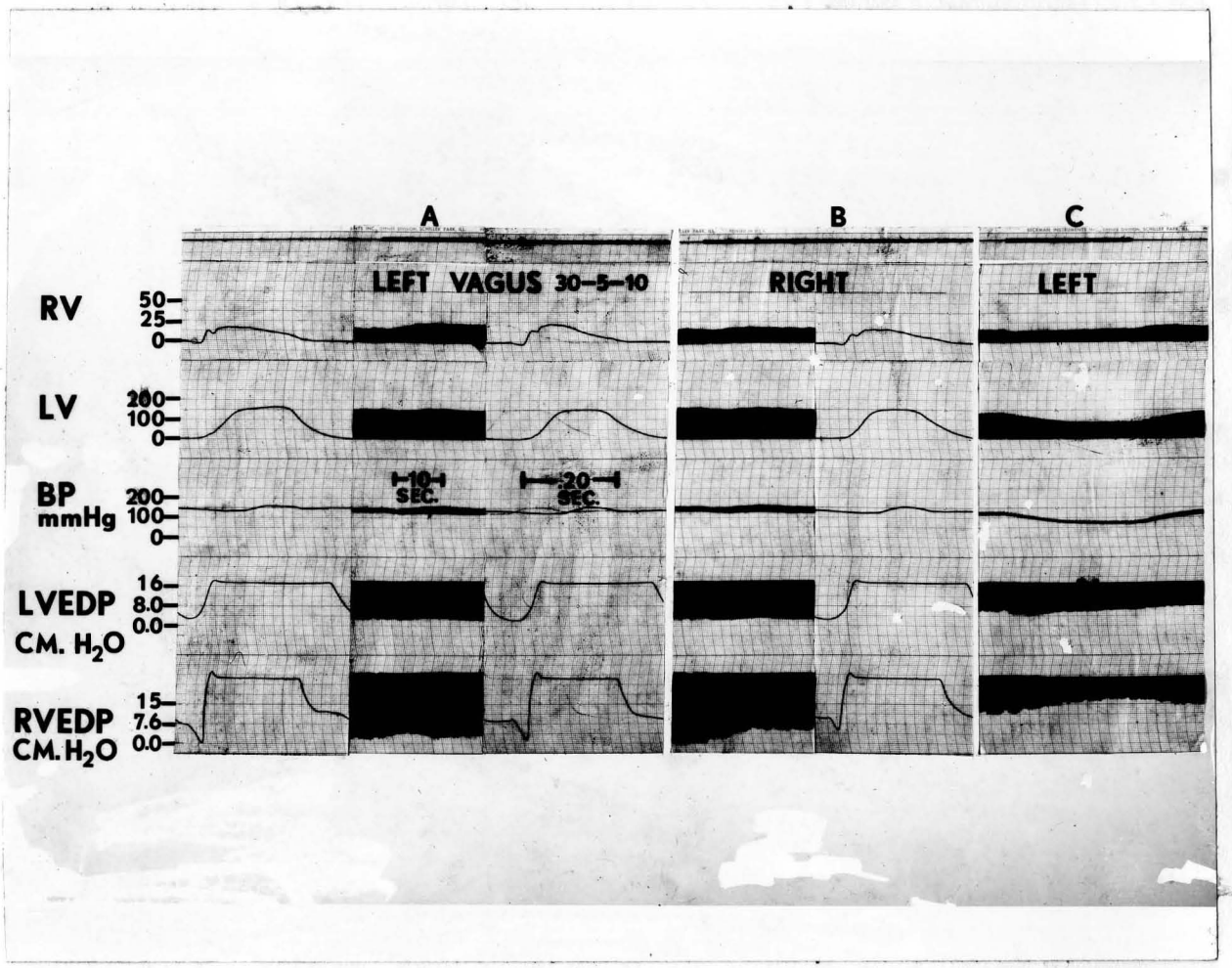

Record showing intraventricular pressure responses resulting from stimulation of right and left cervical vagi. Left vagal stimulation results in greater right ventricular systolic pressure augmentation than that recorded during right vagal stimulation. In addition, right vagal stimulation results in a sustained elevation in RVEDP. In Panel C, left vagal stimulation was repeated after the LV administration of 0.8 mg/Kg propranolol, and results in marked systolic pressure depression in both ventricles.

reveal a more rapid relaxation during early right ventricular diastole and an increased rate of pressure development (dP/dt) in left ventricular pressure, both of which suggest increased sympathetic tone. In addition, vagal stimulation resulted in a slight but definite elevation in pulse pressure in the systemic arterial trace. Panel B illustrates the ventricular responses to right vagal stimulation. The increased right ventricular systolic pressure was accompanied by a marked increase in RVEDP from a control value of 1.52 cm H_2O to 4.56 cm H_2O during right vagal stimulation. The changes in left ventricular dynamics are essentially identical to those recorded during left vagal stimulation. To determine the contribution of adrenergic mechanisms to the observed pressure changes, propranolol was administered intravenously (0.4 mg/Kg), and Panel C illustrates the pressure responses recorded during stimulation of the left cervical vagosympathetic trunk. Stimulation resulted in a distinct decline in both right and left ventricular pressures. RV systolic pressure decreased from 16 mm Hg during the control period to 15 mm Hg at the onset of stimulation. LV systolic pressure decreased from 138 mm Hg to 90 mm Hg. RVEDP increased from 11.4 cm H_2O to 17.5 cm H_2O during stimulation. LVEDP first decreased then increased throughout the period of stimulation.

Table 6 illustrates the magnitudes and directional changes in ventricular dynamics resulting from vagosympathetic stimulation and summarizes the percent changes in all the animals

TABLE VI

AVERAGE PERCENT CHANGE FROM CONTROL DURING

STIMULATION OF RIGHT AND LEFT CERVICAL VAGUS

		Positive Values Average %Δ From Control		Negative Values Average %Δ From Control	
Parameter	Average Control	Left Vagus	Right Vagus	Left Vagus	Right Vagus
BP	110 90	12 (2)* 1 (1)	2.4 (2) - (1)	12 (14) 19 (15)	15 (13) 22 (14)
LVP	108	10.0 (2)	0 (0)	14 (14)	14 (14)
RVP	19.2	36 (12)	30 (11)	8.2 (2)	7.4 (4)
LV dP/dt	1.84	44 (5)	25 (5)	15 (8)	13 (7)
RV dP/dt	0.57	39 (8)	65 (11)	19 (3)	27 (4)
LVEDP	4.81	84 (11)	209 (4)	39 (5)	24 (10)
RVEDP	3.05	76 (13)	113 (14)	7.0 (1)	0 (0)

*Numeral in parentheses represents number of dogs demonstrating that response.

studied. Stimulation resulted in depressed left ventricular pressures in all but 2 of 16 experiments. The average decrease from control was 14% for both right and left vagal stimulations. The rate of left ventricular systolic pressure development (dP/dt) was variable showing increases in 5 of 13 left stimulations and 5 of 12 right stimulations. Average percent increase from control dP/dt values was 44% and 25% for left and right vagosympathetic stimulations respectively. The percent decreases from control were 15% and 14% respectively. The majority of both left and right vagosympathetic stimulations resulted in an increase in right ventricular dP/dt, averages being 39% and 65% respectively. Similarly, right ventricular systolic pressure increased in 12 of 14 left vagal stimulations and in 11 of 15 right vagal stimulations, averaging 36% and 30% respectively. Changes in LVEDP were highly variable, increasing in 11 of 16 left vagal stimulations and decreasing in 10 of 14 right vagal stimulations. On the other hand, RVEDP was found to increase in all but one of 15 left and in all of 15 right vagal stimulations.

CHAPTER V

DISCUSSION

A. Pressure Flow Relations Across the Aortic Valve.

A pressure gradient in the arterial system may be thought of as the sum of three pressure gradients, two acting in the x or axial direction, and a third acting in the y or radial direction. Hence, these pressure gradients are associated with the physical properties and motions of the blood and vascular wall. These components of the pressure gradient are: 1) the pressure gradient along x associated with the acceleration of the blood; 2) the pressure gradient along x related to the frictional resistance to deformation of the blood; and 3) the pressure gradient along y related to the radial distension of the blood vessels (60,147,199).

It is of interest and importance to determine the relative contributions of each of the three components to the observed pressure differential across the aortic valve. The data presented in this study confirm previous reports indicating that the pressure flow relations across the aortic valve during ejection are governed by the inertial flow properties of the blood.

Consequently, the inertial component of the observed pressure difference should represent a large percent of the observed pressure differential across the aortic valve. In order to evaluate this hypothesis, the change in pressure required to accelerate the blood was calculated separately from the following equation (199):

$$\Delta P \text{ inertance} = \frac{\rho l \, dQ/dt}{A} \qquad (10)$$

where, ρ = density of the blood in gm/cm^3

l = distance in centimeters between the aortic and left ventriculat differential pressure catheters

A = cross-sectional area in cm^2 of the ascending aorta

dQ/dt = the maximum rate of flow change in the ascending aorta

ρl is an area density factor, that is, the mass of the column of blood between the pressure tap points expressed per cm^2. The answer to the inertial equation is given in $dynes/cm^2$. In order to convert $dynes/cm^2$ to height in mm Hg, the following relationship is used:

$$h = \frac{P}{\rho \, g} \qquad (11)$$

where, P = inertial change in pressure in $dynes/cm^2$

ρ = density of water in gm/cm^3

g = gravitational constant - 980 cm/sec^2

h = the height of a column of water equivalent to the P in $dynes/cm^2$ calculated from the inertial equation

The value for h in cm H_2O is divided by 1.36 to convert to mm Hg.

TABLE VII

COMPARISON OF CALCULATED AND OBSERVED PRESSURE DIFFERENTIALS

	100 mm Hg Mean Pressure			
Cardiac Output	929	1222	1496	1820
Calculated ΔP*	12.9	16.0	19.7	23.8
Observed ΔP	20.1	26.0	32.8	38.2
Calculated ΔP - % Observed ΔP	64	61	60	62

	75 mm Hg Mean Pressure			
Cardiac Output	929	1222	1496	1820
Calculated ΔP	16.2	20.3	22.6	23.0
Observed ΔP	20.6	26.8	29.4	31.6
Calculated ΔP - % Observed ΔP	78	75	77	72

	50 mm Hg Mean Pressure			
Cardiac Output	929	1222	1496	1820
Calculated ΔP	13.4	16.8	20.9	24.3
Observed ΔP	18.8	23.0	27.4	29.2
Calculated ΔP - % Observed ΔP	71	72	76	83

*ΔP = pressure differential

It should be mentioned that the length over which the inertance is measured corresponds to the distance between the differential catheter tips in the aorta and left ventricle; however, the heart must overcome the inertance of the entire arterial blood mass. In addition, the calculation requires the assumption that a uniform cylinder of blood is accelerated from the ventricle into the ascending aorta, and consequently, neglects variations in cross-sectional area of the ventricular outflow tract, as well as radial distension of the ascending aorta.

The inertial pressure gradient was calculated from the acceleration data in Tables 1, 2, and 3. The cross-sectional area of the aorta was calculated from the dimensions of the flow probe, and amounted to 1.22 cm^2. The average distance between the pressure catheters was 8.5 cm. Table 7 shows the calculated and observed change in pressure values together with the calculated change in pressure expressed as percent of the observed pressure difference across the aortic valve. At 50 and 75 mm Hg mean aortic pressure, the calculated inertial change in pressure amounted to 75% of the observed peak pressure differential across the aortic valve. This indicates that the remaining 25% of the observed change in pressure is directed toward overcoming elastic and frictional opposition to flow. In addition, the value of 75% indicates that the majority of the pressure gradient is directed toward accelerating the stroke volume in the initial phases of ventricular systole. At a mean aortic pressure of 100 mm Hg, the

calculated inertial change in pressure amounted to 62% of the observed change in pressure, indicating that a greater percentage of the change in pressure pulse is directed toward overcoming resistive and elastic opposition to blood motion. Petersen has shown that the change in pressure due to vascular distensibility becomes elevated with increased vessel distensibility. Bergel has demonstrated that vessel distensibility decreases with increases in aortic pressure, from 50 to 150 mm Hg. Consequently, the radially directed change in pressure component should be attenuated at 100 mm Hg mean pressure. These considerations indicate that at 100 mm Hg mean aortic pressure, a large portion of the remaining 38% of the observed pressure difference is directed toward overcoming frictional forces in the blood.

The experiments of Frank and Starling have provided the foundation for most studies concerned with cardiac muscle mechanics (55,209). The length active tension relationship is a useful index for judging contractile changes in the myocardium. The classic studies of A.V. Hill demonstrated that the velocity of muscle shortening is inversely related to the load on the muscle (79). Hill's experiments provided the basis for a more precise understanding of muscle mechanics. Abbott and Mommaerts have shown that the force velocity relationships shown by Hill in skeletal muscle are also integral to cardiac muscle mechanics. Recently, Fry and a series of other investigators, have shown that the maximum velocity of fiber shortening and myocardial wall

tension are inversely related in the intact heart (39,61,108, 171). The relationships of fiber length and afterload to the maximum velocity of fiber shortening, demonstrated by Sonnenblick in the isolated papillary muscle, are applicable to the intact pumping ventricle (203). The relationship between myocardial wall tension and the maximum velocity of fiber shortening, in the intact heart, is an extremely sensitive index of the contractile state of the myocardium. In the intact heart an increase in contractility is said to have occurred when at any given wall tension the contractile element velocity is increased (39).

The ventricular function curves formulated by Sarnoff represent still another method for assessing the contractile state of the myocardium (186). Function curves are derived from the relationship between cardiac work and LVEDP. Therefore, ventricular function curves are an indication of the heart's capacity to do work on the blood. If the ventricle produces more work without a concomitant increase in presystolic fiber length or LVEDP, an increase in contractility is said to have occurred. Covell et al have shown that alterations in force velocity relations could be induced with doses of norepinephrine which produced no changes in the ventricular function curve (39). Consequently, force velocity relations are a more sensitive index for assessing cardiac contractility than are ventricular function curves.

In the last analysis, all assessments of ventricular

contractility must be directed toward judging the heart's ability to move blood. The ventricular function curve is an index of the heart's ability to move blood. However, the exact relations between blood flow from the heart and the force generating the flow are not given by the ventricular function curve. Similarly, force-velocity relations give no information as to the magnitude of the force differential from heart to aorta responsible for the generation of the stroke volume. Both force-velocity relations and the ventricular function curve are primarily indices of the contractile state of the heart muscle, and if these indices are adequate, then the stroke volume and cardiac output are assumed also to be adequate.

The rate of intraventricular pressure development (dP/dt) has also been used as a measure of cardiac performance (68, 162). Force-velocity relations and dP/dt follow each other closely during alterations in the contractile state of the myocardium (171).

There is no denying that dP/dt, ventricular function curves, and force-velocity relations quantitate to some degree the contractile state of the intact heart. Yet, if we are to consider the heart as a pump, we must consider its ability to generate forces responsible for blood flow. It follows then that forces developed in the contracting myocardial fibers must ultimately be transformed into a pressure from heart to ascending aorta or pulmonary artery. This pressure must be composed of a

pressure gradient from the ventricles to a point immediately proximal to the aortic and pulmonic semi-lunar valves. The systolic pressure gradient from heart to aorta has not heretofore been investigated to evaluate ventricular performance.

Tables 1 through 3 and the first graph in Figure 4 show that the peak pressure gradient across the aortic valve increases as a function of left ventricular end diastolic pressure. These data indicate that the energy potential resulting from increases in ventricular fiber length is transformed into an energy gradient from left ventricle to ascending aorta. In the isolated papillary muscle, an increase in fiber length leads to a greater isometric force development (1,203). In the intact heart, elevations in LVEDP shifts the force-velocity relation so that greater myocardial wall tension is developed for a given fiber shortening velocity. However, as in the isolated papillary muscle, increases in preload (LVEDP in intact heart) do not alter the maximum velocity of myocardial muscle fiber shortening (203). Hence, the increased force generated by the contractile elements in the myocardium resulting from elevated preload is transformed into ventricular pressure, establishing a change in the pressure gradient across the aortic valve. In the experiments presented in Tables 1 through 3, increases in LVEDP were produced by elevations in ventricular filling, and were accompanied by increases in stroke volume. It follows therefore, that in order for the heart to eject a larger stroke-volume it must generate more force. This

force is the pressure gradient across the aortic valve during systole. It can be concluded that the relationship between LVEDP and the peak pressure gradient represents an intrinsic mechanism by which the forces generated by the heart on the circulation are adjusted through the fiber length mechanism so that the heart can pump the blood that is presented to it. The afterload was not altered with step changes in cardiac output, since the level of mean aortic pressure was controlled in these experiments.

Figure 4 shows that the relationship between LVEDP and the peak pressure gradient is altered at 100 mm Hg mean pressure. The shift is probably in large part the result of the elevated aortic pressure, to which the heart has adapted heterometrically. Inspection of the results in Table 3 indicates that the magnitudes of the peak pressure gradients measured at 100 mm Hg are elevated above those recorded at either 50 or 75 mm Hg mean pressure at identical output. The elevated peak pressure gradients recorded at 100 mm Hg may be the result of the increased end diastolic pressures.

The ability of the heart to respond to changes in aortic pressure has been known for some time. Sarnoff et al have shown that acute elevations in aortic pressure resulted in an immediate increase in LVEDP, which gradually returned to control levels as the elevation in aortic pressure was maintained. Sarnoff has called this phenomena homeometric autoregulation (195).

In the experiments carried out at 100 mm Hg aortic pressure LVEDP did not return to the levels recorded at either 50 or 75 mm Hg, indicating that homeometric adaptive changes to aortic pressure were not extensive. For this reason it is difficult to evaluate the relative contributions of homeometric and heterometric mechanisms in the ventricular responses recorded at 100 mm Hg mean pressure.

The curvilinear shape of the LVEDP-peak pressure gradient relation at 100 mm Hg resembles static pressure-volume curves recorded for arteries and veins (123). The change in the peak pressure gradient per change in LVEDP is greatly magnified at 100 mm Hg mean pressure, indicating that the elastic limits of the system are exceeded early and the rapidly rising linear portion of the curve represents increased rigidity. The elastic limits of the aorta are not reached at 100 mm Hg; however, Bergel has shown that the elastic modulus of the aorta increases with mean aortic pressure from 20 to 200 mm Hg (13). On the other hand, Peterson has stated that power transfer from heart to aorta is optimal at 90 mm Hg mean pressure, and falls off on either side of this value (147). In addition, Peterson has shown an acceleration transient in the upstroke of the ascending aortic pressure pulse. This initial rapid rise in aortic pressure was attributed to the reluctance of the viscoelastic elements to stretch with the rapid entry of the stroke volume into the ascending aorta. At 100 mm Hg the acceleration

transient may be amplified because of the reduced distensibility at this pressure. Furthermore, Peterson has demonstrated that the pressure required to overcome elasticity increased with vessel compliance (147).

The graphs in Figures 4 and 5 show the relationships of cardiac output, maximum flow velocity, and maximum acceleration to the peak pressure gradient across the aortic valve. Cardiac output increased linearly with the peak pressure gradient. The calculations of Womersley on the relations of pulsatile pressure to flow in the arterial system are based upon the assumption that pressure and flow are linearly related (240). The results in graph 2 of Figure 4 indicate that flow is a linear function of the pressure gradient across the aortic valve. Hence, there is a direct relation between the level of force generated across the aortic valve and the volumetric movement of blood from the heart per unit time.

Similarly, the graphs in Figure 5 show that both peak flow velocity and flow acceleration in the ascending aorta are directly related to the peak pressure gradient. Blood flow in large arterial conduits and across the aortic and pulmonary semi-lunar valves is governed primarily by inertial properties of the blood, that is, the peak pressure gradient is related to flow through acceleration and the mass of blood in the aorta determines the rate of change of volumetric flow resulting from a given pressure gradient (60,63,123,125,140,198,199,201). In

general, the system can be described from Newton's second law of motion:

$$F = ma \qquad (12)$$

where, F = force

m = mass

a = acceleration

Flow in the ascending and descending thoracic aorta does not show the characteristic velocity profile observed in smaller vessels (123). The flow profile is flat indicating little or no velocity gradient among fluid lamina. Consequently, there are slight energy losses through friction. From these considerations it can be stated that most of the pressure energy generated by the heart is directed to overcoming the inertance of the blood mass in the aorta as well as the elastic forces in the blood vessel walls. Spencer and Denison have shown that the blood column in the descending thoracic aorta behaves as a single bar of fluid, the upper and lower ends of which oscillate in phase (202). During ejection then, the pressure gradient across the aortic valve is the ventricular force required to eject a given stroke volume against the elastic and inertial counterforces present in the aorta (145,147).

The temporal relations, during the cardiac cycle, between the peak pressure gradient and the flow pulse in the ascending aorta lends further support to the inertial concept of ventricular ejection. The results of these experiments indicate

that the peak pressure gradient is associated with the point of maximum acceleration on the ascending aortic flow pulse. In addition, when the $\Delta v/\Delta t$ is zero in the ascending aorta the pressure gradient is also zero. On this basis there is reason to believe that pressure flow dynamics across the aortic valve can be conceived through Newton's second law of motion.

The regression of equations in the graphs presented in Figure 6 illustrate this idea. At a given peak flow velocity or maximum acceleration of blood in the ascending aorta, the peak pressure gradient across the aortic valve is increased as the mean aortic pressure is elevated. Elevations in aortic pressure in these experiments resulted in an increase in the volume of blood in the aorta. If the possibility of active aortic constriction is eliminated, then increases in aortic pressure must be accompanied by elevations in blood volume. Here pressure is considered a scalar quantity, having magnitude and not direction. On the other hand, the blood mass in the aorta becomes a vector quantity having both mass and direction when it is multiplied by velocity to yield momentum. Obviously, this increases the aortic blood mass. According to Newton's second law, if the mass is increased the same pressure gradient or force generated by the heart will generate less flow acceleration and less peak flow. Conversely, in order to generate a given flow velocity or acceleration when the aortic pressure is increased, a greater pressure gradient must be developed. These assumptions are realized by

the results obtained through linear regression. The regression lines indicate that the peak flow velocity or flow acceleration is elevated for a given pressure gradient when the aortic pressure is lower. Elevations in aortic pressure or mass cause the maximum flow acceleration and velocity to be reduced for a given pressure gradient. The heart can adapt to elevations in aortic pressure through heterometric autoregulation, and the resultant elevation in presystolic fiber length can produce more isometric tension which is transformed into a larger pressure gradient change across the aortic valve, so that the larger arterial mass can be overcome.

Wilcken et al have shown reductions in flow acceleration and velocity in the ascending aorta following acute elevations in aortic resistance (238). They attributed the elevation in outflow impedance to be responsible for this change. Peak flow velocity was most affected with increases in outflow resistance. In addition, when the abdominal aorta was opened to atmosphere between beats, there was no change in the maximum acceleration of blood in the ascending aorta; however, the stroke volume was augmented. Opening the aorta to atmosphere between beats did not alter the aortic blood mass. The experimental results of Wilcken et al indicate that flow acceleration in the ascending aorta is not dependent upon aortic pressure per se, but is a function of arterial blood mass. Hence, it can be stated that in the arterial system flow accelerations will be affected primarily

by changes in arterial blood mass, and flow velocity by changes in arterial resistance.

Spencer et al have demonstrated that in the abdominal aorta inertial flow could be attenuated by reducing the flow velocity and increasing peripheral resistance. On the other hand, viscous flow was approached when the flow velocity was elevated or when the vessel segment under study was constricted (198).

The trace in Figure 7 illustrates the operation of Newton's second law of motion during ventricular ejection. Cessation of cardiac pumping, induced by stimulation of the vagus nerves, allows the elastic elements in the aorta to recoil, resulting in a reduction of vessel caliber and a decrease in arterial blood volume. The mean aortic pressure preceeding the vagal escape beat was 43 mm Hg, indicating that the volume of blood in the arterial system had been reduced. The vagal escape beat resulted in the generation of a peak pressure gradient equal in magnitude to control, and generated a greater stroke volume and peak flow as well as an increase in the maximum flow acceleration in the ascending aorta. Such experiments indicate that the peak flow and maximum acceleration of blood in the ascending aorta are dependent upon the arterial blood mass and the attendant pressure gradient.

The slope of the line relating the peak pressure gradient and maximum acceleration (Figure 6) yields a ratio expressing the change in the pressure gradient to the change in flow

expressed as acceleration ($\Delta P/dF/dt$). This ratio is an expression of fluid inertance. Elevations in arterial pressure which result in increases in arterial blood mass reduces the slope of the line relating the peak pressure gradient to maximum acceleration. Since during the initial phase of ventricular ejection the force generated by the heart is directed toward overcoming the inertia of the blood column in the aorta, the slope of the line relating the pressure gradient to the rate of change of flow in the aorta is a quantitative measure of the inertial constant of the ascending aorta. In other words, this ratio is an expression of the fluid inertia the heart must overcome in order to eject the stroke volume.

Table 4 and Figure 38 illustrate the effects of stellate ganglion stimulation on pressure-flow relations across the aortic valve. The results in Table 4 indicate that the maximum acceleration was the flow parameter most affected. In some cases this parameter increased to over two times the control value. The changes in peak flow velocity during stimulation were not as extensive as the acceleration changes.

Sonnenblick has shown in the isolated papillary muscle that inotropic interventions can increase both the peak isometric force and the maximum velocity of fiber shortening of the muscle (203). Changes in peak flow and maximum acceleration in the ascending aorta during stimulation were accompanied by elevations in the peak pressure gradient. Hence, ventricular ejection can

be influenced by extrinsic mechanisms through the autonomic nervous system as well as by heterometric autoregulatory processes. In addition, the increase in myocardial synchrony which accompanies stellate ganglion stimulation can contribute to the increased force developed by the contracting myocardium (141,151).

Inspection of the data in Table 4 during vagal bradycardia reveals average increases in peak flow velocity and acceleration in the ascending aorta. Left ventricular dP/dt is reduced along with aortic pressure. However, this peak pressure gradient across the aortic valve shows an average increase over control. The regression lines shown in Figure 6 indicate that for a given peak pressure gradient the maximum flow velocity is elevated at lower mean aortic pressures. Consequently, the augmented peak velocities observed during bradycardia can be explained on this basis. Furthermore, these data tend to support the idea that it is the pressure gradient generated by the heart and not the magnitude of the dP/dt which determines the rate of ventricular emptying.

Reeves has shown a close correlation between dP/dt and the isometric force developed by the contracting left ventricle, at a given end diastolic fiber length (160,162). The reduced dP/dt associated with the vagal escape beat in Figure 7 illustrates that the force of contraction is reduced. Although LVEDP was not measured in this pulse it can be assumed that this parameter increased because of the prolonged filling time associated

with bradycardia. Hence, the vagal stimulation had probably exercised some degree of inhibition on the left ventricle.

Hendersen and Barringer showed that ventricular stroke volume could be augmented with stellate ganglion stimulation (78). Kelso and Randall have concluded from cardiometer experiments that stellate ganglion stimulation could increase ventricular stroke volume (98). According to Rushmer and Wang, stroke volume is not augmented during exercise (176,225). On the other hand, Warner and Toronto have shown that in dogs with electrically paced hearts cardiac output during exercise could be accomplished solely by an increase in ventricular stroke volume (226). The stroke volume data presented in Table 4 were recorded in preparations in which heart rate was allowed to increase with stellate ganglion stimulation. The average results indicate that stellate ganglion stimulation resulted in a small but insignificant increase in ventricular stroke volume. The lack of augmented stroke volume during stimulation is probably the result of the attendant cardioacceleration which reduced the period of diastolic filling. Indeed, the results of Warner and Toronto indicate that elevations in cardiac output during exercise have a significant stroke volume component which is not manifest due to the concomitant elevation in heart rate which accompanies the exercise response.

Noble et al have shown that the maximum acceleration of blood in the ascending aorta may be a sensitive index of the

contractile state of the myocardium (138). The first parameter to be increased during intracoronary infusions of calcium gluconate was the maximum acceleration of blood in the ascending aorta. Similarly, the first parameter to be affected by acute occlusion of the anterior descending coronary artery was the maximum acceleration in blood flow. In addition, during calcium gluconate administration, maximum acceleration increased up to 210% without a change in the stroke volume. Table 4 indicates that inotropic influences such as stellate ganglion stimulation or isoproterenol primarily affects the maximum acceleration of blood flow. Furthermore, Noble et al have shown that changes in position which increased the end diastolic size of the heart generated larger stroke volume primarily through an increase in the peak flow velocity allowing for the additional ejection of blood in late systole (137). In the reclining position, the maximum acceleration was unchanged, but the period of flow acceleration was extended, thus generating the elevated peak flow velocity. In their experiments on conscious dogs, Noble et al state: "The higher peak velocity in early systole indicates extra momentum (mass x velocity) which may have caused much of the additional blood to leave the ventricle passively in late systole. If the force exerted by the heart in early systole is proportional to the acceleration of blood, it would appear that the key feature of the increased cardiac force exerted from a greater initial fiber length is that the same maximum force is exerted for a

longer time, so that there is a greater total force." Indeed, the results in Tables 1 through 3 show that with elevations in left ventricular filling, the period is lengthened over which left ventricular pressure exceeds aortic pressure, indicating that the force exerted by the ventricle is applied for a longer percentage of the ejection period. This point is illustrated in the trace shown in Figure 3. The possibility exists that the peak pressure gradient may be the primary determinant of maximum acceleration and the duration of the peak pressure gradient is the primary determinant of maximum flow velocity.

Noble et al reasoned that the constancy of stroke volume during inotropism is due to forces which counteract the momentum of the blood at peak flow velocity (138). These authors have stated that this opposing force is stored and discharged by the elastic wall of the aorta. At the point of maximum velocity in the ascending aorta the kinetic component is maximal, consequently, it may not be opposed by a lateral force component present in the elastic elements of the aorta. Therefore, some other force should be responsible for the rapid deceleration during inotropism. Cope has shown that the dynamic compliance of the aorta decreases with increases in the frequency of pressure oscillations (37). It follows then that with very rapid ejection of blood into the ascending aorta, the extent of aortic stretch would be decreased so that the energy of ejection would be primarily directed toward overcoming the entire blood mass in

the aorta. In other words, the radial flow component is reduced because of the decrease in dynamic compliance of the aorta, hence the force generated by the heart during inotropism is directed toward overcoming the inertia of the aortic blood column rather than stretching the aortic wall. In addition, rapid acceleration of the aortic blood column can introduce additional impedance through the generation of turbulent flow and high shear rates at the blood vessel-blood column interface (123,124).

The ventricular responses to left stellate stimulation produced changes which were directionally identical to those elicited from a single injection of isoproterenol (0.5 μg/Kg). Numerous workers have shown that isoproterenol can induce ventricular aortic pressure gradients in excess of 50 mm Hg (18,69,99, 100,229,235). Similarly, the results illustrated in Table 4 show that stellate ganglion stimulation can induce large pressure gradients across the aortic valve, indicating that the central nervous system through autonomic pathways can induce functional aortic pressure gradients during systole. This statement has meaning in the light of recent evidence that functional aortic stenosis can be alleviated by the administration of beta-blocking drugs such as propranolol (18). Clinically functional stenosis has been shown to reduce the heart's ability to eject a normal stroke volume, and cardiac output is reduced. In the experiment shown in Figure 8, the secondary increase in pressure gradient across the aortic valve occurred near the peak of ventricular

ejection, but does not appear to offer resistance to ventricular ejection. In addition, functional sub-aortic stenosis may not be due to constriction of sub-valvular musculature. On the contrary the increased levels of ventricular pressure observed during the latter part of systole may be a function of catheter placement (41). In instances in which the left ventricular volume is reduced, such as occurs after hemorrhage, pressure gradients may be reduced or abolished simply by withdrawing the catheter tip to a sub-valvular level (121). These results indicate that high pressure pockets can develop in the apical region of the left ventricle. It has been shown in hemorrhaged dogs that there is a reduction in contrast material in the apical region during systole.

B. Right Ventricular Responses to Autonomic Nerve Stimulation.

Functional obstruction of right ventricular outflow has also been reported (54,90,168,216). The peculiar anatomy and embryology of the infundibular region of the right ventricle provides the basis for functional changes associated with this region (96,97,117,167). Data presented in Table 5 indicates that the sinus and conus regions of the right ventricle are functionally discrete. Normally, a small pressure gradient exists across the infundibular zone of the right ventricle. This gradient can be magnified by inotropic interventions. Tobin et al have shown that calcium, digitalis and isoproterenol can induce large pressure gradients across the infundibular zone (216). The data in Table 5 indicate that large infundibular pressure gradients can

be induced through stimulation of the autonomic nervous system. Electrical excitation of the cervical vagi after atropine can also induce infundibular pressure gradients. In the intact animal, atropine administration may unmask adrenergic fibers present in the vagus nerve, which have a profound effect on heart rate and ventricular force (83,129,156,157). On the other hand, Angelakos and Bloomquist have shown that acetylcholine may increase ventricular contractility through the release of catecholamines from the myocardium (4). Recently, Buccino et al have postulated the existence of a cholinergic receptor which is responsible for the augmentor action of acetylcholine on the ventricular myocardium (24). According to Friedman et al, acetylcholine may act to increase membrane permeability to calcium, thus increasing myocardial contractility (58). The data in Table 5 indicate that stimulation of the cervical vagosympathetic trunk after atropine can induce pressure gradients across the infundibular zone of the right ventricle.

The rate of rise of pressure in the sinus and conus region of the right ventricle is remarkably different during stimulation. Figure 13 is a trace illustrating the effects of left stellate stimulation on right ventricular pressure dynamics. Visual inspection of the rates of pressure development in the sinus and conus regions reveals a much greater dP/dt in the inflow or sinus region of the right ventricle. In addition, peak sinus pressure during stimulation is approximately twice as high as

FIGURE 13

RIGHT VENTRICULAR RESPONSES TO LEFT STELLATE GANGLION STIMULATION

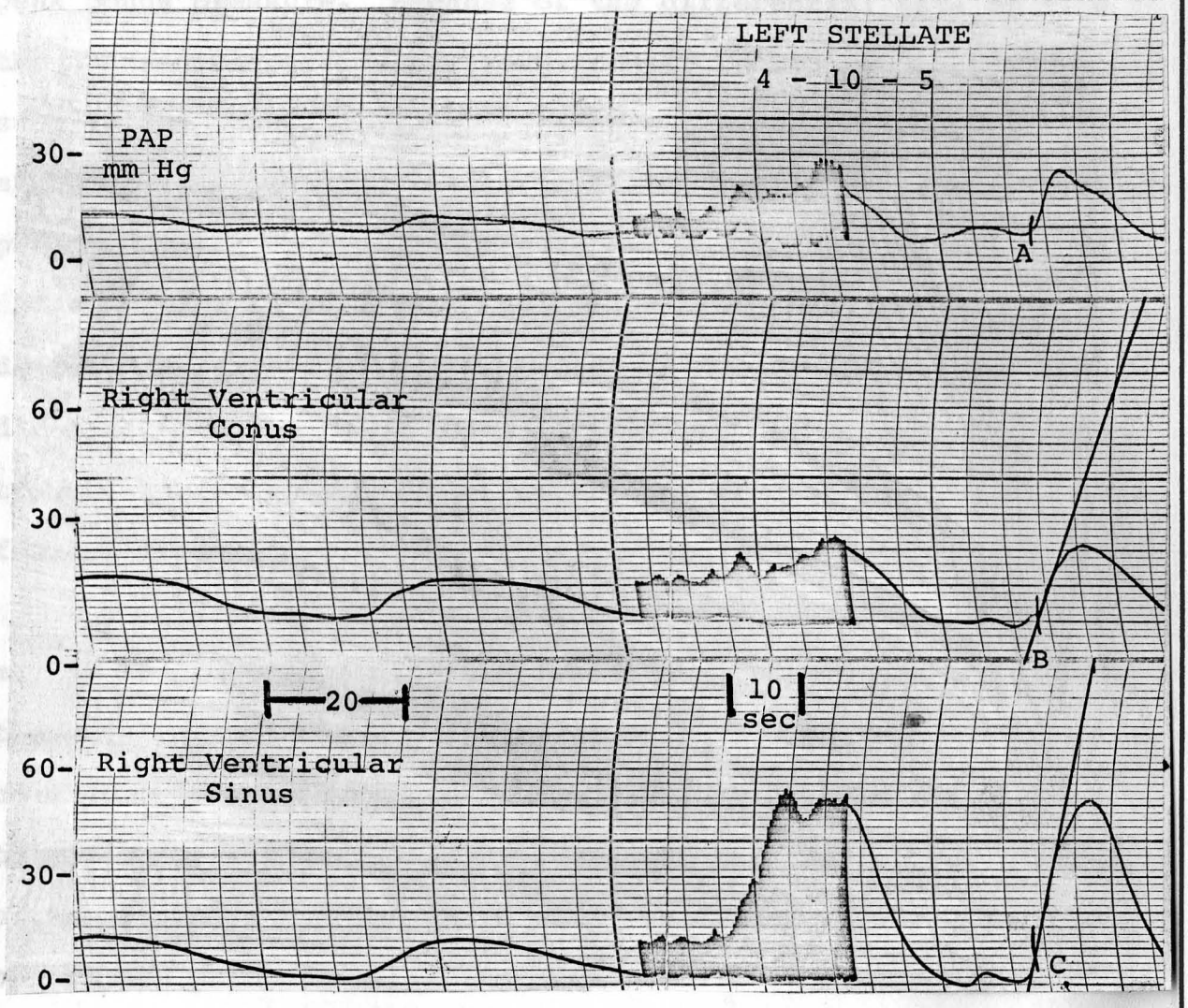

Record showing effects of left stellate ganglion stimulation on right ventricular pressure dynamics. Prior to stimulation, both sinus and conus systolic pressures were identical at 12 mm Hg. During stimulation, peak conus pressure increased to 22 mm Hg while peak sinus pressure reached 52 mm Hg. The slopes on the pressure pulses indicate that the rate of systolic pressure development in the sinus is elevated above that in the conus during stimulation. Systolic pulmonary arterial pressure was increased during stimulation and closely followed right ventricular conus pressure. Simultaneous time marks A and C indicate that sinus or inflow pressure is responsible for pulmonic valve opening. Individual stimulation pulses were 4 volts intensity, 5 msec in duration and occurred at frequency 10 cps.

peak conus pressure. Because of the differential rate of rise in the two regions, sinus pressure reaches pulmonary diastolic pressure before conus pressure. Consequently, transmission of intrasinus pressure through the infundibular region is responsible for pulmonic valve opening.

The phase lag between sinus and conus activation, the differential rates of pressure rise in the two areas, and the different magnitudes of systolic pressure development all contribute to the generation of a pressure gradient across the infundibular region.

The functional significance of these pressure gradients may be of great physiological importance. Brock has shown that the level of pulmonary pressure at which the pulmonic valves become incompetent increased with increases in the contractile tone of the conus region (23). During inotropism strong contractions of the circular muscles surrounding the conus region may help to oppose the pulmonic valve leaflets when their competency is threatened by high pressure loads. Figure 13 indicates that sinus pressure can reach 50 mm Hg during stellate ganglion stimulation. Surely if this pressure were transmitted unattenuated to the pulmonary vasculature, pulmonary edema would develop in a relatively short period. Possibly strong contractions of the infundibular region presents a functional resistance to blood flow through this region. Strictures of the conus region during systole could perform this function. On this basis the conus region may act as

a pressure regulating mechanism, which regulates the pressure gradient from the sinus region to the pulmonic vasculature. On the other hand, the sinus or inflow region may act as a flow pump which maintains volume flow through the stricture generated by the conus region. Therefore, the proper balance of contractile force in the sinus and conus regions of the right ventricle may act to protect and maintain the pulmonary circulation in situations of widespread sympathetic outflow as occurs during hypoxia.

The results presented in Table 5 indicate that cervical vagosympathetic stimulation after atropine blockade can augment right ventricular systolic pressures. However, the effects of cholinergic vagosympathetic mechanisms on right ventricular dynamics has not been investigated.

C. Ventricular Responses to Cervical Vagosympathetic Stimulation.

DeGeest and Levy have demonstrated the existence of vagal cholinergic innervation to the left ventricle and have shown the importance of this innervation in determining the level of left intraventricular pressure during reflex cardiovascular adjustments (45,46,47,48,111). Recently, Randall et al described an adrenergic-mediated effect on the ventricular chambers resulting from stimulation of the cervical vagosympathetic trunk (156). Sympathetic fibers coursing in the vagosympathetic trunk at the cervical level appear to be responsible for these effects. However, we have been unable to locate evidence in the literature for vagally-induced depression of the working right ventricle.

In the majority of animals presented in Table 6, the predominant adrenergic influence exerted by the cervical vagosympathetic trunk appears to be in the right ventricle. Figure 12 illustrates the influence of both cholinergic and adrenergic pathways. After the removal of the sympathetic influence by the beta-adrenergic blocking drug propranolol, vagal stimulation resulted in distinct depression of both ventricular pressures. Atropine was not given in these experiments. Although cardiac sympathetic impulses are channeled primarily through the stellate and caudal cervical ganglion (112), these pathways are not the only ones capable of influencing right heart performance (155). The present observations make it necessary to evaluate the roles of the superior cervical and nodose ganglia in the modulation of ventricular function. Figure 12 demonstrates that ventricular contractility can be regulated over a wide range by the cholinergic and adrenergic components of the vagosympathetic trunk and the interactions of these components may determine the level of right heart performance (110).

Table 6 indicates that vagosympathetic stimulation in the paced heart can induce marked inotropic affects on the right ventricle. Although left ventricular systolic pressure is consistently reduced during vagal stimulation, the rate of systolic pressure development may be increased and the pulse duration reduced, both of which are indications of increased contractility (68,98,162). In addition, LVEDP was found to increase in the

majority of left vagal stimulations and decrease in the majority of right vagal stimulations. Increased LV inotropism as indicated by elevated dP/dt values were not always accompanied by a fall in LVEDP. In fact, these parameters appear to be unrelated functions in these experiments. These results indicate that although peak systolic left ventricular pressure development is inhibited during vagal stimulation, positive inotropic mechanisms are activated, consequently, peak systolic pressure is not a totally accurate index of the inotropic state of the left ventricle during vagosympathetic stimulation. The possibility exists that the fall in systemic arterial pressure may have activated baroreceptor reflexes leading to increased sympathetic tone to the left ventricle, which results in dP/dt elevations (67,190). However, Figure 12 illustrates a record in which vagal stimulation causes elevated LV dP/dt in the absence of changes in systemic arterial pressure. In addition, bilateral transection of the ansa subclavia does not alter the augmentor influences of vagal stimulation (157).

The elevation in right ventricular end diastolic pressure and peak systolic pressure along with declining LVEDP may be explained by excitation of fibers which have a constrictor effect on the pulmonary vascular bed (44). Pulmonary constriction, without consonant increase in RV stroke volume, can lead to decreased pulmonary flow. These factors would attenuate venous return to the left heart. Table 6 indicates such directional changes were

recorded in approximately one-half of the experiments. In the absence of RV inhibition, one would expect the right ventricle to adjust to the elevated afterload by developing greater systolic pressure and stroke volume with restoration of left ventricular systolic and diastolic pressures. The experiment illustrated in Figure 11 reveals that pulmonary occlusion resulting in an elevated RVEDP identical to that recorded during vagal stimulation elicits greater increases in right ventricular pressures. Although such experiments do not completely rule out the possibility of increased pulmonary resistance, the resultant right ventricular depression may be the predominant factor influencing right ventricular stroke volume. Although evidence for pulmonary constrictor outflows is scarce, it now appears likely that stellate ganglion adrenergic mechanisms can induce pulmonary constriction (213). In addition, there is evidence that beta-adrenergic drugs such as isoproterenol can reduce pulmonary vascular resistance (8). The administration of propranolol, beta-adrenergic blocker, completely eliminated the augmented right ventricular pressures resulting from vagosympathetic stimulation. In light of present pharmacological evidence, propranolol could only act to heighten pulmonary vascular resistance by inhibiting a possible beta-adrenergic dilator mechanism present in the pulmonary vasculature.

The marked differences observed in the elevation of right and left ventricular end diastolic pressures in response to

vagosympathetic stimulation may be associated with changes in ventricular distensibility. A decrease in right ventricular distensibility would lead to a higher end diastolic pressure at any given end diastolic volume. Mitchell and his associates showed that, in the intact working heart, neither acetylcholine nor catecholamines, were able to change the indices of distensibility which they measured (131). In addition, end diastolic pressure volume relations in the intact right ventricle appear to be unaffected by norepinephrine or spontaneous tachycardia (102). On the other hand, Hefner et al were able to demonstrate increases in left ventricular distensibility during norepinephrine infusion (76). Measurements in excised hearts have demonstrated that the compliance of the right ventricle is greater than that of the left (103). If this difference is applicable to the in situ working heart, identical filling pressures would result in a greater right ventricular end diastolic volume. Consequently, fiber length changes would be greatest in the right ventricle allowing this chamber to develop systolic pressures which are equal to or greater than control values during vagal stimulation. In other words, as vagal inhibition suppresses contractility of the right ventricle, the RVEDP continues to rise until the fiber length is such that the right ventricle can generate enough tension to increase its stroke volume to equal systemic venous return and counteract prevailing vagal inhibition (187). Such an adaptive change could be met with greater facility

by the right ventricle than by the left because of its greater inherent compliance.

CHAPTER VI

SUMMARY AND CONCLUSIONS

Utilizing the methods of right heart bypass, the effects of filling pressure and afterload on the magnitude of the pressure gradient across the aortic valve were evaluated together with pulsatile flow in the ascending aorta. Sequential alterations in left ventricular filling were performed at 50, 75, and 100 mm Hg mean aortic pressure. The peak pressure gradient across the aortic valve increased as a function of left ventricular end diastolic pressure. Cardiac output, peak flow velocity, and maximum flow acceleration were all found to be linear functions of the peak pressure gradient across the aortic valve. Elevations in aortic pressure caused the peak pressure gradient maximum velocity and the peak pressure gradient maximum acceleration relationships to be altered, such that for a given peak pressure gradient both flow velocity and acceleration were reduced.

The effects of autonomic nerve stimulation on pressure flow relations across the aortic valve were evaluated in intact preparations. Left stellate ganglion stimulation resulted in elevated peak pressure gradients, together with marked elevations

in the maximum acceleration of blood flow in the ascending aorta. Stroke volume was not significantly increased during stimulation. Isoproterenol administration induced changes which were directionally identical to those recorded during electrical excitation of the stellate ganglion. During vagal bradycardia dP/dt was consistently reduced, whereas the maximum acceleration was either increased or unchanged. Increases in peak flow velocity were most marked during vagal bradycardia. In addition, experiments were performed to determine the influence of the autonomic nervous system on right intraventricular pressure gradients. Stimulation of both stellate ganglia caused the generation of marked pressure gradients across the infundibular zone of the right ventricle. Similarly, stimulation of the cervical vagosympathetics after atropine induced pressure gradients across the right ventricle during systole. Elevated right intraventricular sinus pressures along with increased rates of systolic pressure development in the sinus region contributed to the genesis of pressure gradients.

The effects of vagosympathetic stimulation on the paced heart were examined to evaluate the influence of cholinergic mechanisms on ventricular function. Vagosympathetic stimulation consistently reduced left ventricular systolic pressures. On the other hand, right ventricular systolic pressures were either elevated or unchanged during stimulation. Right ventricular end diastolic pressures, however, were consistently and markedly

increased. When the elevation in right ventricular end diastolic pressure recorded during stimulation was matched by partial occlusion of the main pulmonary artery, the resultant systolic pressure development was increased above that recorded during stimulation.

The following conclusions can be drawn from these results:

1) The pressure gradient across the aortic valve increases as a function of LVEDP and represents the ventricular force responsible for the generation of the stroke volume.

2) Cardiac output, peak flow velocity, and the maximum acceleration of blood flow in the ascending aorta are linear functions of the peak pressure gradient. In addition, the peak pressure gradient is associated with the maximum acceleration, and the zero pressure gradient across the aortic valve is associated with peak flow velocity. Hence, the processes of ventricular ejection can be described by Newton's second law of motion ($F = m\ dv/dt$).

3) Increases in afterload increase the effective mass of the arterial system, such that for a given pressure gradient the resultant flow acceleration is reduced when aortic pressure is elevated.

4) Stellate ganglion stimulation can induce large systolic pressure gradients across the aortic valve.

5) Stellate ganglion stimulation results in small increases in stroke volume in open-chest animals.

6) Autonomic nerve stimulation can induce systolic pressure gradients across the infundibular zone of the right ventricle, and appears to have a differential effect on the inflow and outflow regions of this chamber.

7) Vagosympathetic stimulation can result in both a profound depressant and an augmentor action on right ventricular performance.

BIBLIOGRAPHY

1. Abbott, B.C. and W.F.H.M. Mommaerts. A study of inotropic mechanisms in the papillary muscle preparation. J. Gen. Physiol. 42: 533-551, 1959.

2. Alessi, R., M. Nusynowity, J.A. Abildskov, and G.K. Moe. Non-uniform distribution of vagal effects on the atrial refractory period. Am. J. Physiol. 194: 406-410, 1958.

3. Alexander, R.S. The genesis of the aortic standing wave. Circ. Res. 1: 145-151, 1953.

4. Angelakos, E.T. and E. Bloomquist. Release of norepinephrine from isolated hearts by acetylcholine. Arch. Intern. Physiol. 73: 397-402, 1965.

5. Anzola, J. Right ventricular contraction. Am. J. Physiol. 184: 567-571, 1956.

6. Anzola, J. and R.F. Rushmer. Cardiac responses to sympathetic stimulation. Circ. Res. 4: 302-307, 1956.

7. Anrep, G.V. On the part played by the suprarenals in the normal vascular reactions of the body. J. Physiol. 45: 307-317, 1912.

8. Aviado, D.M. The pharmacology of the pulmonary circulation. Pharm. Rev. 12: 159-239, 1960.

9. Bakos, A.C.P. The question of the function of the right ventricular myocardium: An experimental study. Circ. 1: 724-732, 1950.

10. Barger, G. and H.H. Dale. Chemical structure and sympathomimetic action of amines. J. Physiol. 41: 19-59, 1910.

11. Barnett, G.O., J.C. Greenfield, and S.M. Fox. The technique of estimating the instantaneous aortic blood velocity in man from the pressure gradient. Am. H. J. 62: 359-366, 1961.

12. Bayliss, W.M. and E.H. Starling. On some points in the innervation of the mammalian heart. J. Physiol. (London) 13: 407-418, 1892.

13. Bergel, D.H. The dynamic elastic properties of the arterial wall. J. Physiol. 156: 458-469, 1961.

14. Bergel, D.H. The static elastic properties of the arterial wall. J. Physiol. 156: 445-457, 1961.

15. Bielecki, K. and B. Lewartowski. The influence of hemicholinium No. 3 and vagus stimulation on acetylcholine distribution in the cat's heart. Pflügers Arch. Ges. Physiol. 279: 149-155, 1964.

16. Brachfeld, N. and R. Gorlin. Functional subaortic stenosis. Ann. Int. Med. 54: 1-11, 1961.

17. Braunwald, E., E.C. Brockenbrough, and R.L. Frye. Studies on digitalis. V. Comparison of the effects of ouabain on left ventricular dynamics in valvular aortic stenosis and hypertrophic subaortic stenosis. Circ. 26: 166-173, 1962.

18. Braunwald, E., C.T. Lambrew, S.D. Rockoff, John Ross, Jr., and A.G. Morrow. Idiopathic hypertrophic subaortic stenosis: I. A description of the disease based upon an analysis of 64 patients. Circ. (Suppl. 4) 30: 98, 1964.

19. Braunwald, E., S.J. Sarnoff, and W.N. Stainsby. Determinants of duration and mean rate of ventricular ejection. Circ. Res. 6: 319-325, 1958.

20. Brecher, G.A. Critical review of recent work on ventricular diastolic suction. Circ. Res. 6: 554-566, 1958.

21. Brecher, G.A. and A.T. Kissen. Ventricular diastolic suction at normal arterial pressures. Circ. Res. 6: 100-106, 1958.

22. Brigton, J.D., R.E. Ferguson, M. Fredric, and E. Rapaport. Thermodilution studies of ventricular volume changes due to isoproterenol and bleeding. J. Appl. Physiol. 18: 129-133, 1963.

23. Brock, R. Control mechanisms in the outflow tract of the right ventricle in health and disease. Guy's Hosp. Rep. 104: 356-379, 1955.

24. Buccino, R.A., E.H. Sonnenblick, T. Cooper, and E. Braunwald. Direct positive inotropic effect of acetylcholine on myocardium. Evidence for multiple cholinergic receptors in the heart. Circ. Res. 19: 1097-1108, 1966.

25. Buckley, N.M., E. Ogden, and R.C. McPherson. The effect of inotropic drugs on filling of the isolated right ventricle of the dog. H. Circ. Res. 3: 447-453, 1955.

26. Buckley, N.M., E. Ogden, and D.S. Linton, Jr. The effects of work load and heart rate on the filling of the isolated right ventricle of the dog. Circ. Res. 3: 434-446, 1955.

27. Burchell, H.B. and M.D. Visscher. The changes in the form of the beating mammalian heart, as demonstrated by high-speed photography. Am. H. J. 22: 794-803, 1941.

28. Burn, J.H. and M.J. Rand. Sympathetic postganglionic mechanism. Nature 184: 163-166, 1959.

29. Burton, A.C. Physiology and Biophysics of the Circulation. Yearbook Medical Publishers, Inc., 1965. 143 p.

30. Calvin, L., J.K. Perloff, P.W. Conrad, and C.A. Hufnagel. Idiopathic hypertrophic subaortic stenosis. Am. H. J. 63: 447-484, 1962.

31. Campeti, F.L. Infundibular dynamics studied by cinea ngiocardiography in pure valvular pulmonary stenosis. Abstracted, Circ. 14: 918-918, 1956.

32. Cannon, W.B., J.T. Lewis, and S.W. Britton. Studies on the conditions of activity in endocrine glands. XVIII. A lasting preparation of the denervated heart for detecting internal secretion, with evidence for accessory accelerator fibers from the thoracic sympathetic chain. Am. J. Physiol. 77: 326-351, 1926.

33. Cannon, W.B. and A. Rosenblueth. A comparative study of sympathin and adrenine. Am. J. Physiol. 112: 268-276, 1935.

34. Cannon, W.B. and A. Rosenblueth. A comparison of the effects of sympathin and adrenine on the iris. Am. J. Physiol. 113: 251-258, 1935.

35. Cannon, W.B. and A. Rosenblueth. Studies on conditions of activity in endocrine organs. XXIX. Sympathin E and sympathin I. Am. J. Physiol. 104: 557-573, 1933.

36. Carlsten, A., B. Folkow, and C.A. Hamberger. Cardiovascular effect of direct vagal stimulation in man. Acta Physiol. Scand. 41: 68-76, 1957.

37. Cope, F.W. Elastic characteristics of isolated segments of human aortae under dynamic conditions. J. Appl. Physiol. 14: 55-59, 1959.

38. Cotten, M.DeV. Circulatory changes affecting measurements of heart force in situ with strain gauge arches. Am. J. Physiol. 174: 365-370, 1953.

39. Covell, J.W., J. Ross, Jr., E.H. Sonnenblick, and E. Braunwald. Comparison of the force-velocity relation and the ventricular function curve as measures of the contractile state of the intact heart. Circ. Res. 19: 364-372, 1966.

40. Criley, M.J., K.B. Lewis, R.J. White, Jr., and R.S. Ross. Pressure gradients without obstruction. A new concept of "hypertrophic subaortic stenosis". Circ. 32: 851-887, 1965.

41. Cullis, W. and E.M. Tribe. Distributions of nerves in the heart. J. Physiol. 46: 141-150, 1913.

42. Daggett, W.M., E.C. Nugent, P.W. Carr, P.C. Powers, and Y. Harada. Influence of vagal stimulation in ventricular contractility, O_2 consumption, and coronary flow. Am. J. Physiol. 212: 8-18, 1967.

43. Dale, H.H. Nomenclature of fibers in the autonomic system and their effects. J. Physiol. 80: 10-11, 1933.

44. Daly, De.B.I. and O.C. Hebb. Pulmonary vasomotor fibers in the cervical vagosympathetic nerve of the dog. Quart. J. Exptl. Physiol. 37: 19-43, 1952.

45. DeGeest, H., M.N. Levy, and H. Zieske. Carotid chemoreceptor stimulation and ventricular performances. Am. J. Physiol. 209: 564-570, 1965.

46. DeGeest, H., M.N. Levy, and H. Zieske. Negative inotropic effect of the vagus nerves upon the canine ventricle. Science 144: 1223-1225, 1964.

47. DeGeest, H., M.N. Levy, and H. Zieske. Reflex effects of cephalic hypoxia, hypercapnia, and ischemia upon ventricular contractility. Circ. Res. 17: 349-358, 1965.

48. DeGeest, H., M.N. Levy, H. Zieske, and R.I. Lipman. Depression of ventricular contractility by stimulation of the vagus nerve. Circ. Res. 17: 222-235, 1965.

49. DeMattos, A.D., M.N. Levy, and H. Zieske, Jr. Response of the heart to increased peripheral resistance. Circ. Res. 13: 33-38, 1963.

50. Denison, A.B., Jr. and H.D. Green. Effects of autonomic nerves and their mediators on the coronary circulation and myocardial contraction. Circ. Res. 6: 633-643, 1958.

51. Driscol, T.E. and R.W. Eckstein. Systolic pressure gradients across the aortic valve and in the ascending aorta. Am. J. Physiol. 210: 557-565, 1965.

52. Drury, A.N. The influence of vagal stimulation upon the force of contraction and the refractory period of ventricular muscle in the dog's heart. Heart 10: 405-413, 1923.

53. Eckstein, R.W., M. Stroud, III, R. Eckel, C.V. Dowling, and W.H. Pritchard. Effects of control of cardiac work upon coronary flow and O_2 consumption after sympathetic nerve stimulation. Am. J. Physiol. 163: 539-544, 1950.

54. Engle, M.A., G.R. Holswade, H.P. Goldberg, D.S. Lukas, and F. Glenn. Regression after open valvotomy of infundibular stenosis accompanying severe valvular pulmonic stenosis. Circ. 17: 862-873, 1958.

55. Frank, O. On the dynamics of cardiac muscle. Translated by C.B. Chapman and E. Wasserman. Am. H. J. 58: 282-317, 1959, and 58: 467-478, 1959.

56. Franklin, D.L., R.L. VanCitters, and R.F. Rushmer. Left ventricular function described in physical terms. Circ. Res. 11: 702-711, 1962.

57. Freis, E.D. and W.C. Heath. Hydrodynamics of aortic blood flow. Circ. Res. 14: 105-116, 1963.

58. Friedman, W.F., R.A. Buccino, E.H. Sonnenblick, and E. Braunwald. Effects of frequency in contraction and ionic environment on the responses of heart muscle to acetylcholine. Circ. Res. 21: 573-582, 1967.

59. Fry, D.L. Physiologic recording by modern instruments with particular reference to pressure recording. Physiol. Rev. 40: 753-788, 1960.

60. Fry, D.L. The measurement of pulsatile blood flow by the computed pressure gradient technique. IRE Tr. Biomed. Elec., ME 6: 259-264, 1959.

61. Fry, D.L., D.M. Griggs, Jr., and J.C. Greenfield, Jr. Myocardial mechanics: Tension-velocity-length relationships of heart muscle. Circ. Res. 14: 73-85, 1964.

62. Fry, D.L., A.J. Mallos, and A.G.T. Casper. A catheter tip method for measurement of the instantaneous aortic blood velocity. Circ. Res. 4: 627-632, 1956.

63. Fry, D.L., F.W. Noble, and A.J. Mallos. An electric device for instantaneous and continuous computation of aortic blood velocity. Circ. Res. 5: 75-78, 1957.

64. Fry, D.L., D.J. Patel, and F.M. DeFreitas. Relation of geometry to certain aspects of hydrodynamics in larger pulmonary arteries. J. Appl. Physiol. 17: 492-496, 1962.

65. Gauer, O.H. Volume changes of the left ventricle during blood pooling and exercise in the intact animal. Their effects on left ventricular performance. Physiol. Rev. 35: 143-155, 1955.

66. Gesell, R.A. Cardiodynamics in heart block as affected by auricular systole, auricular fibrillation and stimulation of the vagus nerve. Am. J. Physiol. 40: 267-313, 1916.

67. Gilmore, J.P. and J.H. Siegel. Myocardial catecholamines and ventricular performance during carotid artery occlusion. Am. J. Physiol. 207: 672-676, 1964.

68. Gleason, W.C. and E. Braunwald. Studies of the first derivative of the ventricular pulse in man. J. Clin. Invest. 41: 80-91, 1962.

69. Gorlin, R., L.S. Cohen, W.C. Elliott, M.D. Klein, and F.J. Lawe, Cardiomyopathies. Ciba Foundation Symposia. London: Churchill, 1964. 76 p.

70. Green, H.D. Circulatory system: Physical principles. In: Medical Physics. Ed. Glasser. Chicago: Year Book Publishers, 1950. Vol. 2, 228-251 p.

71. Hamilton, W.F. Role of Starling's concept in regulation of the normal circulation. Physiol. Rev. 35: 160-168, 1955.

72. Hamilton, W.F. and E.S. Bracket. Dynamic considerations on the relation between aortic and ventricular pressure curves. Am. J. Physiol. 112: 130-138, 1935.

73. Hamilton, W.F. and J.W. Remington. Some factors in the regulation of the stroke volume. Am. J. Physiol. 153: 287-297, 1948.

74. Haney, H.F., A.J. Lindgren, and W.B. Youmans. An experimentor analysis, by means of acetylcholine hypotension, of the problem of vagal cardioaccelerator fibers. Am. J. Physiol. 144: 513-520, 1945.

75. Hawthorne, E.W. Instantaneous dimensional changes of the left ventricle in dogs. Circ. Res. 9: 110-119, 1961.

76. Hefner, L.L., H.C. Coughlan, W.B. Jones, and T.J. Reeves. Distensibility of the dog's left ventricle. Am. J. Physiol. 201: 97-101, 1961.

77. Helps, E.B.W. and D.A. McDonald. Arterial blood flow calculated from pressure gradients. J. Physiol. 124: 30-31, 1954.

78. Henderson, Y. and T.B. Barringer. The conditions determining the volume of the arterial blood stream. Am. J. Physiol. 31: 289-299, 1913.

79. Hill, A.Y. The heat of shortening and the dynamic constants of muscle. Proc. Roy. Soc. London, Ser., 126: 136-195, 1938.

80. Hirsch, E.F., G.C. Kaiser, and T. Cooper. Experimental heart block in the dog. III. Distribution of the vagus and sympathetic nerves in the septum. Arch. Pathol. 79: 441-452, 1965.

81. Hirsch, E.F., C.A. Nigh, M.P. Kaye, and T. Cooper. Terminal innervation of the heart. II. Studies of the perimysial innervation apparatus and of sensory receptors in the rabbit and in the dog with the techniques of total extrinsic denervation, bilateral, cervical vagotomy, and bilateral thoracic sympathectomy. Arch. Path. 77: 172-187, 1964.

82. Hirsch, E.F., V.L. Willman, M. Jellinek, and T. Cooper. The terminal innervation of the heart. I. Quantitative correlations of the myocardial catecholamines with the perimysial plexus in normal cardiac tissues of the rabbit and dog and in the heart of the dog after total extrinsic denervation. Arch. Path. 76: 677-692, 1963.

83. Hoffmann, F., E.J. Hoffmann, S. Middleton, and J. Talesnik. The stimulating effect of acetylcholine on the mammalian heart and the liberation of an epinephrine-like substance by the isolated heart. Am. J. Physiol. 144: 187-198, 1945.

84. Hoffmann, B.F., A.A. Siebens, and C.M. Brooks. Effect of vagal stimulation on cardiac excitability. Am. J. Physiol. 169: 377-383, 1952.

85. Hollenberg, M., S. Carriere, and A.C. Barger. Biphasic action of acetylcholine on ventricular myocardium. Circ. Res. 16: 527-536, 1965.

86. Holt, J.P. Estimation of the risidual volume of the ventricle of the dog's heart by two indicator dilution techniques. Circ. Res. 4: 187-195, 1956.

87. Holt, J.P. and J. Allensworth. Estimation of the residual volume of the right ventricle of the dog. Circ. Res. 5: 323-326, 1957.

88. Howell, W.H. and W.W. Duke. Experiments on the isolated mammalian heart to show the relation of the inorganic salts to the action of the accelerator and inhibitory nerves. J. Physiol. (London) 35: 131-150, 1906.

89. Imperial, E.S., M.N. Levy, and H. Zieske, Jr. Outflow resistance as an independent determinant of cardiac performance. Circ. Res. 9: 1148-1155, 1961.

90. Johnson, A.M. Functional infundibular stenosis: Its differentiation from structural stenosis and its importance in atrial septal defect. Guy's Hosp. Rep. 108: 373-387, 1959.

91. Jourdan, F. and S.J.G. Nowak. Etude experimentale chez Le chien Des fibres cardioacceleratrices Du vague. Arch. Intern. Pharmacodyn. 53: 121-135, 1936.

92. Kabat, H. Cardioaccelerator fibers in the vagus nerve of the dog. Am. J. Physiol. 128: 246-257, 1939.

93. Kagan, A. Dynamic responses of the right ventricle following extensive damage by cauterization. Circ. 1: 816-823, 1952.

94. Kassebaum, D.G. and A.R. Van Dyke. Electrophysiological effects of isoproterenol on purkinje fibers of the heart. Circ. Res. 19: 940-946, 1966.

95. Katz, L.N. Factors modifying the duration of ventricular systole. J. Lab. Clin. Med. 6: 291-311, 1921.

96. Keith, A. Fate of the bulbus cordis in the human heart. Lancet 2: 1267-1273, 1924.

97. Keith, A. The evolution and action of certain muscular structures of the heart. Lancet 1: 703-707, 1904.

98. Kelso, A.F. and W.C. Randall. Ventricular changes associated with sympathetic augmentation of cardiovascular pressure pulses. Am. J. Physiol. 196: 731-744, 1959.

99. Krasnow, N., E. Rollet, W.B. Hood, Jr., P.M. Yurchak, and R. Gorlin. Reversible obstruction of the ventricular outflow tract. Am. J. Card. 11: 1-7, 1963.

100. Krasnow, N., E.L. Rolett, P.M. Yurchak, W.B. Hood, Jr., and R. Gorlin. Isoproterenol and cardiovascular performance. Am. J. Med. 37: 514-525, 1964.

101. Kurovetz, W.R., M.E. Hess, J. Shanfeld, and N. Haugaard. The action of sympathomimetic amines on isometric contraction and phosphorylase activity of the isolated rat heart. J. Pharm. & Exp. Therap. 127: 122-127, 1959.

102. LaFonant, R.L., H. Finebergh, and L.M. Katz. Pressure volume relations in the right ventricle. Circ. Res. 11: 699-701, 1962.

103. Laks, M.M., D. Garner, and H.J.C. Swan. Volumes and compliances measured simultaneously in the right and left ventricles of the dog. Circ. Res. 20: 565-569, 1967.

104. Lawton, R.W. Measurements on the elasticity and damping of isolated aortic strips of the dog. Circ. Res. 3: 403-408, 1955.

105. Leaders, F.E. Local cholinergic adrenergic interaction: Mechanism for the biphasic chronotropic response to nerve stimulation. J. Pharm. & Exp. Therap. 142: 31-32, 1963.

106. Lee, W.C. and F.E. Shideman. Mechanism of the positive inotropic response to certain ganglionic stimulants. J. Pharm. & Exp. Therap. 126: 239-249, 1959.

107. Levine, H.J. and N.A. Britman. Force velocity relations in the intact dog heart. J. Clin. Invest. 43: 1383-1396, 1964.

108. Levine, H.J., S.A. Forward, K.M. McIntyre, and E. Schechter. Effect of afterload on force-velocity relations and contractile element work in the intact dog heart. Circ. Res. 18: 729-744, 1966.

109. Levy, M.N., M. Ng, R.I. Lipman, and H. Zieske. Vagus nerves and baroreceptor control of ventricular performance. Circ. Res. 18: 101-106, 1966.

110. Levy, M.N., M.L. Ng, P. Martin, and H. Zieske. Sympathetic and parasympathetic interactions upon the left ventricle of the dog. Circ. Res. 19: 5-10, 1966.

111. Levy, M.N., M.L. Ng, and H. Zieske. Cardiac and respiratory effects of aortic arch baroreceptor stimulation. Circ. Res. 19: 935-939, 1966.

112. Levy, M.N., M.L. Ng, and H. Zieske. Functional distribution of the peripheral cardiac sympathetic pathways. Circ. Res. 19: 650-661, 1966.

113. Linden, R.J. and J.H. Mitchell. Relation between left ventricular diastolic pressure and myocardial segment length and observations on contribution of atrial systole. Circ. Res. 8: 1092-1099, 1960.

114. MacWilliam, J.A. On the phenomena of inhibition in the mammalian heart. J. Physiol. (London) 9: 346-395, 1888.

115. MacWilliam, J.A. The action of the vagus nerves on the mammalian heart. Quart. J. Exp. Physiol. 20: 149-192, 1930.

116. Mall, F. Development of the human heart. Am. J. Anat. 13: 249-298, 1912.

117. Mall, F.P. On the muscular architecture of the ventricles of the human heart. Am. J. Anat. 2: 211-266, 1911.

118. March, H.W. The persistence of a functioning bulbus cordis homologue in the turtle heart. Am. J. Physiol. 201: 1109-1112, 1961.

119. March, H.W., J.K. Ross, and R.R. Lower. Observations on the behavior of the right ventricular outflow tract, with reference to its developmental origins. Am. J. Med. 32: 835-845, 1962.

120. March, H.W. and S.P. Stephanos. The use of high speed cinematography in the analysis of cardiovascular motion. Am. H. J. 62: 652-658, 1961.

121. Martin, A.M., Jr., D.B. Hackel, M.S. Spach, M.P. Capp, and E. Mikat. Cineangiocardiography in hemorrhagic shock. Am. H. J. 69: 283-287, 1964.

122. Mayer, S.E. and N.C. Moran. Relation between pharmacologic augmentation of cardiac contractile force and the activation of myocardial glycogen phosphorylase. J. Pharm. & Exp. Therap. 129: 271-281, 1960.

123. McDonald, D.A. Blood Flow in Arteries. London: Edward Arnold, Ltd., 1960.

124. McDonald, D.A. The occurrence of turbulent flow in the rabbit aorta. J. Physiol. 118: 340-347, 1952.

125. McDonald, D.A. The relation of pulsatile pressure to flow in arteries. J. Physiol. 127: 533-552, 1955.

126. McDonald, D.A. The velocity of blood flow in the rabbit aorta studied with high speed cinematography. J. Physiol. 118: 328-339, 1952.

127. McDowall, R.J.S. The stimulating action of acetylcholine on the heart. J. Physiol. (London) 104: 392-403, 1946.

128. Meisner, J.E. and R.F. Rushmer. Eddy formation and turbulence in flowing liquids. Circ. Res. 12: 455-463, 1965.

129. Middleton, S., H.H. Middleton, and J. Toha. Adrenergic mechanisms of vagal cardiostimulation. Am. J. Physiol. 158: 31-37, 1949.

130. Mitchell, J.H., J.P. Gilmore, and S.J. Sarnoff. The transport function of the atrium. Factors influencing the relation between mean left atrial pressure and left ventricular end diastolic pressure. Am. J. Cardiol. 9: 237-247, 1962.

131. Mitchell, J.H., R.J. Linden, and S.J. Sarnoff. Influence of cardial sympathetic and vagal nerve stimulation on the relation between left ventricular diastolic pressure and myocardial segment length. Circ. Res. 8: 1100-1107, 1960.

132. Mitchell, J.H., A.G. Wallace, and N.S. Skinner, Jr. Relation between end diastolic pressure and mean rate of ejection of left ventricle. Am. J. Physiol. 211: 83-87, 1966.

133. Mizeres, N.J. The origin and course of the cardioaccelerator fibers in the dog. Anat. Rec. 132: 261-279, 1958.

134. Morrow, A.G. and E. Braunwald. Functional aortic stenosis: A malformation characterized by resistance to left ventricular outflow without anatomic obstruction. Circ. 20: 181-189, 1959.

135. Napolitano, L.M., V.L. William, C.R. Hanlon, and T. Cooper. Intrinsic innervation of the heart. Am. J. Physiol. 208: 455-458, 1965.

136. Ninomiya, I. Direct evidence of nonuniform distribution of vagal effects on dog atria. Circ. Res. 19: 516-683, 1966.

137. Noble, M.I.M., D. Trenchard, and A. Guz. Left ventricular ejection in conscious dogs. II. Determinants of stroke volume. Circ. Res. 19: 148-152, 1966.

138. Noble, M.I.M., D. Trenchard, and A. Guz. Left ventricular ejection in conscious dogs. I. Measurement and significance of the maximum acceleration of blood from the left ventricle. Circ. Res. 19: 139-147, 1966.

139. Nonidez, J.F. Studies on the innervation of the heart. I. Distribution of the cardiac nerves, with special reference to the identification of the sympathetic and parasympathetic postganglionics. Am. J. Anat. 65: 361-410, 1939.

140. Okino, O. and M.P. Spencer. Relationships between blood ejection and pressure gradient across the pulmonary valve. Fed. Proc. 21: 135-135, 1962.

141. Osadjan, C.E. and W.C. Randall. Effects of left stellate ganglion stimulation on left ventricular synchrony in dogs. Am. J. Physiol. 207: 181-186, 1964.

142. Patterson, S.W., H. Piper, and E.H. Starling. The regulation of the heart beat. J. Physiol. 48: 465-513, 1914.

143. Patterson, S.W. and E.H. Starling. On the mechanical factors which determine the output of the ventricles. J. Physiol. 48: 357-379, 1914.

144. Peserico, E. Influence of mechanical factors of the circulation upon the heart volume. J. Physiol. 65: 146-156, 1928.

145. Peterson, L.H. Certain physical characteristics of the cardiovascular system and their significance in the problem of calculating stroke volume from the arterial pulse. Fed. Proc. 11: 762-766, 1952.

146. Peterson, L.H. Some characteristics of certain reflexes which modify the circulation in man. Circ. 2: 351-362, 1950.

147. Peterson, L.H. The dynamics of pulsatile blood flow. Circ. Res. 2: 127-139, 1954.

148. Piemme, T.E., D. Barnett, and L. Dexter. Relationship of heart sounds to acceleration of blood flow. Circ. Res. 18: 303-315, 1966.

149. Porjé, I.G. and E. Rudewald. Hemodynamic studies with differential pressure technique. Acta Physiol. Scand. 51: 116-135, 1961.

150. Priola, D.V., C.E. Osadjan, and W.C. Randall. Functional characteristics of the left ventricular inflow and outflow tracts. Circ. Res. 17: 123-129, 1965.

151. Priola, D.V. and W.C. Randall. Alterations in cardiac synchrony induced by the cardiac sympathetic nerves. Circ. Res. 15: 463-472, 1964.

152. Puff, A. Die morphologie Des Bewegungsablaufes Der Herzkammern (Eine Utersuchung über Die Importance Beeimflussung Des Kontraktionsaalaufes Im rechten und Linken Ventrikel). Anat. Anz. 108: 342-350, 1960.

153. Puff, A. Systemum-Stellungen Der Muskelfasern in Kontraktionsvorgang an der Rechten Herzkammer. Verh. Anat. Ges. Anat. Anz. 105: 355-360, 1958.

154. Randall, W.C., H. McMally, J. Cowan, L. Caliguiri, and W.G. Rohse. Functional analysis of the cardioaugmentor and cardioaccelerator pathways in the dog. Am. J. Physiol. 191: 213-217, 1957.

155. Randall, W.C. and C.N. Peiss. Anomalous autonomic outflows to the heart and blood vessels. In Baroreceptors in Hypertension. Ed. P. Kezdi. Amsterdam: Elsevier, 1967.

156. Randall, W.C., D.V. Priola, and J.B. Pace. Responses of individual cardiac chambers to stimulation of the cervical vagosympathetic trunk in atropinized dogs. Circ. Res. 20: 534-544, 1967.

157. Randall, W.C., D.V. Priola, J.B. Pace, and J.S. Wechsler. Ventricular augmentor fibers in the cervical vagosympathetic trunk. Proc. Soc. Exp. Bio. & Med. 125: 1254-1257, 1967.

158. Randall, W.C., D.V. Priola, and R.H. Ulmer. A functional study of distribution of cardiac sympathetic nerves. Am. J. Physiol. 205: 1227-1231, 1963.

159. Randall, W.C. and W.G. Rohse. The augmentor action of the sympathetic cardiac nerves. Circ. Res. 4: 470-475, 1956.

160. Reeves, T.J. and L.L. Hefner. Isometric contraction and contractility in the intact mammalian ventricle. Am. H. J. 64: 525-538, 1962.

161. Reeves, T.J. and L.L. Hefner. The effect of vagal stimulation on ventricular contractility. Trans. Assoc. Am. Physicians 74: 260-270, 1961.

162. Reeves, T.J., L.L. Hefner, W.B. Jones, C. Coghan, G. Prieto, and J. Carroll. Hemodynamic determinants of the rate of change in pressure in the left ventricle during isometric contraction. Am. H. J. 60: 745-761, 1960.

163. Remington, J.W. Unexplained features of the left ventricular pressure pulse. Am. J. Physiol. 199: 328-330,

164. Remington, J.A. and R.P. Ahlquist. Effect of sympathomimetic drugs on the Q-T interval and on the duration of ejection. Am. J. Physiol. 174: 165-170, 1953.

165. Remington, J.W., W.F. Hamilton, and R.P. Ahlquist. Interrelation between the length of systole stroke volume and left ventricular work in the dog. Am. J. Physiol. 154: 6-15, 1948.

166. Remington, J.W. and R.A. Huggins. Relation of left ventricular ejection period to the Q-T interval of the electrocardiogram. Am. J. Physiol. 175: 185-190, 1953.

167. Robb, J.S. and R.C. Robb. The normal heart. Am. H. J. 23: 455-467, 1942.

168. Rodbardo, S., A. Shaffer, and P. Brostoff. Contraction of the pulmonary infundibular ring as a mode of stenosis in man. J. Lab. & Clin. Med. 44: 917-918, 1954.

169. Rosenblueth, A. The chemical mediation of autonomic nervous impulses as evidenced by summation of responses. Am. J. Physiol. 102: 12-38, 1932.

170. Rosenblueth, A.J., E. Alanis, Lopez, and R. Rubio. The adaptation of ventricular muscle to different circulatory conditions. Arch. Intern. Physiol. et. Biochem. 67: 358-373, 1959.

171. Ross, J., Jr., J.W. Covell, E.H. Sonnenblick, and E. Braunwald. Contractile state of the heart characterized by force-velocity relations in variably afterloaded and isovolumic beats. Circ. Res. 18: 149-163, 1966.

172. Rothberger, C.J. and D. Scherf. Wirkt der vagus auf die Kontraktionsstärke der Kammern des Säugetierherzens. Z. ges. exp. med. 71: 274-283, 1930.

173. Rudewald, Borje. Hemodynamics of the human ascending aorta as studied by means of a differential pressure technique. Acta Physiol. Scand. 54, Suppl. 187: 7-64, 1961.

174. Rushmer, R.F. Autonomic balance in cardiac control. Am. J. Physiol. 192: 631-634, 1958.

175. Rushmer, R.F. Cardiovascular Dynamics. Second edition. W.B. Saunders & Co.: Philadelphia and London, 1961. 182-184 p.

176. Rushmer, R.F. Constancy of stroke volume in ventricular responses to ejection. Am. J. Physiol. 196: 745-750, 1959.

177. Rushmer, R.F. Initial ventricular impulse. A potential key to cardiac evaluation. Circ. Res. 29: 268-283, 1964.

178. Rushmer, R.F. Continuous measurements of left ventricular dimensions in intact, unanesthetized dogs. Circ. Res. 2: 14-21, 1954.

179. Rushmer, R.F. and D.K. Crystal. Changes in configuration of the ventricular chambers during the cardiac cycle. Circ. 4: 211-218, 1951.

180. Rushmer, R.F., D.K. Crystal, and C. Wagner. The functional anatomy of ventricular contraction. Circ. Res. 1: 162-170, 1953.

181. Rushmer, R.F., O. Smith, and D. Franklin. Mechanism of cardiac control in exercise. Circ. Res. 7: 602-627, 1959.

182. Rushmer, R.F. and N. Thal. The mechanisms of ventricular contraction: A cinefluorographic study. Circ. Res. 4: 219-228, 1951.

183. Rushmer, R.F. and T.C. West. Role of autonomic hormones on left ventricular performance continuously analyzed by electronic computers. Circ. Res. 5: 240-246, 1957.

184. Rushmer, R.F., N. Watson, D. Harding, and D. Baker. Effects of acute coronary occlusion on performance of right and left ventricles in intact unanesthetized dogs. Am. H. J. 66: 522-531, 1963.

185. Samaan, Adli. The antagonistic cardiac nerves and heart rate. J. Physiol. 83: 332-340, 1935.

186. Sarnoff, S.J. Myocardial contractility as described by ventricular function curves; observations on Starling's law of the heart. Physiol. Rev. 35: 107-122, 1955.

187. Sarnoff, S.J. and E. Berglund. Ventricular function. I. Starling's law of the heart studied by means of simultaneous right and left ventricular function curves in the dog. Circ. 9: 706-718, 1954.

188. Sarnoff, S.J., E. Braunwald, G.H. Welch, R.B. Case, W.N. Stainsby, and R. Macruz. Hemodynamic determinants of oxgen consumption of the heart with special reference to the time-tension index. Am. J. Physiol. 192: 148-156, 1958.

189. Sarnoff, S.J., S.K. Brockman, J.P. Gilmore, R.J. Linden, and J.H. Mitchell. Regulation of ventricular contraction influence of cardiac sympathetic and vagal nerve stimulation on atrial and ventricular dynamics. Circ. Res. 8: 1108-1122, 1960.

190. Sarnoff, S.J., J.P. Gilmore, S.K. Brockman, J.H. Mitchell, and R.J. Linden. Regulation of ventricular contraction by the carotid sinus: Its effect on atrial and ventricular dynamics. Circ. Res. 8: 1123-1136, 1960.

191. Sarnoff, S.J., J.P. Gilmore, and J.H. Mitchell. Influence of atrial contraction and relaxation on closure of mitral valve. Observations on effects of autonomic nerve activity. Circ. Res. 11: 26-35, 1962.

192. Sarnoff, S.J., J.P. Gilmore, and A.G. Wallace. Influence of autonomic nerve activity on the adaptive mechanisms in the heart. In The Nervous Control of the Heart. Ed. W.C. Randall. Baltimore: Williams & Wilkins, 1965. 54-129 p.

193. Sarnoff, S.J. and J.H. Mitchell. The control of the function of the heart. In Handbook of Physiology, Section 2, Circulation. Ed. W.F. Hamilton and Philip Dow. Washington, D.C.: American Physiological Society, 1962. 489 p.

194. Sarnoff, S.J. and J.H. Mitchell. The regulation of the performance of the heart. Am. J. Med. 30: 747-771, 1961.

195. Sarnoff, S.J., J.H. Mitchell, J.P. Gilmore, and J.P. Remensnyder. Homeometric autoregulation in the heart. Circ. Res. 8: 1077-1091, 1960.

196. Schreiner, G.L., E. Berglund, N.G. Borst, and R.G. Monroe. Effects of vagal stimulation and of acetylcholine on myocardial contractility, oxygen consumption and coronary flow in dogs. Circ. Res. 5: 563-567, 1957.

197. Shipley, R.E. and D.E. Gregg. The cardiac response to stimulation of the stellate ganglia and cardiac nerves. Am. J. Physiol. 143: 396-401, 1945.

198. Spencer, M.P. and A.B. Denison, Jr. Aortic flow pulse as related to differential pressure. Circ. Res. 4: 476-484, 1956.

199. Spencer, M.R. and A.B. Denison. Pulsatile blood flow in the vascular system. Handbook of Physiology. Section 2, Circulation. Washington, D.C.: American Physiological Society, 1963.

200. Spencer, M.P. and A.B. Denison, Jr. Square wave electromagnetic flowmeter: Theory of operation and design of magnetic probes for clinical and experimental applications. IRE Tr. Biomed. Elec., ME 6: 220-228, 1959.

201. Spencer, M.P. and F.C. Greiss. Dynamics of ventricular ejection. Circ. Res. 10: 274-279, 1962.

202. Spencer, M.P., F.R. Johnston, and A.B. Denison, Jr. Dynamics of the normal aorta. Inertiance and compliance of the arterial system which transforms the cardiac ejection pulse. Circ. Res. 6: 491-500, 1958.

203. Sonnenblick, E.H. Force velocity relations in mammalian heart muscle. Am. J. Physiol. 202: 931-939, 1962.

204. Sonnenblick, E.H. Instantaneous force-velocity-length determinants in the contraction of heart muscle. Circ. Res. 16: 441-451, 1965.

205. Sonnenblick, E.H. and S.E. Downing. Afterload as a primary determinant of ventricular performance. Am. J. Physiol. 204: 604-610, 1963.

206. Sonnenblick, E.H., J. Ross, Jr., J.W. Covell, G.A. Kaiser, and E. Braunwald. Velocity of contraction as a determinant of myocardial oxygen consumption. Am. J. Physiol. 209: 919-927, 1965.

207. Sonnenblick, E.H., J.H. Siegel, and S.J. Sarnoff. Ventricular distensibility and pressure-volume curve during sympathetic stimulation. Am. J. Physiol. 204: 1-8, 1963.

208. Stainsby, W.N., S.J. Sarnoff, E. Braunwald, R.B. Case, and G.H. Welch. Effects of independent alterations of stroke volume, aortic pressure and heart rate on left ventricular function. Fed. Proc. 15: 177-178, 1956.

209. Starling, E.H. The Linacre Lecture on the Law of the Heart (given at Cambridge, 1915). London: Longmans, Green, 1918.

210. Starr, I., W.A. Jeffers, and R.H. Meade. The absence of conspicuous increments of venous pressure after severe damage in the right ventricle of the dog, with a discussion of the relation between clinical congestive failure and heart disease. Am. H. J. 26: 291-301, 1943.

211. Straub, H. Der Einfluss des Vagus auf Rhythmic und Dynamik des Säugetierherzens. Z. ges. exp. Med. 53: 197-232, 1926.

212. Szentivanyi, M., J.B. Pace, J.S. Wechsler, and W.C. Randall. Localized myocardial responses to stimulation of cardiac sympathetic nerves. Circ. Res. 21: 691-702, 1967.

213. Szidon, J.P., R.H. Ingram, and A.P. Fishman. Effects of sympathetic stimulation on the pulmonary circulation. Fed. Proc. 26: 271-271, 1967.

214. Taylor, R.R., H.E. Cingolani, and R.H. McDonald, Jr. Relationship between left ventricular volume, ejected fraction, and wall stress. Am. J. Physiol. 211: 674-680, 1966.

215. Tcheng, K.T. Innervation of the dog's heart. Am. H. J. 41: 512-524, 1951.

216. Tobin, J.R., P.E. Blundell, R.G. Goodrich, and H.J.C. Swan. Induced pressure gradients across infundibular zone of right ventricle in normal dogs. Circ. Res. 16: 162-173, 1965.

217. Truex, K.D., J.C. Scott, D.M. Long, and M.Q. Smythe. Effect of vagus nerves on heart rate of young dogs: An anatomic-physiologic study. Anat. Rec. 123: 201-221, 1955.

218. Tulgan, J. A study of the relation of afferent impulses to the activity of the central cardiovascular nervous mechanism. Am. J. Physiol. 65: 174-179, 1923.

219. Ulmer, R.H. and W.C. Randall. Atrioventricular pressures and their relationships during stellate stimulation. Am. J. Physiol. 201: 134-138, 1961.

220. Von Euler, J.S. The nature of adrenergic nerve mediators. Pharm. Rev. 3: 247-277, 1951.

221. Wallace, A.O., J.H. Mitchell, N.S. Skinner, and S.J. Sarnoff. Hemodynamic variables affecting the relation between mean left atrial and left ventricular end diastolic pressures. Circ. Res. 13: 261-270, 1963.

222. Wallace, A.G. and S.J. Sarnoff. Effects of cardiac sympathetic nerve stimulation on conduction in the heart. Circ. Res. 14: 86-92, 1964.

223. Wallace, A.G., W.G. Troyer, M.A. Lesage, and E.F. Zotti. Electrophysiologic effects of isoproterenol and beta-blocking agents in awake dogs. Circ. Res. 18: 140-148, 1966.

224. Wang, H.H., M.R. Blumenthal, and S.C. Wang. Effect of efferent vagal stimulation on coronary sinus outflow and cardial work in the anesthetized dog. Circ. Res. 8: 271-277, 1960.

225. Wang, Y., R.J. Marshall, and J.T. Shephard. Stroke volume in the dog during graded exercise. Circ. Res. 4: 558-563, 1960.

226. Warner, H.R. and A.F. Toronto. Regulation of cardiac output through stroke volume. Circ. Res. 8: 549-552, 1960.

227. Weissler, A.M., R.G. Peeler, and W.H. Ruehil. Relationships between left ventricular ejection time, stroke volume, and heart rate in normal individuals and patients with cardiovascular disease. Am. H. J. 62: 367-378, 1961.

228. West, T.C. and R.F. Rushmer. Comparative effects of epinephrine and levarterenol (l-norepinephrine) on left ventricular performance in conscious and anesthetized dogs. J. Pharm. & Exp. Therap. 120: 361-370, 1957.

229. Whalen, R.E., A.I. Cohen, R.G. Summer, and H.D. McIntosh. Demonstration of the dynamic nature of idiopathic hypertrophic subaortic stenosis. Am. J. Cardiol. 11: 8-16, 1963.

230. Wiggers, C.J. The Physiology of Shock. New York: Commonwealth, 1950.

231. Wiggers, C.J. Studies on the cardiodynamic actions of drugs. I. The application of optical methods of pressure registration in the study of cardiac stimulants and depressants. J. Pharm. & Exp. Therap. 30: 233-250, 1926-27.

232. Wiggers, C.J. The influence of vascular factors on mean pressure, pulse pressure, and phasic peripheral flow. Am. J. Physiol. 123: 644-658, 1938.

233. Wiggers, Carl J., II. The influence of the vagus nerves on the fractionate contraction of the right auricle. Am. J. Physiol. 42: 133-140, 1916.

234. Wiggers, C.J. and L.N. Katz. The specific influence of the accelerator nerves on the duration of ventricular systole. Am. J. Physicl. 53: 49-64, 1920.

235. Wigle, E.D. Cardiovascular drugs in muscular subaortic stenosis. Fed. Proc. 24: 1279-1286, 1965.

236. Wigle, E.D., A. Chrysohou, and W.G. Bigelow. Results of ventriculotomy in muscular subacrtic stenosis. Am. J. Cardiol. 11: 572-586, 1963.

237. Wigle, E.D., P.R. David, C.J. LaBrosse, and T. McMeekan. Muscular subaortic stenosis. Am. J. Cardiol. 15: 761-772, 1965.

238. Wilcken, D.E.L., A.A. Charlier, J.I.E. Hoffman, and A. Guz. Effects of alterations in aortic impedance on the performance of the ventricles. Circ. Res. 14: 283-293, 1964.

239. Womersley, J.R. Method for the calculation of velocity, rate of flow and viscous drag in arteries when the pressure gradient is known. J. Physiol. 127: 553-563, 1955.

240. Womersley, J.R. The mathematical analysis of the arterial circulation in a state of oscillatory motion. Wright Air Development Center. Technical Report WADC-TR-56-614, 1958.

241. Woodbury, R.A. and G.G. Robertson. The one ventricle pump and the pulmonary arterial pressure of the turtle. Am. J. Physiol. 137: 628-636, 1942.

242. Woollard, H.H. The innervation of the heart. J. Anat. 60: 345-373, 1926A.

243. Yanowitz, F., J.B. Preston, and J.A. Abildskov. Functional distribution of right and left stellate innervation to the ventricles: Production of neurogenic electrocardiographic changes by unilateral alteration of sympathetic tone. Circ. Res. 18: 416-428, 1966.

APPROVAL SHEET

The dissertation submitted by John Blaise Pace has been read and approved by five members of the Dissertation Committee.

The final copies have been examined by the director of the dissertation and the signature which appears below verifies the fact that necessary changes have been incorporated, and that the dissertation is now given final approval with reference to content, form, and mechanical accuracy.

The dissertation is therefore accepted in partial fulfillment of the requirements for the degree of Doctor of Philosophy.

May 27, 1968
Date

Walter C. Randall
Signature of Advisor